EFFECTS OF SURFACE FUNCTIONAL GROUPS AND NATURAL ORGANIC MATTER ON

CLOFIBRIC ACID ADSORPTION BY MESOPOROUS SILICATE SBA-15

Miss Jutima Permrungruang

A Thesis Submitted in Partial Fulfillment of the Requirements

for the Degree of Master of Science Program in Environmental Management

(Interdisciplinary Program)

Graduate School

Chulalongkorn University

Academic Year 2013

Copyright of Chulalongkorn University

ผลของหมู่ฟังก์ชันบนพื้นผิวตัวดูดซับและสารอินทรีย์ธรรมชาติต่อกระบวนการการดูดซับ
กรดคลอไฟบริคโดยตัวกลางดูดซับเมโซพอรัสซิลิเกตเอสบีเอ-15

นางสาวจุติมา เพิ่มรุ่งเรือง

| | |
|---|---|
| Thesis Title | EFFECTS OF SURFACE FUNCTIONAL GROUPS AND NATURAL ORGANIC MATTER ON CLOFIBRIC ACID ADSORPTION BY MESOPOROUS SILICATE SBA-15 |
| By | Miss Jutima Permrungruang |
| Field of Study | Environmental Management |
| Thesis Advisor | Assistant Professor Patiparn Punyapalakul, Ph.D. |
| Thesis Co-Advisor | Aunnop Wongrueng, Ph.D. |

Accepted by the Graduate School, Chulalongkorn University in Partial Fulfillment of the Requirements for the Master's Degree

⋯⋯⋯⋯⋯⋯⋯⋯⋯⋯⋯⋯⋯⋯⋯Dean of the Graduate School

(Associate Professor Amon Petsom, Ph.D.)

THESIS COMMITTEE

⋯⋯⋯⋯⋯⋯⋯⋯⋯⋯⋯⋯⋯⋯⋯Chairman

(Assistant Professor Chantra Tongcumpou, Ph.D.)

⋯⋯⋯⋯⋯⋯⋯⋯⋯⋯⋯⋯⋯⋯⋯Thesis Advisor

(Assistant Professor Patiparn Punyapalakul, Ph.D.)

⋯⋯⋯⋯⋯⋯⋯⋯⋯⋯⋯⋯⋯⋯⋯Thesis Co-Advisor

(Aunnop Wongrueng, Ph.D.)

⋯⋯⋯⋯⋯⋯⋯⋯⋯⋯⋯⋯⋯⋯⋯Examiner

(Assistant Professor Chawalit Ngamcharussrivichai, Ph.D.)

⋯⋯⋯⋯⋯⋯⋯⋯⋯⋯⋯⋯⋯⋯⋯External Examiner

(Assistant Professor Suwanna Kitpatiboontanon, Ph.D.)

iv

จุติมา เพิ่มรุ่งเรือง : ผลของหมู่ฟังก์ชันบนพื้นผิวตัวดูดซับและสารอินทรีย์ธรรมชาติต่อ
กระบวนการการดูดซับกรดคลอไฟบริคโดยตัวกลางดูดซับเมโซพอรัสซิลิเกตเอสบีเอ-15.
(EFFECTS OF SURFACE FUNCTIONAL GROUPS AND NATURAL ORGANIC
MATTER ON CLOFIBRIC ACID ADSORPTION BY MESOPOROUS SILICATE SBA-
15) อ.ที่ปรึกษาวิทยานิพนธ์หลัก: ผศ. ดร. ปฏิภาณ ปัญญาพลกุล, อ.ที่ปรึกษา
วิทยานิพนธ์ร่วม: อ. ดร. อรรณพ วงศ์เรือง, 127 หน้า.

งานวิจัยนี้มีจุดประสงค์เพื่อศึกษาผลของหมู่ฟังก์ชันบนพื้นผิวและประเมินผลกระทบ
ของสารอินทรีย์ธรรมชาติ(NOM) ที่มีความชอบน้ำ (HPI) และความไม่ชอบน้ำ (HPO) ต่อการดูด
ซับกรดคลอไฟบริก(CFA) รวมถึงรายงานค่าพารามิเตอร์ที่เกี่ยวข้องกับการถ่ายเทมวลสารสำหรับ
การออกแบบระบบดูดซับแบบตัวกลางอยู่กับที่โดยใช้ตัวกลางดูดซับซิลิเกตชนิดซานตาบาบาราแอ
ซิก(SBA-15) ที่ปรับปรุงพื้นผิวด้วยการต่อติดหมู่ฟังก์ชัน ได้แก่ หมู่ 3-
(trimethoxysilylpropyl)diethylenetriamine และหมู่3-mercaptopropyltriethoxy (3N-
SBA-15 และ M-SBA-15 ตามลำดับ) จากการทดลองที่ความเข้มข้นสูงของ CFA พบว่าตัวกลาง
ดูดซับทุกชนิดเกิดการดูดซับอย่างรวดเร็วใน 1 ชั่วโมงแรกและเข้าสู่สมดุลภายใน 6 ชั่วโมง
จลนพลศาสตร์และไอโซเทอมในการดูดซับสอดคล้องกับสมการจลนพลศาสตร์อันดับที่ 2 เทียม
และไอโซเทอมแบบฟรุนดริช ตามลำดับ 3N-SBA-15 มีประสิทธิภาพการดูดซับ CFA สูงสุด เมื่อ
pH มีค่าน้อยลง (pH 5) พบว่าความสามารถในการดูดซับ CFA มีค่าสูงขึ้นแต่เมื่อ pH สูงขึ้นพบว่า
ความสามารถในการดูดซับลดลง นอกจากนั้นตัวกลางดูดซับชนิดชอบน้ำมีแนวโน้มในการดูดซับ
CFA สูงกว่าตัวกลางดูดซับชนิดไม่ชอบน้ำ พันธะไฮโดรเจนและแรงดึงดูดทางประจุไฟฟ้าอาจจะมี
บทบาทสำคัญต่อกระบวนการดูดซับร่วมกัน นอกจากนั้นไอโซเทอมการดูดซับ CFA ที่ความเข้มข้น
ต่ำ (50-250 ไมโครกรัมต่อลิตร) สอดคล้องกับไอโซเทอมแบบเส้นตรง จากการศึกษาผลกระทบ
ของ NOM ต่อการดูดซับ CFA แสดงให้เห็นว่าการมีอยู่ของ NOM ทำให้เกิดการดูดซับ CFA ลดลง
ซึ่งอาจจะเกิดจากการแข่งขันโดยตรงของ NOM กับ CFA และ การบดบังรูพรุนบนตัวดูดซับชนิด
3N-SBA-15 การรายงานค่าพารามิเตอร์ที่เกี่ยวข้องกับการถ่ายเทมวลสารประกอบด้วย
สัมประสิทธิ์การแพร่ในชั้นฟิล์มของเหลว (kf) สัมประสิทธิ์การแพร่จากชั้นฟิล์มเข้าสู่ของแข็ง (ks)
สัมประสิทธิ์การถ่ายเทมวลสารจากชั้นของเหลวโดยรวม (Kf) สัมประสิทธิ์การถ่ายเทมวลสารเข้าสู่
ชั้นของแข็งโดยรวม (Ks) และค่าการแพร่ (Ds) ซึ่งสามารถคำนวณได้จากผลของการศึกษา
จลนพลศาสตร์การดูดซับ

สาขาวิชา    การจัดการสิ่งแวดล้อม          ลายมือชื่อนิสิต .............................................
ปีการศึกษา  2556                           ลายมือชื่อ อ.ที่ปรึกษาวิทยานิพนธ์หลัก .............
                                          ลายมือชื่อ อ.ที่ปรึกษาวิทยานิพนธ์ร่วม ...............

# # 5587520220 : MAJOR ENVIRONMENTAL MANAGEMENT

KEYWORDS: SURFACE FUNCTIONAL GROUPS / CLOFIBRIC ACID / ADSORPTION / SBA-15 / MESOPOROUS SILICATE

JUTIMA PERMRUNGRUANG: EFFECTS OF SURFACE FUNCTIONAL GROUPS AND NATURAL ORGANIC MATTER ON CLOFIBRIC ACID ADSORPTION BY MESOPOROUS SILICATE SBA-15. ADVISOR: ASST. PROF. PATIPARN PUNYAPALAKUL, Ph.D., CO-ADVISOR: AUNNOP WONGRUENG, Ph.D., 127 pp.

The objectives of this study are to study the effect of surface functional groups on CFA adsorption mechanism by SBA-15 and to evaluate the effect of hydrophilic (HPI) and/or hydrophobic (HPO) natural organic matter (NOM) on clofibric acid (CFA) adsorption, including to calculate mass transfer parameters for design of the fixed bed adsorption. SBA-15 was synthesized via surfactant template method. 3N-SBA-15 and M-SBA-15 were synthesized via post-grafting method with 3-(trimethoxysilylpropyl)diethylenetriamine and 3-mercaptopropyl-triethoxysilane, respectively. The adsorption of CFA onto all adsorbents at high concentration was increased rapidly in the first 1 hr. and reach equilibrium within 6 hr. The adsorption kinetic and isotherm were compatible with pseudo-second-order and Freundlich isotherm, respectively. 3N-SBA-15 had highest CFA adsorption capacity. Highest removal capacities of CFA were achieved in acidic condition (pH 5), but decreased with increase in pH. Furthermore, the main role adsorption mechanisms were supposed to be a hydrophilic interaction through hydrogen bonding and electrostatic interaction. Moreover, adsorption isotherm of CFA at low concentration (50-250 microgram/liter) of 3N-SBA-15 was investigated and was compatible with Linear isotherm. The presence of HPO and HPI NOM can decrease the CFA adsorption capacity, which might be caused by direct adsorption competition and pore blocking onto 3N-SBA-15. The reported mass transfer parameters consist of liquid film mass transfer coefficient (kf), solid film mass transfer coefficient (ks), overall solid-phase mass transfer coefficient (Ks), overall liquid-phase mass transfer coefficient (Kf), and constant diffusivity (Ds), which was calculated from the adsorption kinetic data.

| | | |
|---|---|---|
| Field of Study: Environmental Management | Student's Signature | ................................. |
| | Advisor's Signature | ................................. |
| Academic Year: 2013 | Co-Advisor's Signature | ................................. |

## ACKNOWLEDGEMENTS

## CONTENTS

LIST OF FIGURES

## LIST OF TABLES

CHAPTER I

INTRODUCTION

1.1 STATE OF PROBLEM

Recently, pharmaceutical compounds are widely used in large quantities in the farming industry, agriculture, and the treatment of several bacterial infections in humans and animals. Some pharmaceutical agents are the emergence and dissemination of resistant bacteria and resistance genes. In consequence of incomplete degradation efficiencies from hospital wastewater, municipal wastewater and effluent of drug manufacturers, they are eventually released into soils, sediments and aquatic environments such as rivers, streams, lakes and ground waters through different pathways (Loffler, Rombke, Meller, & Ternes, 2005). Some researchers reported that the presence of pharmaceutical drugs even at low concentration (ranging from μg/L to ng/L) may lead to public health problems (Rosal et al., 2008).

Clofibric acid (CFA), which is the active metabolite of blood lipid regulators is one of the most widely used to lower elevated serum lipids. Toxicological studies of CFA have been reported the effect on aquatic species (Saravanan, Karthika, Malarvizhi, & Ramesh, 2011). CFA are resistant to physical and biological treatment processes. Furthermore, the effects of degradation by-products of CFA are still uncleared and supposed to be more toxic than the mother compound. Therefore, physicochemical treatment such as adsorption should be the appropriate treatment process for removal of CFA from wastewater (Carabineiro, Thavorn-Amornsri, Pereira, & Figueiredo, 2011). Adsorption is a well-known equilibrium separation process and an effective method for water decontamination applications (Ahmad et al., 2009; Dabrowski, 2001; Rafatullah, Sulaiman, Hashim, & Ahmad, 2009). Several studies have

been used adsorption for removal pharmaceuticals by using different absorbent such as zeolites (Rossner, Snyder, & Knappe, 2009), activated carbon (Yu, Peldszus, & Huck, 2008), montmorillonite (Molu & Yurdakoç, 2010), and mesoporous silica (Bui, Kang, Lee, & Choi, 2011). Activated carbon is the most famous adsorbent because it can produces high levels of treatment and has a high stability. Although activated carbon presented efficient removal of pharmaceuticals; however, disadvantages of the adsorption activated carbon are low selectivity and regeneration of PAC after used can cause the toxic compound.

Moreover, in the real treatment process those natural organic matters (NOM) are found in wastewater. Therefore, NOM has the possibility to interact with adsorbent and absorbate (Matilainen et al., 2011). In the conventional treatment plants which use activated carbon for the removal of micro contaminants, NOM has a significant effect on its effectiveness and NOM always offers competition for adsorption sites that result in higher dose requirements and shorter lifetime for activated carbon (Hepplewhite, Newcombe, & Knappe, 2004; Newcombe & Cook, 2002). Therefore, the adsorbent that is capable to adsorb the micro-pollutant without limitation should be developed.

Mesoporous silicates have been widely used for micro-pollutants removal as the adsorbent because of their high surface area, uniform pore size, high selectivity and tunable pore structure, so in this study was used Santa Brabara Acid-15 (SBA-15) that was grafted with surface functional groups by post-grafting method to modify and increase selectivity of adsorbents for removal CFA. Kinetic parameters, isotherm parameters and mass transfer parameters can be calculated from the adsorption information from batch adsorption experiments. In real situation, treatment process

design needs to apply adsorption parameter such as adsorption capacity, adsorption rate and mass transfer parameters for designing adsorption column. Hence, this study was focused on batch adsorption for removal CFA and used the treated discharge wastewater to study the effect of NOM on CFA adsorption by using silica base porous material and their functionalized.

## 1.2 OBJECTIVES

1. To study the effect of surface modification of mesoporous silicate Santa Brabara Acid-15 (SBA-15) on clofibric acid (CFA) adsorption mechanism.

2. To evaluate the effect of hydrophilic and/or hydrophobic natural organic matter (NOM) on clofibric acid (CFA) adsorption.

3. To calculate mass transfer parameters for the design of the fixed bed adsorption.

## 1.3 HYPOTHESES

1. Surface modification via the post-grafting method of mesoporous silicate SBA-15 with hydrophilic and positive charged functional group can increase the adsorption capacity of clofibric acid (CFA).

2. The electrostatic attraction and hydrogen bonding between adsorbents and adsorbate may be the important roles in the adsorption of clofibric acid (CFA).

3. Natural organic matter (NOM) may be decrease adsorption capacity of adsorbent by adsorption competition and/or pore blocking mechanism.

## 1.4 SCOPES OF THE STUDY

A diagram in **Figure 1. 1** shows a descriptive of this research which divided into five phases, which are: 1) synthesis and characterization of SBA-15 and their functionalized, 2) removal of CFA by SBA-15 and their functionalized at high concentration, 3) removal of CFA by an effective functionalized SBA-15 at low concentration, 4) removal of CFA in treated wastewater from swine farm and 5) calculation of mass transfer parameters for fixed bed unit operation.
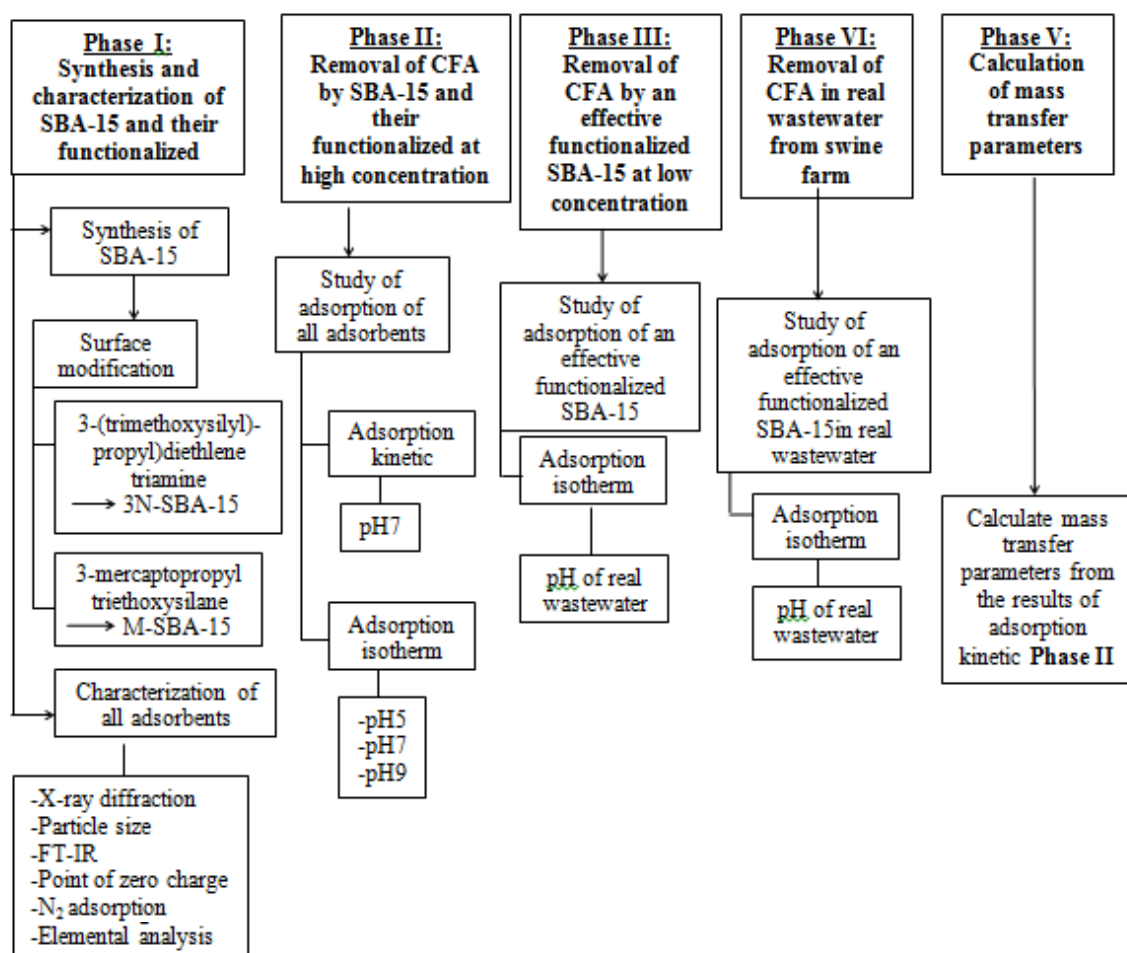
**Figure 1. 1** Overview of this research

**Phase I: Synthesis and characterization of SBA-15 and their functionalized.**

SBA-15 and their functionalized (amino and mercapto functional groups) were synthesized via post-grafting method and used as adsorbents in this study. The physicochemical properties of adsorbents were characterized which consist of X-ray diffraction (XRD) pattern, $N_2$ adsorption-desorption isotherm, Fourier transform infrared spectrometer (FT-IR), particle size, nitrogen content, sulfur content, and point of zero charge (PZC).

**Phase II: Removal of CFA by SBA-15 and their functionalized at high concentration.**

Adsorption experiments of clofibric acid (CFA) were conducted as batch experiments and the experiments of adsorption were included both of adsorption kinetic and adsorption isotherm. Adsorption kinetic experiments were performed by varying contact time at pH7 with the initial concentration of clofibric acid (CFA) 10 mg/L. The ratio of adsorbent to clofibric acid (CFA) solution was set at 1 g/L. The adsorption kinetic data was analyzed by the pseudo-first-order model, the pseudo-second-order model and intraparticle diffusion model to study adsorption mechanism. Adsorption isotherms experiments were performed by varying concentration of clofibric acid (CFA) solution (6-15 mg/L) and varying pH of solution at 5, 7 and 9. The ratio of adsorbent to clofibric acid (CFA) solution was also set at 1 g/L. The Linear, Langmuir and Freundlich isotherm were considered at this study.

**Phase III: Removal of CFA by an effective functionalized SBA-15 at low concentration.**

Adsorption of clofibric acid (CFA) at low concentration was studied with the most effective adsorbent from **Phase II**. Adsorption isotherms will be performed by varying concentration of clofibric acid (CFA) solution (50-250 µg/L) at pH at treated swine farm wastewater. The ratio of adsorbent to clofibric acid (CFA) solution was set at 1 g/L.

**Phase IV: Removal of CFA in treated wastewater from swine farm.**

Adsorption of clofibric acid (CFA) in the discharge wastewater from wastewater treatment plant (WWTP) of swine farm in Chiang Mai province of Thailand was studied with the most effective adsorbent from **Phase II** at pH of treated wastewater. Before using, water sample was done by fractionation to separate natural organic matter (NOM) that were hydrophobic NOM and hydrophilic NOM. Adsorption isotherm was performed by varying concentration that clofibric acid (CFA) in the discharge wastewater from wastewater treatment plant (WWTP) of swine farm between 6-15 mg/L. The amount ratio of adsorbent to clofibric acid (CFA) solution was set at 1 g/L. The Linear, Langmuir and Freundlich isotherm were considered at this study.

**Phase V: Calculation of mass transfer parameters.**

The mass transfer parameters that were liquid film mass transfer coefficient ($k_f$), solid film mass transfer coefficient ($k_s$), overall solid-phase mass transfer coefficient ($K_s$), overall liquid-phase mass transfer coefficient ($K_f$), and constant diffusivity ($D_s$) were calculated from the results of adsorption kinetic of **Phase II**.

**1.5 EXPECTED OUTCOMES**

1. To suggest the appropriate surface functional groups to enhance the adsorption efficiency of clofibric acid (CFA) in treated swine farm wastewater.

2. Describe adsorption mechanisms between synthetic mesoporous silicates and clofibric acid (CFA) and effect of natural organic matter on adsorption capacity.

3. Report mass transfer parameters for the design of the fixed bed adsorption column.

CHAPTER II

THERETICAL BACKGROUD AND LITERATURE REVIEWS

## 2.1 PHARMACEUTICALS

Recently, pharmaceutical compounds are widely used in large quantities in the farming industry, agriculture, and the treatment of several bacterial infections in humans and animals. In consequence of incomplete metabolism in humans, the disposal of domestic animal, hospital waste, wastewater irrigation, effluent of drug manufacturers and runoff from agricultural fields, they are eventually released into soils, sediments and aquatic environments such as rivers, lakes, streams, and ground waters through different pathways (Figueroa, Leonard, & MacKay, 2004; Halling-Sorensen, Holten Lützhøft, Andersen, & Ingerslev, 2000; T. Heberer, 2002; Loffler et al., 2005). Some researchers reported that even in low concentration pharmaceutical drugs (ranging from μg/L to ng/L) can lead to public health problems (Rosal et al., 2008). Some pharmaceuticals can cause environmental effects such as the development of antibiotic resistant bacteria and endocrine disruption.
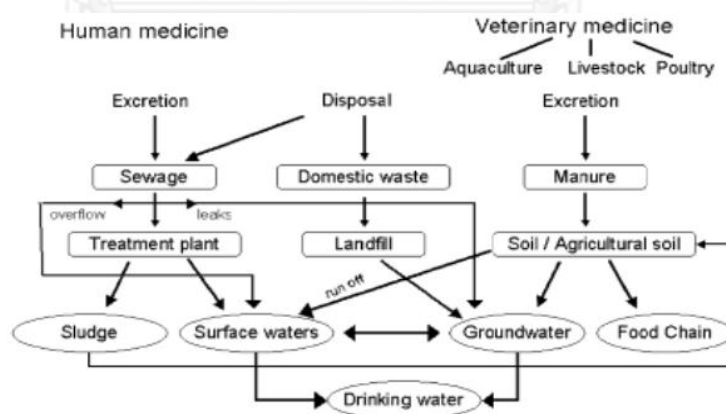


**Figure 2. 1** Origin and routes of pharmaceutical compounds (Diaz-Cruz & Barcelo, 2006)

**Figure 2. 1** shows origin and routes of pharmaceutical compounds that used in human and veterinary medicine (Diaz-Cruz & Barcelo, 2006). The research shows

many classes of pharmaceutically active compounds such as antibiotics, antiepileptic, anti-inflammatory and antiseptic are found in drinking water supplys (Yang, Zheng, Xue, & Lu, 2001), wastewater (Gros, Petrovic, Ginebreda, & Barcelo, 2010), surface water (Kolpin et al., 2002) and ground water (Barnes et al., 2008; Ye, Weinberg, & Meyer, 2007). The occurrence of pharmaceuticals and their active metabolites were reported in groundwater (Lindsey, Meyer, & Thurman, 2001), surface water, suspended solids and sediments (Haller, Muller, McArdell, Alder, & Suter, 2002; Schlusener, Bester, & Spiteller, 2003).

The ecotoxicology of pharmaceuticals found that antibiotic residuals can remain in food products or they can release into the environment by human and animal effluents (Fabrega, Sanchez-Cespedes, Soto, & Vila, 2008). Some pharmaceuticals are resistant to physical and biological treatment (Yang et al., 2001). Therefore, chemical treatment (ozonation and oxidation) (Gogate & Pandit, 2004) and physicochemical treatment such as adsorption (Carabineiro et al., 2011) and membrane filtration have been used for removal of pharmaceutical compounds from wastewater (Yang et al., 2001).

## 2.2 CLOFIBRIC ACID (CFA)

Clofibric acid (CFA), which is the active metabolite of blood lipid regulators or antilipidemic group is one of the most widely used to lower elevated serum lipids by decreasing the low density lipoprotein fraction that has high level in triglycerides (Goodman, Gilman, Rall, Nies, & Taylor, 1990).

**Table 2. 1** Properties of Clofibric acid (CFA)

| Name | Clofibric acid |
|---|---|
| Abbreviations | CFA |
| Formula | $C_{10}H_{11}O_3Cl$ |
| Molecular weight (g.) | 214.5 |
| Log Kow | 2.84 |
| pKa | 3.18 |
| Solubility (mg/L) | 582.5 |
| Functional group | COOH |
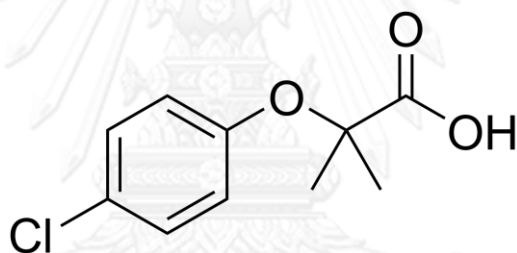


**Figure 2. 2** Molecular structure of clofibric acid (CFA)

Clofibric acid (CFA) is an active derivative substance of clofibrate and fibrates (Cunningham, Binks, & Olson, 2009; Saravanan et al., 2011). Clofibrate can be hydrolyzed into clofibric acid (CFA) by light and oxidation. It can be classified as a plant growth regulator (antiauxin) pesticide and it can be a structural isomer of the herbicide mecoprop that regularly used as a preemergent herbicide in agriculture (Ray, Melin, & B, 2008).

These drugs can release to aquatic environment through excretion via water, domestic waste waters disposal from hospitals, sewage treatment systems, and

runoff from agricultural fields (Kar & Roy, 2010; Rosal et al., 2008; Sanderson et al., 2004). It has been found in surface water, groundwater, effluents of wastewater treatment plant (WWTP), drinking water treatment plants (DWTP) and soils and sediments (Lindsey et al., 2001; Tixier, Singer, & Oellers, 2003; Vazquez-Roig, Segarra, Blasco, Andreu, & Picó, 2009; Westerhoff, Yoon, Snyder, & Wert, 2005). The presence of pharmaceuticals in the environment indicates that pharmaceuticals cannot be removed completely in sewage treatment plants (STPs) (Castiglioni et al., 2006). Moreover, the biological treatment such as activated sludge wastewater treatment plants showed biodegradation efficiency that it cannot remove clofibric acid (CFA) (T. Heberer, 2002), while removal in biological trickling filters was 15% (Stumpf, Ternes, Wilken, Rodrigues, & Bauman, 1999). Therefore, physicochemical process was suggested for water treatment (Boyd, Reemtsma, Grimm, & Mitra, 2003).

Toxicological studies of clofibric acid (CFA) have been found that effect on aquatic species such as an Indian major carp (Cirrhinus mrigala) and a common carp (Cyprinus carpio) (Saravanan et al., 2011; Saravanan & Ramesh, 2013).

The removal of clofibric acid (CFA) by adsorption is one of the most interesting techniques, because of low setup, low operation cost, low area requirements and no production of undesirable by products (Bui, Pham, Le, & Choi, 2013). Activated carbon is the most famous adsorbent because it consistently produces high levels of treatment but disadvantages of the adsorption activated carbon are low selectivity and regeneration. Moreover, the capacity of activated carbon decreases when natural organic matter presented, and the regeneration after use of activated carbon could cause the toxic compound from halogen atom

presented on the molecule of pollutants (Domínguez, González, Palo, & Cuerda-Correa, 2011).

Therefore, the adsorbent that is capable to adsorb the micro-pollutant without limitation in regeneration should be the adsorbent that are modified and developed for the higher selectivity such as silica porous materials.

## 2.3 NATURAL ORGANIC MATTER (NOM)

Natural organic matter (NOM) refers to a group of carbon-based compounds that are found in surface water and groundwater. They are the product of various decomposition of plant and animal residues. NOM composing of aromatic, aliphatic, phenolic, and quinonic structures with various molecular sizes and properties. It can be characterized by separating it into different fractions that can be classified in to the hydrophobic and hydrophilic NOM. Hydrophobic NOM consist poly-aromatic carbon, phenolic functional group and conjugated double bonds moieties in the molecule, while hydrophilic NOM consists higher aliphatic carbon and nitrogenous compound (Matilainen et al., 2011). Therefore, NOM has the possibility to interact with adsorbent and absorbate.

## 2.4 MESOPOROUS SILICA ADSORBENT

Since mesoporous silicas was found in 1992 by Mobil scientists (Tanev & Chibwe, 1994), these materials have widely used in separation, catalysis and adsorption because of their many advantages such as high surface area, large and uniform pore size, tunable pore structure, large pore volume, and tunable surface functional groups, which can improve adsorption capacity and selective adsorption. Dickey has used sol-gel process to synthesize silica based adsorbent that he can control pore size and shape of the inorganic porous materials by molecular imprinting or molecular templating (Dickey, 1949).

There are three steps to prepare amorphous porous material. First step is the synthesis by surfactant template. Second step is the frying process to remove water from materials. Last step is the template removal process. In generally, the reagents that are used in the synthesis are silica source, surfactant template, catalyst and water.

Mesoporous materials SBA-15 which have hexagonal array uniform channel of controlled pore size. In 1998, It has the first report of SBA-15 by Zhoa et al. (Zhao et al., 1998) that is synthesized by surfactant template. SBA-15 is synthesized with triblock copolymers pluronic P123 as a structure directing agent and tetraethyl orthosilicate (TEOS) as the silica source in acid condition. The surfactant head group interacts with inorganic precursor of SBA-15 by hydrogen bonding and electrostatic attraction.

## 2.5 ADSORBENT SURFACE MODIFICATION

The modification of porous material by the organic functional groups of the active sites of silica walls can be applied in many fields such as adsorption, nanotechnology, and biology. There are two methods to functionalize, the post method or grafting and the direct method or co-condensation.

### 2.5.1 Post synthetic or grafting method

The post synthetic or grafting method has two steps. The first step is synthesis of mesoporous materials. The second step is grafting an functional group onto the surface under reflux condition with appropriate solvent. Mesoporous silicates silanol (Si-OH) groups that act as active site to form a layer of covalently coupled surface functional groups (Stein, Melde, & Schroden, 2000). Advantage of this method is good preservation of their structure after post-grafting, but limited the

functional groups that are grafted due to the density of reactive silanols on surface are limited.
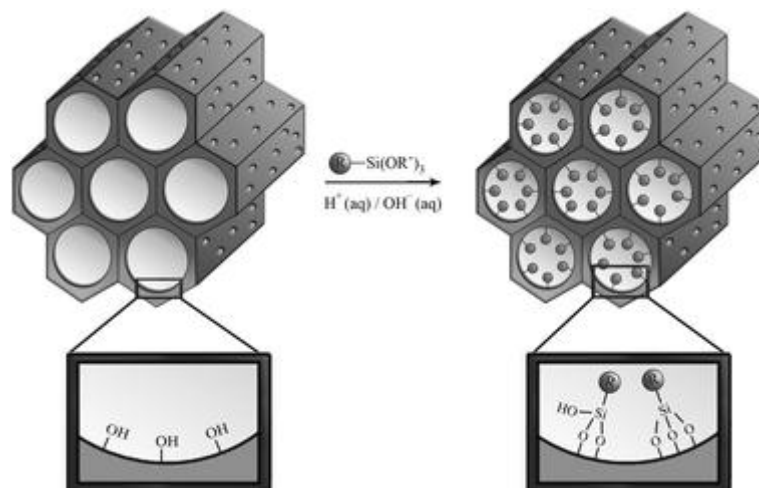


**Figure 2. 3** Functionalization of mesoporous silicates by post grafting (Van Der Voort, Vercaemst, Schaubroeck, & Verpoort, 2008)

## 2.5.2 Co-condensation method or direct synthesis

The co-condensation or direct synthesis method is the method that the functional groups are added during the synthesis to the surfactant template. Advantages of this method are high uniform surface coverage of functionality, but loss in original structure and poor control of functional group on the surface (Hoffmann, Cornelius, Morell, & Froba, 2006).
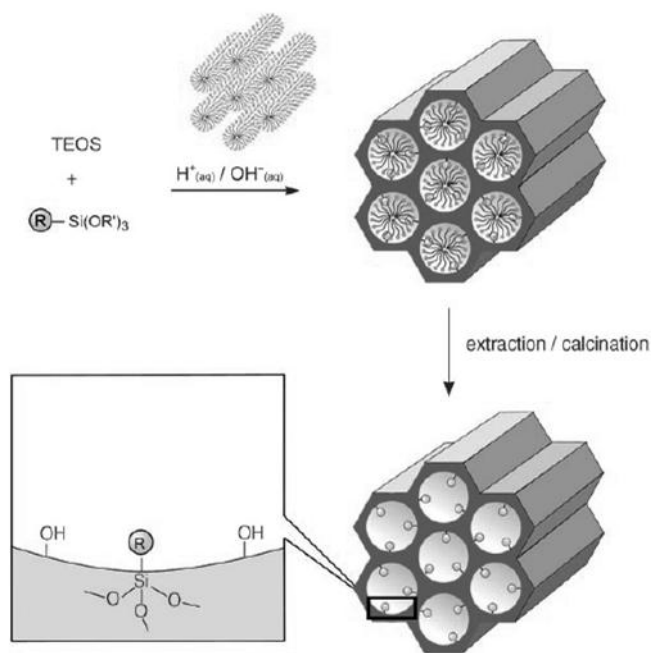
**Figure 2. 4** Co-condensation method for the modification of mesoporous, R= organic functional group (Hoffmann et al., 2006)

## 2.6 ADSORPTION THEORY

Adsorption is a fundamental process in the physicochemical treatment that attracts and retains the molecules of a substance on the surface of a liquid or a solid. The substance that adsorbed on the surface is usually described as the adsorbate, while the substance that is absorbed is usually described as adsorbent.

### 2.6.1 Types of adsorption

Types of adsorption depending on the nature of forces that exist between adsorbate and adsorbent that the adsorption can be divided into two types.

### *2.6.1.1 Physical adsorption (physisorption)*

Physisorption or physical adsorption that involves the balancing of a weak attractive force between adsorbate and adsorbent and is associated with van der Waals-type interactions. This process is always exothermic and energy given out on

adsorption. Because of the weak force of attraction, this type can be reversed by heating or reducing the driving force such as concentration.

### 2.6.1.2 Chemical adsorption (chemisorption)

Chemisorption or chemical adsorption describes the adsorption which a strong chemical bond between the surface and the adsorbate. It has the exchange of electrons between the adsorbing molecule and the surface. In chemisorption the force of attraction is very strong, so adsorption can be difficultly reversed.

### 2.6.2 Adsorption phenomena

In the adsorption mechanism of solid-liquid adsorption has three steps (Albadarin et al., 2012). The first step is film diffusion process that presents the transport of adsorbate to external surface of adsorbent. The second step is intraparticle diffusion process that presents the diffusion of adsorbate to an adsorption site through the liquid filled pore. The last step is adsorption process that presents the adsorption of the adsorbate to a site (internal or external) on the surface of the adsorbent. Normally, the last step is very fast when compared with other steps, so it can be considered negligible. Therefore, the rate limiting step can be film diffusion or intraparticle diffusion.
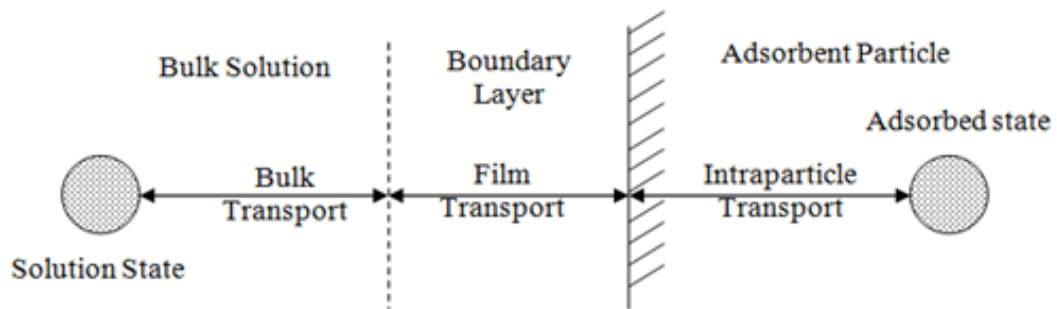
Figure 2. 5 The Steps of mass transfer of adsorption
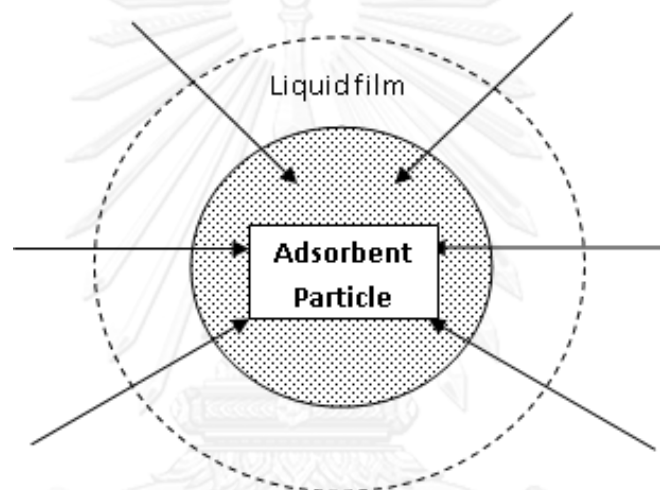


Figure 2. 6 Schematic of adsorbent particle (Cooney, 1998)

## 2.6.3 Adsorption kinetic

Kinetics is concerned about a system gets from an initial state to final state and the time required for the transition, hence it gives ideal about the mechanism of adsorption (Abechi, Gimba, Uzairu, & Kagbu, 2011).

### 2.6.3.1 The pseudo-first-order model

Adsorption kinetics of pharmaceuticals was examined using the first-order model as **Equation 2.1** (Lagergren, 1898)

$$\ln(q_e - q_t) = \ln q_e - k_1 t \qquad (2.1)$$

Where $k_1$ is the pseudo-first-order rate constant (mg/g) and $q_t$ is amounts of adsorbate (mg/g) at time $t$ (min). When plot between $\ln(q_e - q_t)$ and t, the values of $q_e$ and $k_1$ are calculated from the intercept and slope, respectively.

### 2.6.3.2 The pseudo-second-order model

The pseudo-second-order model can be presented in the following form (Ho & Mckay, 1999) that shows in **Equation 2.2.**

$$\frac{t}{q_t} = \frac{1}{k_2 q_e^2} + \frac{t}{q_e}$$
(2.2)

Where $k_2$ is the pseudo- second-order rate constant (g/mg.min). Moreover, the initial adsorption rate can also be obtained from this model as **Equation 2.3.**

$$h = k_2 q_e^2$$
(2.3)

Where $h$ is the initial sorption rate (µg/g.min).

### 2.6.3.3 Intraparticle diffusion model

Weber and Morris had presented the intraparticle diffusion model in 1962 that is used to predict the rate-controlling step in an adsorption process for understanding the mechanism of the sorption (Weber & Morris, 1962). The intraparticle diffusion equation can be expressed as **Equation 2.4.**

$$q_t = k_i t^{1/2} + C$$
(2.4)

Where $q_t$ is the amount of adsorbate adsorbed (mg/g) at time $t^{1/2}$ (min$^{1/2}$), $k_i$ is the intraparticle diffusion rate constant (mg/g.min$^{1/2}$) and $C$ is the interception, which can be determined from the plot of $q_t$ versus $t^{1/2}$.

### 2.6.4 Mass transfer

Adsorbent particle has liquid film that adsorbate will transport through liquid film in adsorption. Mass transfer will occur when concentration of solution is different that a high concentration will diffuse to a low concentration. Mass transfer through liquid film is depended on mass transfer resistance that if mass transfer resistance decreases, it means that adsorbate can transfer through liquid film easily. Mass transfer through liquid film can write in rate law that calls "Linear driving force" (LDF) as shown **Equation 2.5**.

$$\frac{\partial \overline{q}}{\partial t} = k_f S_0 (C - C_i) \tag{2.5}$$

$\overline{q}$ is the average solute concentration in solid (M/V). $C$ is the concentration of the solute in bulk solution (M/V). $C_i$ is the concentration of solute in liquid interface (M/V). $S_0$ is the surface area of particle per unit volume of adsorbent (M/V) and $k_f$ is the liquid film mass transfer coefficient (L/T).

Mass transfer through particle pore can describe by "Homogeneous solid diffusion model" (HSDM) that has Diffusivity ($D_s$) as shown in **Equation 2.6**.

$$\frac{\partial q}{\partial t} = \frac{D_s}{r^2} \frac{\partial}{\partial r} (r^2 - \frac{\partial q}{\partial r}) \tag{2.6}$$

$r$ is the radial position (L) and $D_s$ is constant diffusivity (L$^2$/T). Crank presents the solution to solve **Equation 2.6** that can be rewritten in **Equation 2.7** (Crank, 1956)

$$\frac{\overline{q}}{q_\infty} = 6 \left( \frac{D_s t}{R^2} \right)^{1/2} \left[ \pi^{1/2} + L \right] \tag{2.7}$$

The slope of a plot between $\dfrac{\overline{q}}{q_\infty}$ and $t^{1/2}$ is $6 \left( \dfrac{D_s}{\pi R^2} \right)^{1/2}$ that can calculate $D_s$ from the slope value and $q_\infty$ is average solute concentration in solid at infinite time.

Mass transfer through solid film can write in rate law that calls "Linear driving force" (LDF) as shown in **Equation 2.8**.

$$\frac{\partial \overline{q}}{\partial t} = k_s S_0 (q_i - \overline{q})$$  (2.8)

$q_i$ is the solid concentration at interface (M/V) and $k_s$ is the solid film mass transfer coefficient (L/T).

The presence of Overall solid-phase mass transfer coefficient ($K_s$) can be rewritten as **Equation 2.9.**

$$\frac{\partial \overline{q}}{\partial t} = K_s S_0 (q_e - \overline{q})$$  (2.9)

$K_s$ is Overall solid-phase mass transfer coefficient and $q_e$ is value of $q$ at equilibrium (M/V).

$$\frac{1}{K_s} = \frac{m}{k_f} + \frac{1}{mk_s}$$  (2.10)

$m$ is slope of a plot between $q$ and $C$. In case of the presence of Overall liquid-phase mass transfer coefficient ($K_f$) can be rewritten as **Equation 2.11**.

$$\frac{\partial \overline{q}}{\partial t} = K_f S_0 (C - C_e)$$  (2.11)

$C_e$ is value of $C$ at equilibrium (M/V).

$$\frac{1}{K_f} = \frac{1}{k_f} + \frac{1}{mk_s}$$  (2.12)

According to **Equation 2.10** and **2.12**, it has relationship between $K_s$ and $K_f$ as **Equation 2.13**.

$$K_f = mK_s$$  (2.13)

The design of the fixed bed adsorption column have to use of the mass transfer parameters that are $k_f, k_s, K_s, K_f$, and $D_s$ to predict and calculate breakthrough curve follow the mass transfer models.

## 2.6.5 Adsorption Isotherm

Adsorption isotherm study is the study of adsorption capacity of the adsorbent at equilibrium state at the different initial concentration. Adsorption isotherms are plots between the amount of solute retained per mass unit of the solid adsorbent at equilibrium ($q$) and the equilibrium concentration of solute remaining in the solution at constant temperature ($C_e$). The adsorption capacity, $q$ (mg/g), can compute by **Equation 2.14.**

$$q = \frac{(C_0 - C_e)V}{W} \tag{2.14}$$

Where $C_0$ is the initial concentration of the adsorbate (mg/L), $C_e$ is the concentration of adsorbate at equilibrium (mg/L), $V$ is a volume of the solution (L), and $W$ is the weight of adsorbent (g).The adsorption isotherm relationship can also be mathematically expressed and can predict and evaluate the efficiency of adsorption process. Linear, Langmuir and Freundlich isotherm are applied to use for describing the adsorption of pharmaceuticals onto mesoporous adsorbents.

### 2.6.5.1 The Linear Isotherm

Linear isotherm is the equation that shows the relationship between concentration of adsorbate and the amount of absorbate that was adsorbed at equilibrium. The linear form of the Linear isotherm is given by **Equation 2.15**.

$$q_e = K_P C_e \tag{2.15}$$

$q_e$ is the amount of adsorbate adsorbed at equilibrium (mg/L) and $K_p$ is the Linear constant (L/mg). $C_e$ is the concentration of adsorbate at equilibrium (mg/L).

### 2.6.5.2 The Langmuir Isotherm

In 1916 Irving Langmuir proposed another adsorption isotherm known as Langmuir adsorption isotherm. The linear form of the Langmuir isotherm is given by **Equation 2.16** (Langmuir, 1916).

$$\frac{1}{q_e} = \frac{1}{K_L q_m C_e} + \frac{1}{q_m} \tag{2.16}$$

Where $q_m$ defines the maximum adsorption capacity (mg/g), $q_e$ is the amount of adsorbate adsorbed at equilibrium (mg/L) and $K_L$ is the Langmuir constant (L/mg).

### 2.6.5.3 The Freundlich Isotherm

Freundlich presented an empirical expression that present the isothermal variation of adsorption of a quantity of adsorbate adsorbed by unit mass of adsorbent with pressure. **Equation 2.17** described the Freundlich isotherm.

$$q_e = \frac{x}{m} = K_f C_e^{1/n} \tag{2.17}$$

Where $X$ is the mass of the adsorbate adsorbed on mass $m$ of the adsorbent, $C_e$ is equilibrium concentration of adsorbate, $K_f$ and $n$ are constants whose values depend upon adsorbent and adsorbate at particular temperature.

Freundlich model can be linearized by plotting it in a log-log format as **Equation 2.18.**

$$\log q_e = \log K_{fr} + \frac{1}{n} \log C_e \tag{2.18}$$

Where $K_{fr}$ is the Freundlich constant and n is the adsorption intensity (dimentionless).

## 2.7 LITERATURE REVIEWS

### 2.7.1 Pharmaceuticals

The pharmaceutical residues are frequently found in the environment. Many researchers reported the occurrence of pharmaceuticals in surface water, ground water, sediments and suspended solids. The literature showed that they found two pharmaceutical compounds (sulfonamides and tetracyclines) in ground water were detected in unit of microgram per liter (Lindsey et al., 2001). In soil and sediment was measured animal-origin pharmaceuticals in manure were reported that two sulfonamides (sufamethazine and sulfathiazole) were detected in the range 0.10–12.4 µg/kg (Haller et al., 2002). The other research found that two antibiotics (macrolides, ionophore polyethers) in soil had the concentration at 11 and 43 µg/kg of tiamulin and salinomycin, respectively (Schlusener et al., 2003). Surface water was analyzed from two lakes in India. In the two lakes, the high concentrations of ciprofloxacin (up to 6.5 mg/L), cetirizine (up to 1.2 mg/L), norfloxacin (up to 0.52 mg/L), and enoxacin (up to 0.16 mg/L) were also found (Fick et al., 2009).

The ecotoxicology of pharmaceuticals found that the human population can be infected by resistant bacteria from animals by food products of animal or direct contact. Finally, antibiotic residuals can remain in food products or they can be released into the environment by effluents of animal and human (Fabrega et al., 2008).

Some pharmaceuticals are resistant to physical and biological treatment (Yang et al., 2001). Therefore, chemical treatment (ozonation and oxidation) (Gogate

& Pandit, 2004; Pocostales, Álvarez, & Beltrán, 2011) and physicochemical treatment such as adsorption (Carabineiro et al., 2011) and membrane filtration have been used for removal of pharmaceutical compounds from aqueous solution and wastewater (Yang et al., 2001). For experiment of ozonation shows that degradation efficiency of enrofloxacin (ENR) are 99.5% (Li, Zhang, Liang, & Yediler, 2013) and use of Fenton and photo-Fenton processes can achieve a degradation efficiency of 91% by Fenton oxidation and 100% by photo-Fenton. The treatment of pharmaceuticals (cyclophosphamide and ciprofloxacin) has been investigated by using a nanofiltration membrane bioreactor (NF-MBR) in concentration of 6–143 ng/L for cyclophosphamide and 249–405 ng/L for ciprofloxacin from treatment plants (WWTP).

### 2.7.2 Adsorption of pharmaceuticals

Adsorption is a well-known equilibrium separation process and it is most widely used for removal contaminated wastewater. Several studies have been used adsorption for removal pharmaceuticals by using different absorbent such as zeolites activated carbon, montmorillonite and mesoporous silica. Adsorption of pharmaceuticals by silica based porous material has been used to removal pharmaceutical compounds.

Punyapalakul and Sitthisorn studied the removal of Carbamazepine (CBZ) and Ciprofloxacin (CIP) by HMS and functionalized HMSs in the concentration ranged from 6-9 mg/L (Punyapalakul & Sitthisorn, 2010). They discovered that their adsorbents can remove targeted compounds due to hydrophobicity and hydrogen bonding. The results showed that the adsorption capacities of adsorbents were lower than PAC. They found that the adsorption kinetics and isotherms results were fitted well with

pseudo-second order model and Langmuir isotherm, respectively. The pH values affected the adsorption capacities because of hydrogen bonding between adsorbate and adsorbent.

Minmin Liu studied the adsorption of tetracycline (TC) from aqueous solution on zeolite A modified MCM-41 (A-MCM-41) in the concentration ranged from 100-500 mg/L (Liu et al., 2013). They found that after modification the adsorption capability of A-MCM-41 increased dramatically. The pH effects on TC adsorption had higher adsorption performance in acidic and neutral condition. The adsorption isotherms and the adsorption kinetics were fitted with Langmuir isotherm and both of pseudo second order equation and the intra-particle diffusion model, respectively.

Nakorn Suriyanon studied the adsorption of diclofenac and carbamazepine on hexagonal mesoporous silicate (HMS), and functionalized HMS with the amine and mercapto (A-HMS and M-HMS, respectively) that were compared with SBA-15 and MCM-41 plus powdered activated carbon (PAC) (Suriyanon, Punyapalakul, & Ngamcharussrivichai, 2013). They found that adsorption mechanism depended on surface functional groups, pH and temperature. The adsorption kinetic and isotherm were followed a pseudo-second order kinetic model and a linear isotherm, respectively. The adsorption capacity was increased for DCF and CBZ due to increased hydrogen bonding and hydrophobic interactions when using M-HSM. The highest adsorption capacities of M-HMS, A-HMS and HMS were pH 5, because the electrostatic interactions and hydrogen bonding at this pH. M-HMS was endothermic and spontaneous in nature for thermodynamic analysis. The molecular size of the adsorbate might be related to the adsorption capacity of adsorbent.

### 2.7.3 Clofibric acid (CFA)

Clofibric acid (CFA), which is the active metabolite of blood lipid regulators that used to lower elevated serum lipids. It can release to environment by many pathways such as domestic wastewaters, effluents from hospital, sewage treatment systems, and runoff from agricultural fields.

### *2.7.3.1 Occurrence of clofibric acid (CFA)*

It has been found pharmaceuticals in surface water, groundwater, and conventional sewage treatment. Clofibric acid (CFA) was measured in ground water samples at concentrations 7.3 µg/L (T. Heberer, Butz, & Stan, 1995). It has been found in surface waters of Swiss lakes in 0.55 µg/L (Buser, Müller, & Theobald, 1998). It was also reported in the effluent of wastewater treatment plant (WWTP) in the concentrations reached 0.06 mg/L (Tixier et al., 2003). In drinking water treatment plants (DWTP), clofibric acid was also observed (Westerhoff et al., 2005). The presence of pharmaceutical compounds indicate that these contaminants cannot be removed completely in sewage treatment plants (STPs) (Castiglioni et al., 2006). In Berlin, it also detected clofibric acid (CFA) in drinking water samples at concentrations in 0.3 µg/L (Rosal, Rodríguez, & Gaecia-Calvo, 2009) and also detected in soils and sediments in 35.62 µg/kg (Vazquez-Roig et al., 2009).

### *2.7.3.2 The ecotoxicology of clofibric acid (CFA)*

Additionally, toxicological studies have been showed that clofibric acid (CFA) affected to aquatic species. The study of chronic effect that shows in **Figure 2. 7**, the following NOEC were found for clofibric acid (CFA) in *C. dubia* [NOEC (7 days) = 640 µg/L], the rotifer *B. calyciflorus* [NOEC (2 days) = 246 µg/L], and in early life stages of zebrafish [NOEC (10 days) = 70 mg/L] (Ferrari, Paxéus, Giudice, Pollio, & Garric, 2003).

The literature reported acute toxicity that shows in **Figure 2. 8** at different concentrations of clofibrate and clofibric acid (CFA) that affect to aquatic organisms; for example, clofibrate indicated LC50 values in the range of 7.7-39.7 mg/L that can harm to the fish Gambusia holbrooki at 96 h (Fent, Weston, & Caminada, 2006).

The investigation of study indicated that clofibric acid (CFA) caused of changing biochemical and ionoregulatory responses of an Indian major carp *(Cirrhinus mrigala* ) at concentration 1, 10 and 100 µg/L (Saravanan & Ramesh, 2013) and in a common carp (*Cyprinus carpio*) was investigated on the toxic effects of CFA at concentrations 1, 10 and 100 µg/L for a short term period of 96 hr. The results showed that in fish treated with CFA, red blood cell (RBC), plasma sodium ($Na^+$), potassium ($K^+$), and glutamate oxaloacetate transaminase (GOT) levels were decreased (Saravanan et al., 2011).
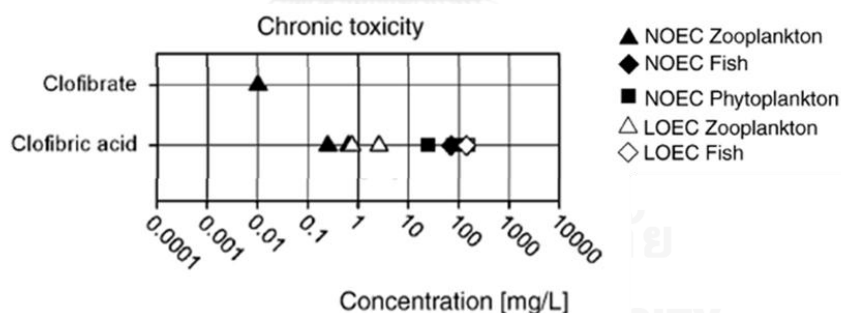


**Figure 2. 7** Chronic toxicity of clofibrate and clofibric acid (CFA) to aquatic organisms

(Fent et al., 2006)
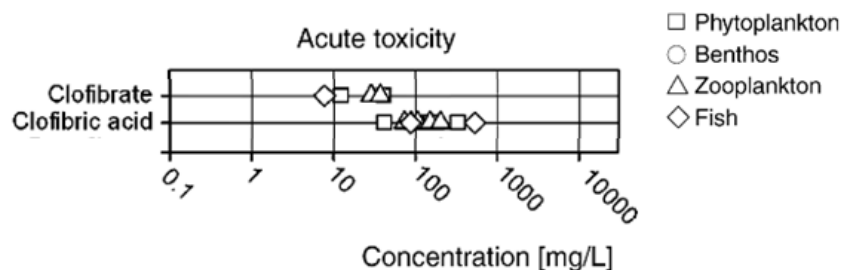
**Figure 2. 8** Acute toxicity of clofibrate and clofibric acid (CFA). EC50 and LC50 for different organisms and different endpoint and exposure time (Fent et al., 2006)

### 2.7.3.3 The removal of clofibric acid (CFA)

The conventional wastewater treatment such as municipal STPs that consists of the steps mechanical pre-treatment (homogenisation, removal of solids), preliminary treatment (addition of flocculation agents), primary sedimentation and biological treatment (aerobic nitrification, anaerobic denitrification and phosphate removal) can remove clofibric acid (CFA) 27.7%. However, researchers reported the effective removal of clofibric acid (CFA) by the membrane bioreactor (MBR) that can remove 71.8% (Radjenovic, Petrovic, & Barcelo, 2007). Although membrane filtration has a good percentage of removal, their limitations in its applicability for chemical behavior have been reported in the real full-scale treatment system. The membranes can be fouled during the operation by generating precipitated chemicals or the growth of microbial. Physicochemical properties of the membrane surface were changed when the system was fouling that affect the separation mechanisms such as size and electrostatic interactions.

In some studies used ozonation and especially advanced oxidation processes is the effective treatment by using $O_3/H_2O_2$ molar ratio ($O_3/H_2O_2$) = 2:1. The results showed the removal of 50%-90% (Ternes et al., 2002; Zwiener & Frimmel, 2000). Some literatures found that ozonation at a small ozone dose of 0.5 mg/L, the concentrations of clofibric acid (CFA) were decreased by only 10-15%. Nevertheless,

ozonation is the formation of by products that may be more harmful than the parent substances (Thomas & Adriano, 2006)

Removal of clofibric acid (CFA) by adsorption is one of the most interesting techniques, because of its simplicity, low area requirements, low operation cost, low set up and no production of undesirable by products (Bui et al., 2013). Activated carbon is the most famous adsorbent because it consistently produces high levels of treatment and has a high degree of stability and reliability. Although activated carbon presented efficient removal of hydrophobic pharmaceuticals, but inefficient removal for hydrophilic pharmaceuticals has been observed. However, disadvantages of the adsorption activated carbon are low selectivity and regeneration since the thermal regeneration of PAC after used could cause the toxic compound from halogen atom presented on the molecule of pollutants. Moreover, the capacity of activated carbon extremely decreases when natural organic matter presented, and the regeneration of these adsorbents is questionable (Domínguez et al., 2011). Therefore, the adsorbent that is capable to adsorb the micro-pollutant without limitation in regeneration should be developed or explored to handle with pharmaceutical residues and the surface of the adsorbent should be modified and developed for the higher selectivity such as silica porous materials.

### 2.7.3.4 Adsorption of clofibric acid (CFA) by silica based porous materials

Mesoporous silica such as HMS, MCM-41, MCM-48, and SBA-15 are widely used because of its advantages such as uniform structure and high surface area (up to 1000 $m^2$/g).

Tung Xuan Bui studied the adsorption of mixture pharmaceuticals by using SBA-15 in concentration of solution 10-300 μg/L (Bui & Choi, 2009). The rate removal

adsorptions of pharmaceuticals were achieved in acidic media (pH 3–5). At pH 3, carbamazepine reached 85.2%, 88.3% for diclofenac, 93.0% for ibuprofen, 94.3% for ketoprofen, and 49.0% for clofibric acid (CFA). On the other hand, it decreased with increase in pH. Moreover, SBA-15 and mesoporous silica-based materials can be regenerated without loss by combustion because of stability of mesoporous silica structure up to 850 °C. Based on results, hydrophilic interaction was the mechanism of the selected pharmaceuticals. This study suggest that SBA-15 can also remove pharmaceuticals from wastewater of pharmaceutical manufactures.

Two years later, Tung Xuan Bui studied the adsorption of pharmaceuticals by using SBA-15 and three grated SBA-15 (hydroxymethyl group (HM-SBA-15), aminopropyl group (AP-SBA-15), and trimethylsilyl (TMS-SBA-15) in initial concentration of approximately 100 μg/L (Bui et al., 2011). They found that acidic compounds in cases of clofibric acid (CFA) and diclofenac may prefer for adsorption onto AP-SBA-15. THM-SBA-15 had the highest adsorption capacities than SBA-15 that showed seven compounds, including carbamazabine, diclofenac, estrone, gemfibrozil, ibuprofen, ketoprofen, and trimethoprim, had the adsorption percentage as 70.6–98.9% onto TMS-SBA-15 except clofibric acid (CFA) at pH 5.5. They suggested that TMS-SBA-15 may be adsorbent for removal of pharmaceuticals from drug manufacturers wastewater and TMS-SBA-15 can regenerate.

## 2.7.4 Natural organic matter (NOM)

Natural organic matter (NOM) refers to a group of carbon-based compounds that consist of aliphatic, aromatic, phenolic, and quinonic structures with varying molecular sizes and properties. Pharmaceuticals are usually found in the environment in low concentration (ng/L to μg/L); however, it also contains natural

organic matter (NOM), which higher concentration (mg/L) than pharmaceutical compounds. Therefore, NOM will have effect on the adsorption of pharmaceuticals.

### 2.7.4.1 Effect of NOM on pharmaceutical adsorption

In 2012, Ridder studied influence of natural organic matter (NOM) on adsorption of neutral and charged pharmaceuticals onto activated carbon. The result indicated that NOM can influence pharmaceutical adsorption by two mechanisms that were direct adsorption competition and pore blocking onto granular activated carbon (GAC). Moreover, the higher hydrophobicity of NOM, indicating that competition of NOM might influence adsorption ability more than pore blocking (Ridder et al., 2011). The other literatures showed the adsorption of pharmaceuticals to another adsorbent that was silica. Tung Xuan Bui studied the influence of natural organic matter (NOM) on the adsorption of pharmaceuticals to silica (Bui & Choi, 2010). These results suggest that NOM can affect the adsorption of pharmaceuticals and thus the ultimate fate of pharmaceuticals in the aqueous environment. Moreover, the adsorption of pharmaceuticals was reduced when NOM presented except for diclofenac.

### 2.7.4.2 Interaction between NOM and pharmaceuticals

Dissolved organic matter (DOM) is the dissolved fraction of the NOM in natural water. Interactions between DOM and PPCPs can detect and quantify of these compounds (Lajeunesse & Gagnon, 2007).

Many literature studied interaction between PPCPs and DOM. In 2008, Bai studied interaction between carbamazepine and humic substances (HS) by using a fluorescence spectroscopy (Bai et al., 2008). They used a landfill leachate in their

study. The result showed that hydrophobic adsorption or partitioning might be the major force for carbamazepine binding to HS.

The other literature studied interaction between PPCPs and DOM that they hypothesized that the types of bonding form between PPCPs and DOM depended on physico-chemical properties of both DOM and PPCPs (Hernandez-Ruiz, Abrell, Wickramasekara, Chefetz, & Chorover, 2012). In the experiment they used fluorescence spectroscopy to investigate DOM-PPCP molecular interaction, and tandem mass spectrometry to measure DOM affected on analysis of quantification. Log $K_{ow}$ was used to predict that hydrophobic interactions were important, while polar functional groups may in fact mediate association between ionized chemicals and oxygen containing DOM moieties (Pan, Ning, & Xing, 2009). Hydrogen bonding, ¶–¶ and van der Waals interactions were predominately interaction between carbamazepine and DOM (Navon, Hernandez-Ruiz, Chorover, & Chefetz, 2011). Prior research has suggested that hydrophobic interactions may be the key role the partitioning of PPCP contaminants to dissolved organic matter. (Pan et al., 2009).

## 2.8 CONCLUSION

The literature reviews show that there are a few studies on removal pharmaceutical residues by adsorption on SBA-15 and their functionalized. The studies by Bui et al. have been related with this research that they study adsorption of CFA onto SBA-15 and modified SBA-15 (Bui & Choi, 2009; Bui et al., 2013). The literature review shows that modified SBA-15 with amino functional group has higher CFA adsorption than SBA-15 because of acid-base and hydrophilic interaction (pKa = 3.81 as acidic pharmaceutical and log $K_{ow}$ = 2.84 as hydrophilic compound), so in the presence of higher density of amino group such as tri-amino may cause the higher

adsorption capacity than mono-amino group. Therefore, in this research SBA-15 will be modified by tri-amino (hydrophilic) and mercapto group (hydrophobic) to improve adsorption capacities of adsorbents.

In this research, the treated wastewater sample will be used as background water sample which is representative of NOM in surface water. NOM are supposed to affect adsorption capacity of CFA. The study of Ridder mentions that NOM can influence pharmaceutical adsorption by two mechanisms that are direct adsorption competition and pore blocking onto adsorbent (Ridder et al., 2011). Moreover, Navon studies NOM can interact with pharmaceuticals by hydrogen bonding, ¶–¶ and van der Waals interactions (Navon et al., 2011). From the literature reviews show that surface modification of SBA-15 and the presence of NOM can affect to adsorption capacity of CFA, so in this research will investigate the effect of surface functional groups and NOM on CFA adsorption by mesoporous silicate SBA-15 to adsorption efficiency of CFA.

CHAPTER III

MATERIALS AND METHODS

## 3.1 MATERIALS

### 3.1.1 Chemical Reagents

| | | | |
|---|---|---|---|
| 1. | Acetone | HPLC | LAB SCAN |
| 2. | Acetonitrile | HPLC | LAB SCAN |
| 3. | Clofibric acid (CFA) | 97% | Sigma Aldrich |
| 4. | Dipotassium hydrogenphosphate | >97% | Ajax Finechem |
| 5. | Ethyl alcohol absolute | RPE-ACS | CARLO ERBA |
| 6. | Hydrochloric acid | 37% | CARLO ERBA |
| 7. | Sodium hydroxide | 99% | MERCK |
| 8. | Sodium chloride | 99.5% | CARLO ERBA |
| 9. | Tetraethoxysilane (TEOS) | 98% | Fluka |
| 10. | Toluene | 98% | LAB SCAN |
| 11. | 3-(trimethoxysilyl)-propyl)diethylenetriamine | >98% | Fluka |
| 12. | 3-mercaptopropyltrimethoxysilane | >98% | Fluka |
| 13. | Methanol | HPLC | LAB SCAN |
| 14. | Nitrogen gas | 99.5% | Praxair |
| 15. | Pluronic P123 | | |
| 16. | Powdered activated carbon | | ShirasakiS-10 enviroChemicals, Ltd. |
| 17. | Potassium dihydrogenphosphate | >99.5% | Volchem |

### 3.1.2 Laboratory Equipment

1. High Performance Liquid Chromatography (HPLC) (Varian, Prostar, USA)

2. Column C18 (C18 4.6 x 250 mm (5 μm), GLS Science, USA)

3. Solid Phase Extraction (SPE)

4. C18 Cartridge (500mg/3 ml) Cleanert ODS-SPE

5. Oasis HLB Cartridge (6ml, Water Corporation, USA)

6. Syringe filter (Nylon, 0.45 μm, 13 mm, Chrom Tech)

7. Membrane filter (Nylon, 0.45μm, 47 mm, )

8. Membrane filter (Cellulose acetate, 0.45μm, 47 mm, Hyper Fil)

9. Glass Microfiber filters (GF/C, 0.12 μm, size 25 mm, Whatman)

10. Filter papers (Qualitative 1, 90 mm, Whatman)

11. Magnetic stirrer (REXIM RS-6D, AS ONE)

12. Balance 4 digit (Pioneer, OHAUS)

13. Vacuum filtration apparatus

14. Vacuum pump

15. Oven (ED/FD, Binder)

16. Fume hood

17. Muffle furnace

18. Thermometer

19. pH meter (Hach, Sension2)

20. TDS meter (Amtast, Con900)

### 3.1.3 Treated wastewater sample

In this study, discharged wastewater from wastewater treatment plant (WWTP) of swine farm in Chiang Mai province of Thailand was applied as a

background sample of this study which is representative of NOM in wastewater. Natural organic matter (NOM) in wastewater sample was separated hydrophilic and hydrophobic portion by fractionation. And CFA was dissolved in water sample in concentration 100 mg/L as stock solution stored at 4°C prior to use.

**Table 3. 1** Measured parameters for treated wastewater sample

| Parameters | Instruments |
|---|---|
| pH | pH meter |
| Dissolve organic carbon | Total organic carbon analyzer |

## 3.2 METHODOLOGY

The experimental frame work of this research is shown in **Figure 1. 1**. The detail of this study was divided into 5 phases.

### 3.2.1  Phase I: Synthesis and characterization of SBA-15 and their functionalized.

#### *3.2.1.1 Preparation of adsorbents*

SBA-15 was synthesized in acidic condition by using pluronic P123 as a structure directing agent and TEOS as silica source (Zhao et al., 1998). Pluronic P123 4 g. was dissolved in 2.73 g. of HCl 37 % and 116.28 g. of deionized water in a 250 mL beaker with stirring. The homogeneous solution was heated to 40 °C before adding drop wise 8.52 g. of TEOS under stirring. The resulting gel was aged at 40 °C for 24 hr. and finally was transferred into hydrothermal bottle then was aged at 100 °C for 24 hr. The product was filtered and was washed thoroughly with deionized water. The obtained solid precipitate was dried at room temperature overnight. To remove surfactant, the material was calcined at 550 °C for 5 hr.

### 3.2.1.2 Functionalization of SBA-15

*3.2.1.2.1 3-(trimethoxysilyl)-propyl)diethylenetriamine grafting procedure*

Modification of SBA-15 by 3-(trimethoxysilyl)-propyl)diethylenetriaminewas prepared by post-grafting method and was applied from literature (Punyapalakul & Sitthisorn, 2010). Firstly, calcined SBA-15 4 g. was pretreated at 150 ℃ for 20 hr. The pretreated SBA-15 was added in toluene 57.5 mL and 3-(trimethoxysilyl)-propyl)diethylenetriamine was added 2.6 g. under stirring at 150 rpm for 24 hr. Reactions were kept at room temperature. After reaction, the product was filtered and was washed with toluene. Finally, the sample was dried at 150 ℃ for 4 hr. and was stored in desiccator. The functionalized sample was named as 3N-SBA-15.
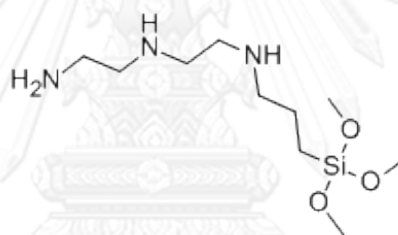


**Figure 3. 1** 3-(trimethoxysilyl)-propyl)diethylenetriamine

*3.2.1.2.2 3-mercaptopropyltriethoxysilane grafting procedure*

Modification of SBA-15 by 3-mercaptopropyltriethoxysilanewas prepared by post-grafting methods and was applied from literature (Hongsawat, Prarat, Ngamcharussrivichai, & Punyapalakul, 2013). Firstly, 1 g. calcined SBA-15 was dehydrated at 105 $^{\circ}$C in an oven for 24 hr., and then stirred in 60 mL of toluene containing 2 g. of 3-mercaptopropyltriethoxysilane under refluxing conditions for 24 hr. The product was filtrated, and then was washed with toluene. Finally, the product was dried at 85 $^{\circ}$C for 2 hr.
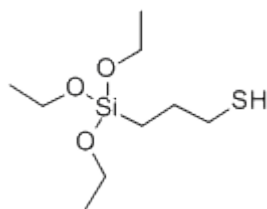
**Figure 3. 2** 3-mercaptopropyltriethoxysilane

*3.2.1.3 Characterization of SBA-15 and funtionalized SBA-15*

**Table 3. 2** Characterization of SBA-15 and functionalized SBA-15

| Parameter | Measurement |
|---|---|
| Silica porous structures | X–Ray Diffractometer<br>(Broker AXS Model D8 Discover) |
| $N_2$adsorption-desorption isotherms | Surface Area Analyzer<br>(Autosorb-1 Model Thermo Finnigan) |
| The presence of surface functional groups | Fourier Transform Infrared Spectrometer (FT-IR)<br>(Perkin Elmer Model Spectrum One) |
| Point of zero charges (PZC) | Acid-base titration method |
| Amount of S and N | Elemental analyzer<br>(LECO Model CHNSO) |
| Particle size distribution | Laser Particle Size Distribution Analyzer (MALVERN Model Mastersizer S) |

**3.2.2 Phase II: Removal of CFA by SBA-15 and their functionalized at high concentration.**

*3.2.2.1 Preparation of stock solution*

Clofibric acid (CFA) standard stock solution was prepared with deionized water as synthetic wastewater in concentration of 100 mg/L and was stored in the dark at 4 °C.

*3.2.2.2 Adsorption experiments*

*3.2.2.2.1 Adsorption kinetic study*

Adsorption kinetic experiment was performed by varying the contact time and initial concentration of clofibric acid (CFA) solution was set at 10 mg/L in 2 mM phosphate buffer at pH 7. Ratio of adsorbent and solution was fixed 1 g/L. The mixture was stirred in beaker at static condition at 25 °C, and then the supernatant solution was filtrated through a nylon syringe filter (pore size 0.45 mm). Then, the remaining clofibric acid (CFA) concentration was analyzed by reverse phase high performance liquid chromatography (HPLC) equipped with UV detector (230 nm) The C18 column (4 × 250 mm, 5μm) was used in this study. The elution gradient was conducted by using water (A) and acetonitrile (B) at room temperature. The initial elution condition was a mobile phase B 100% v/v reach to 70% in 5 min and the flow rate was set at 1mL/min. Chromatogram of CFA measured by HPLC equipped with UV detector are shown in **Figure 3. 3**.
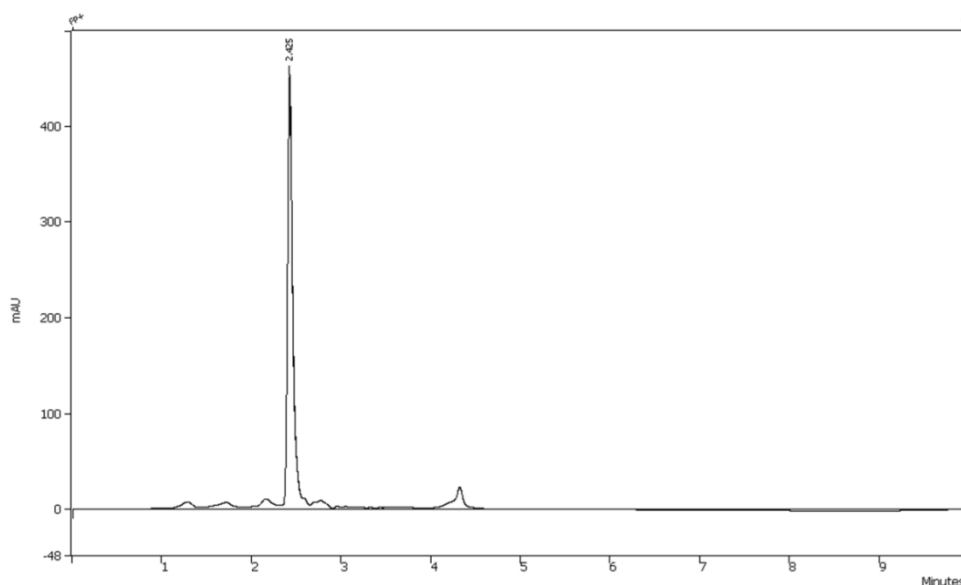
**Figure 3. 3** Chromatogram of CFA by HPLC with UV detector

**Table 3. 3** Retention time of CFA and Limit of detection from analyzed by HPLC in Phase II.

| Name | Clofibric acid |
|---|---|
| Retention time | 2.425 |
| *Limit of detection | 50 µg/L |

*Limit of detection (LOD) at signal to noise ratio (S/N) = 3

*3.2.2.2.2 Adsorption isotherm study*

Adsorption isotherm was conducted with the initial concentration range between 6-15 mg/L and 1 g/L of adsorbent. The ionic strength of the solution was fixed using 2 mM phosphate buffer at either pH 5, 7 or 9. The sample was stirred in beaker at static condition at 25 $^{\circ}$C until the equilibrium is reached, and then the supernatant solution was filtrated through a nylon syringe filter (pore size 0.45 mm). Then, the remaining clofibric acid (CFA) concentration was analyzed by reverse phase high performance liquid chromatography (HPLC) equipped with UV detector (230 nm). The C18 column (4 × 250 mm, 5µm) was used in this study. The elution

gradient was conducted by using water (A) and acetonitrile (B) at room temperature. The initial elution condition was a mobile phase B 100% v/v reach to 70% in 5 min and the flow rate was set at 1mL/min.

### 3.2.3 Phase III: Removal of CFA by an effective functionalized SBA-15 at low concentration.

The effective functionalized SBA-15 was used as adsorbent in this study. Adsorption isotherm was conducted with the initial concentration range between 50-250 µg/L and 1 g/L of adsorbent. The ionic strength of the solution was fixed using 2 mM phosphate buffer at pH of treated wastewater. The sample was stirred in beaker at static condition at 25 $^{\circ}$C until the equilibrium is reached, and then the supernatant solution was filtrated through a nylon syringe filter (pore size 0.45 mm). Before analysis, the filtrate was concentrated by a solid-phase extraction (SPE) using a 500 mg C18 cartridge (Agela, Japan). The cartridge was washed as a conditioning step with methanol 5 mL and followed by 10 mL of deionized water, and then the sample was fed into the cartridges. After that the cartridge was washed with deionized water 10 mL, the cartridge was eluted with methanol 10 mL and the liquid samples were evaporated with nitrogen gas. The volume of samples was adjusted to 0.5 mL of methanol. Then, the remaining clofibric acid (CFA) concentration was analyzed by reverse phase high performance liquid chromatography (HPLC) equipped with UV detector (230 nm). The C18 column (4 × 250 mm, 5µm) was used in this study. The elution gradient was conducted by using water (A) and acetonitrile (B) at room temperature. The initial elution condition was a mobile phase B 100% v/v reach to 70% in 5 min and the flow rate was set at 1mL/min. Recovery percentage was 95.3% ± 1.97.

**Table 3. 4** Recovery percentage of CFA after SPE and analyzed by HPLC with UV detector.

| Name | % recovery | | | Average of % recovery | SD | %RSD |
|---|---|---|---|---|---|---|
| | 1 | 2 | 3 | | | |
| CFA | 95.6 | 93.2 | 97.1 | 95.3 | 1.97 | 2.06 |

**3.2.4 Phase IV: Removal of CFA in the discharge wastewater from swine farm**

*3.2.4.1 Wastewater sample preparation*

The discharge wastewater from wastewater treatment plant (WWTP) of swine farm in Chiang Mai province of Thailand was used as background water sample of this study. Collected wastewater was fractionated to separate hydrophobic and hydrophilic natural organic matters (NOMs). Water sample was filtered through a glass fiber filter (GF/F, pore size 0.75 μm) and then was adjusted to pH 2 by using $H_2SO_4$. Then the water sample was fed through resin (DAX-8) at flow rate 20 mL/min. The first water sample released from column was hydrophilic NOM. Hydrophobic NOM was eluted with 0.1 N of NaOH 25mL and 0.01 N of NaOH 125 mL at flow rate 200mL/hr. Stock clofibric acid (CFA) was prepared in concentration 100 mg/L by deionize water and it was diluted by fractionated water for using in adsorption experiment.

**Table 3. 5** pH and ionic strength (IS) of wastewater sample

| Natural organic matter (NOM) | pH | IS |
|---|---|---|
| Hydrophilic NOM | 6.17 | 2 mM* |
| Hydrophobic NOM | 7.35 | 2 mM* |

*Calculate from TDS (Total dissolve solid)

*3.2.4.2 NOM concentration measurement*

The concentration of NOM in wastewater sample was analyzed by using dissolve organic carbon measurement (TOC) and reverse phase high performance liquid chromatography (HPLC) with UV detector (230 nm.). **Figure 3. 4** and **Figure 3. 5** illustrated the chromatograms of CFA in the presence of hydrophobic and hydrophilic NOM, respectively. **Table 3. 4** reported the HPLC's retention time data of CFA, hydrophobic and hydrophilic NOM. And **Table 3. 5** showed the TOC results of hydrophobic and hydrophilic NOM.
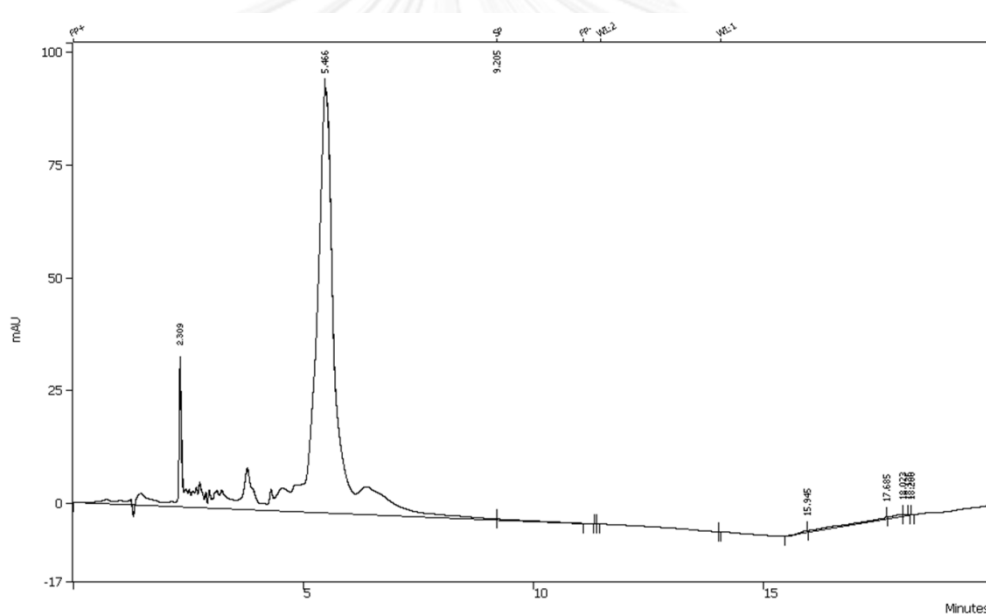


**Figure 3. 4** Chromatogram of hydrophobic NOM and CFA by HPLC with UV detector
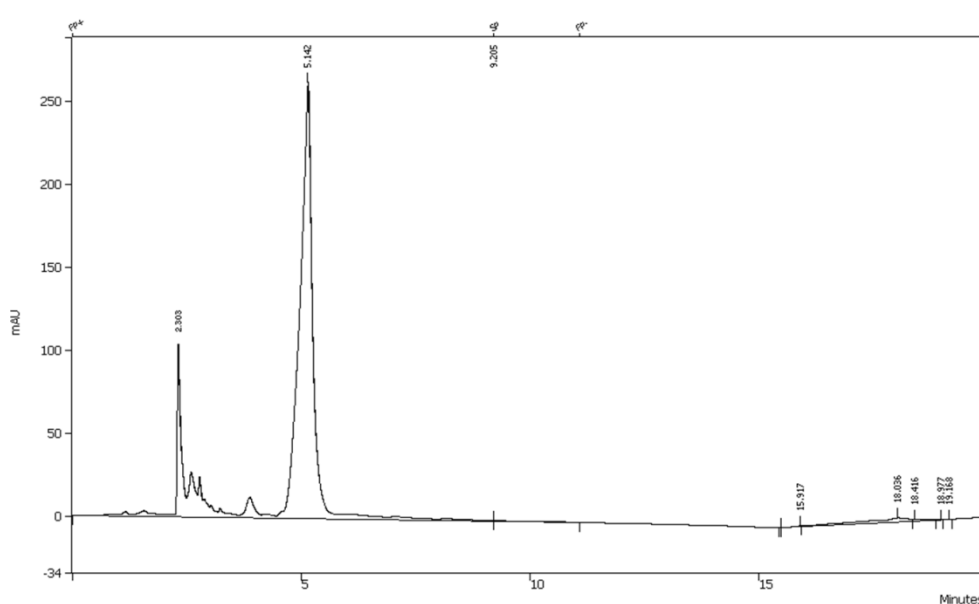
**Figure 3. 5** Chromatogram of hydrophilic NOM and CFA by HPLC with UV detector

**Table 3. 6** Retention time of NOM and CFA from analyzed by HPLC of Phase IV

| Name | Retention time (min.) |
|---|---|
| CFA | 2.309 and 2.303 |
| Hydrophobic NOM | 5.466 |
| Hydrophilic NOM | 5.142 |

**Table 3. 7** Dissolve organic carbon concentration of NOM

| Name | Dissolve organic carbon (mg/L) | | |
|---|---|---|---|
| | 1 | 2 | Average of dissolve organic carbon (mg/L) |
| Hydrophobic NOM | 0.7181 | 0.7176 | 0.7179 |
| Hydrophilic NOM | 0.7772 | 0.7880 | 0.7880 |

### 3.2.4.3 Adsorption experiments

The most effective functionalized SBA-15 (from phase II) was used as adsorbent in this study. Adsorption isotherm was conducted with the initial

concentration range between 6-15 mg/L and 1 g/L of adsorbent at pH of treated wastewater. The sample was stirred in beaker at static condition at 25 $^{\circ}$C until the equilibrium condition was reached, and then the supernatant solution was filtrated through a nylon syringe filter (pore size 0.45 mm). Then, the remaining clofibric acid (CFA) concentration was analyzed by reverse phase high performance liquid chromatography (HPLC) equipped with UV detector (230 nm). The C18 column (4 × 250 mm, 5μm) was used in this study. The elution gradient was conducted by using water (A) and acetonitrile (B) at room temperature. The initial elution condition was a mobile phase B 100% v/v reach to 0% in 10 min and the flow rate was set at 1mL/min.

### 3.2.5   Phase V: Calculation of the mass transfer parameters

In this phase, the mass transfer parameters such as liquid film mass transfer coefficient($k_f$), solid film mass transfer coefficient ($k_s$), overall solid-phase mass transfer coefficient ($K_s$), overall liquid-phase mass transfer coefficient($K_f$), and constant diffusivity ($D_s$) were calculated from the results of adsorption kinetics of **Phase II** by using **Equation 2.5-2.13** to predict those parameters which required for calculation of breakthrough curve follow the mass transfer models for the design of the fixed bed adsorption column.

CHAPTER IV

RESULTS AND DISCUSSION

## 4.1 CHARECTERIZATION

The synthesized mesoporous silica SBA-15 via surfactant template method and SBA-15 modified surface by two different surface functional groups (3N-SBA-15 and M-SBA-15) were characterized the physico-chemical properties by various methods.

### 4.1.1 X-ray Diffraction

X-ray diffraction (XRD) was used to evaluate silica structure of mesoporous silicates at $2\theta$ angel of $0.5^{\circ} - 10.0^{\circ}$. The powder XRD diffraction pattern of SBA-15 as shown in **Figure 4. 1** that showed three main reflections corresponding to the (100), (110), and (200) at $2\theta = 0.91°$, 1.57° and 1.80° respectively that indicated the hexagonal structure of SBA-15 (Hamoudi, El-Nemr, & Belkacemi, 2010).
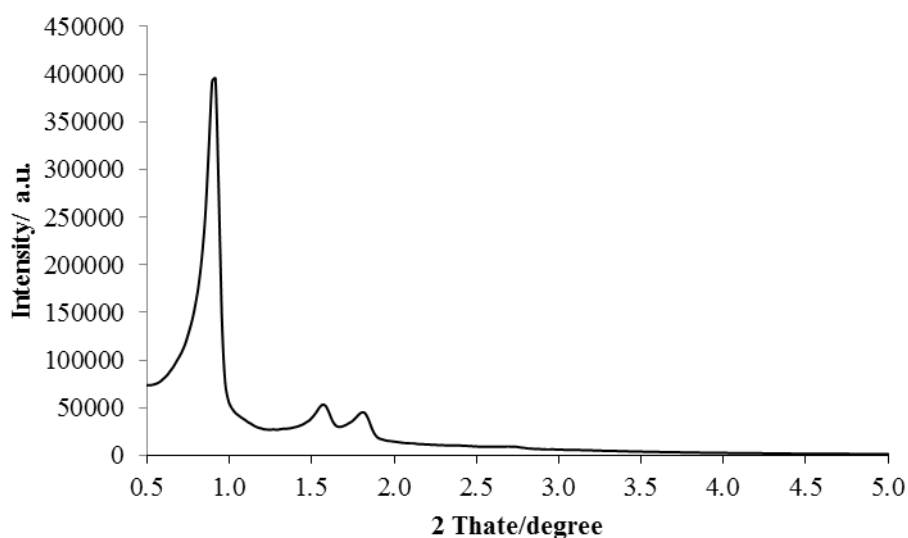


**Figure 4. 1** Low angel XRD pattern of SBA-15

**4.1.2 N$_2$ adsorption-desorption isotherms**

N$_2$ adsorption-desorption isotherms were used to characterize surface area, pore size, and pore volume of SBA-15 and functionalized SBA-15 **as shown in Figure 4. 2.**
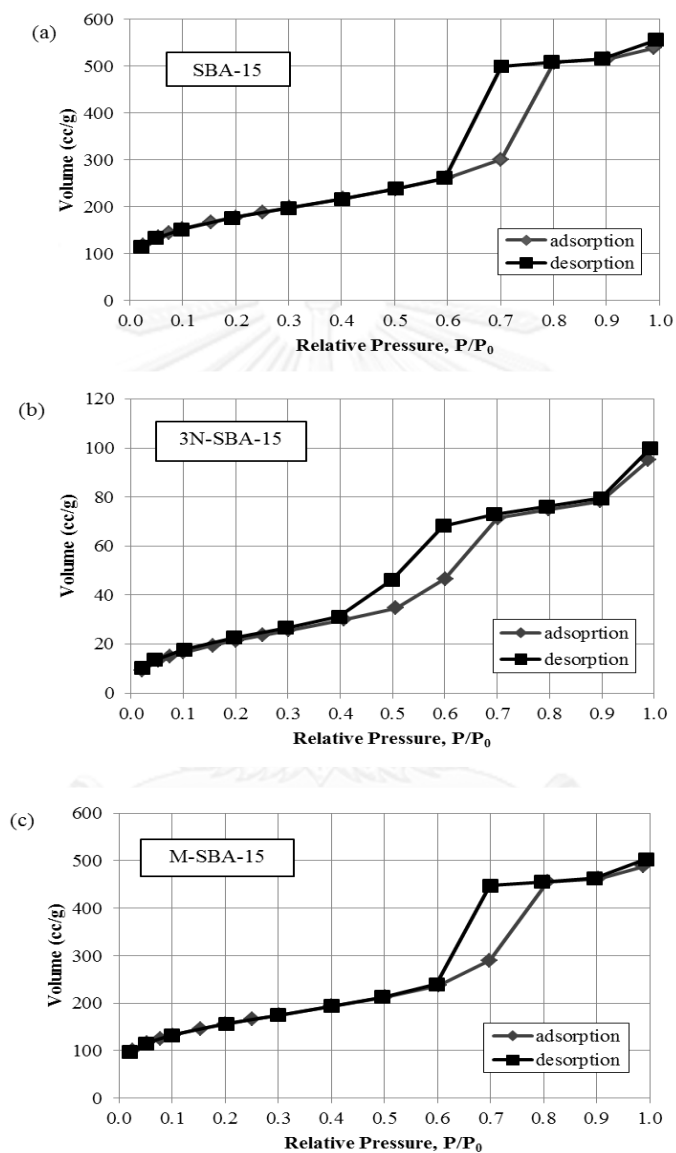


**Figure 4. 2** N$_2$ Adsorption-desorption isotherms of synthesized SBA-15 (a), 3N-SBA-15 (b) and M-SBA-15 (c)

N$_2$ adsorption-desorption isotherms were used to characterize surface area, pore size, and pore volume of SBA-15 and functionalized SBA-15s. In case of surface

area, Brunauer-Emmett-Teller (BET) isotherm was used to calculate specific surface area. The calculation of pore size distribution and pore volume of the adsorbents were used equation of Barrett-Joyner-Halenda (BJH) by assuming a cylindrical pore geometry from nitrogen desorption data (obtained at 77 K). The $N_2$ adsorption-desorption isotherms of SBA-15 and functionalized SBA-15s were Type IV isotherm that presented the mesoporous structure (2-50 nm.) and had a hysteresis loop that generated by the capillary condensation of the adsorbate ($N_2$) in the mesoporous of the solid.
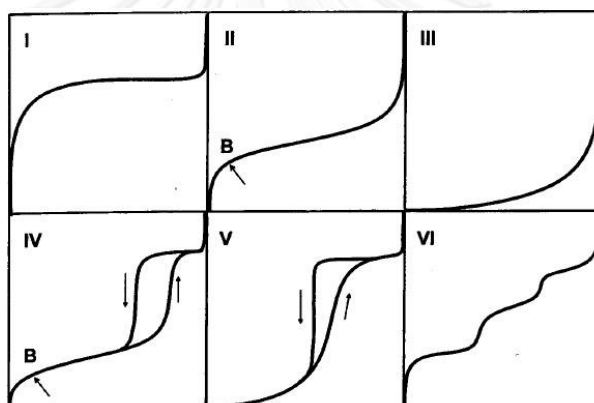


**Figure 4. 3** Classification of the isotherm types by IUPAC (Sing, 1982)

The calculated parameters from the $N_2$ adsorption-desorption isotherms are summarized in **Table 4. 1.** The results from **Table 4. 1** showed that the pore volume of SBA-15 was larger than M-SBA-15 and 3N-SBA-15, while the BET surface area of the synthesized adsorbents followed the order: SBA-15>M-SBA-15>3N-SBA-15. The decrease of pore volume and surface area can indicate the grafting of organo-functional group inside the pores. According to the results of 3N-SBA-15, which had the smallest pore diameter, the pore structure of 3N-SBA-15 may be covered by steric of tri-amino functional group and cause the smallest pore diameter of 3N-SBA-15 compared with others.

**Table 4. 1** The calculated parameters from the $N_2$ adsorption-desorption isotherms

| Adsorbents | Surface functional groups | Surface characteristic | BET surface area ($m^2$/g) | Pore volume (cc/g) | Pore diameter (Å) |
|---|---|---|---|---|---|
| SBA-15 | Silanol | Hydrophilic | 614.89 | 0.83 | 61.24 |
| 3N-SBA-15 | Amino and silanol | Hydrophilic | 83.69 | 0.15 | 46.09 |
| M-SBA-15 | Mercapto and silanol | Hydrophobic | 547.65 | 0.76 | 61.21 |
| PAC[a,b] | Carboxyl, phenyl and etc. | Hydrophobic | 980.00 | 0.83 | 54.16 |

[a] (Prarat, Ngamcharussrivichai, Khaodhiar, & Punyapalakul, 2011)

[b] (Suriyanon et al., 2013)

The mean pore size of synthesized SBA-15 calculated from pore size distribution results by Barrett-Joyner-Halenda (BJH) method are shown in **Table 4. 1 and Figure 4. 4**. The results showed that pore size of SBA-15, 3N-SBA-15 and M-SBA-15 were 61.24, 46.09, and 61.21, respectively. 3N-SBA-15 had the smallest pore size, it may be caused by the cover of steric functional group between amino functional group and silicate structure of SBA-15 during the grafting process. From comparison between pore size of all adsorbents comparing and molecular size of CFA, it was found that molecule size of CFA (0.94 nm.) (Nie, Deng, Wang, Huang, & Yu, 2013) was smaller than pore size of all synthesized adsorbents. Therefore, CFA adsorption can be occurred at both of external surface and internal surface area of adsorbents.
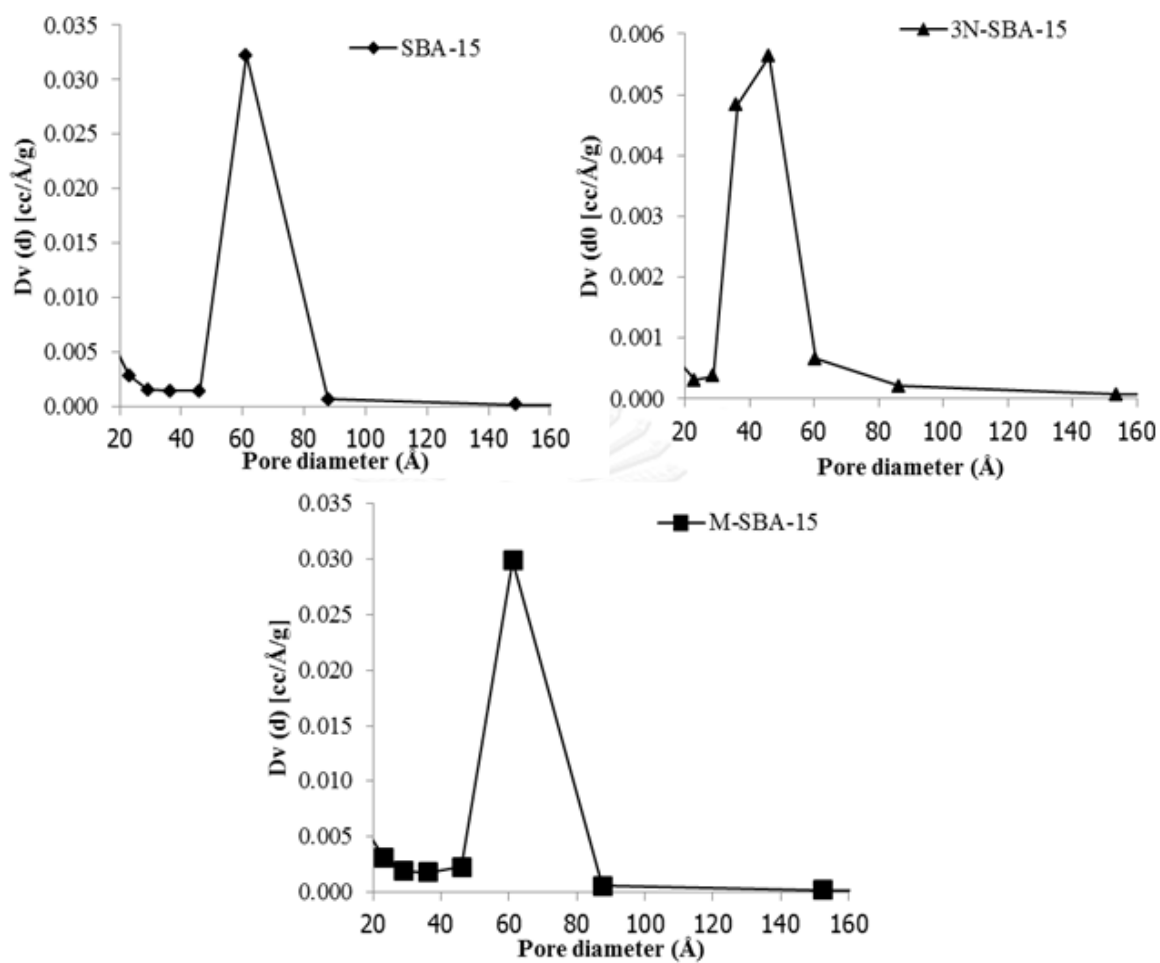
**Figure 4. 4** Pore size distribution (BJH) of synthesized SBA-15

### 4.1.3 Fourier transforms infrared spectroscopy

FTIR spectroscopy was used to confirm the presence of surface functional groups that grafting on the surface of adsorbents.
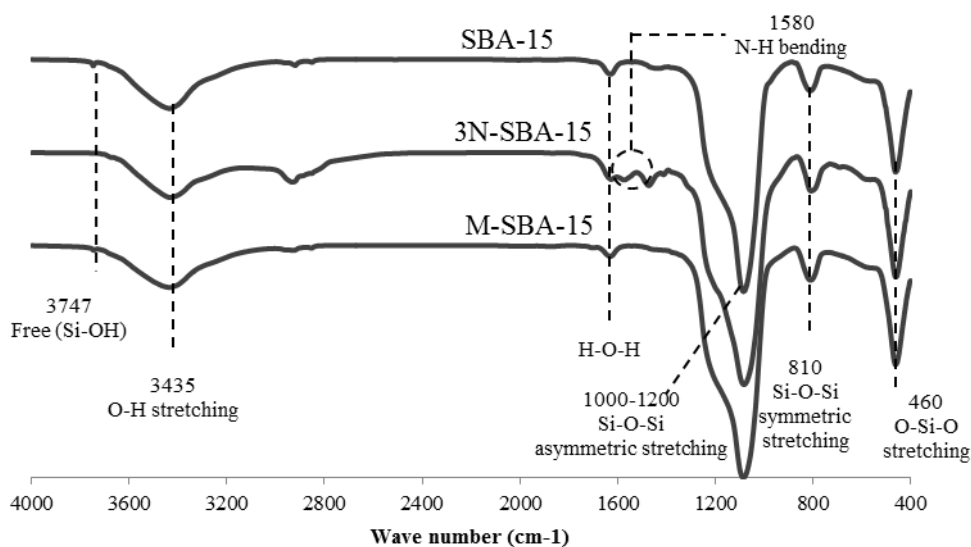
**Figure 4. 5** FT-IR spectra of SBA-15 and functionalized SBA-15

According to **Figure 4. 5**, FTIR spectra of all adsorbents shown a peak at 3747 $cm^{-1}$ which relate to the free silanol group (Si-OH). The peak at 3435 $cm^{-1}$ indicated the O-H stretching of silanol group on the surface. It can be indicated that all adsorbents had silanol group on their surface. The asymmetric Si-O-Si band around 1000-1200 $cm^{-1}$, the symmetric Si-O-Si around 810 $cm^{-1}$ and O-Si-O stretching around 460 $cm^{-1}$ can associate with the silica network of all adsorbents. In case of 3N-SBA-15 that has amino functional group, the bands of primary amine should be around 3300-3500 $cm^{-1}$ and N-H bending around 1580 $cm^{-1}$, however it was difficult to identify those two peaks for the amino functional group attached to the surface of adsorbent because of the overlapping of broad O-H stretching. In case of mercapto functional group on M-SBA-15, the band peak of S-H stretching should be around 2490-2580 $cm^{-1}$, but it could not be clearly identified. However, the presence of mercapto functional group could be confirmed by CHONS elemental analysis for sulfur content.

**4.1.4 CHONS Elemental Analysis**

The elemental analysis was applied to determine the amount of nitrogen and sulfur content on the surface of 3N-SBA-15 and M-SBA-15, respectively.
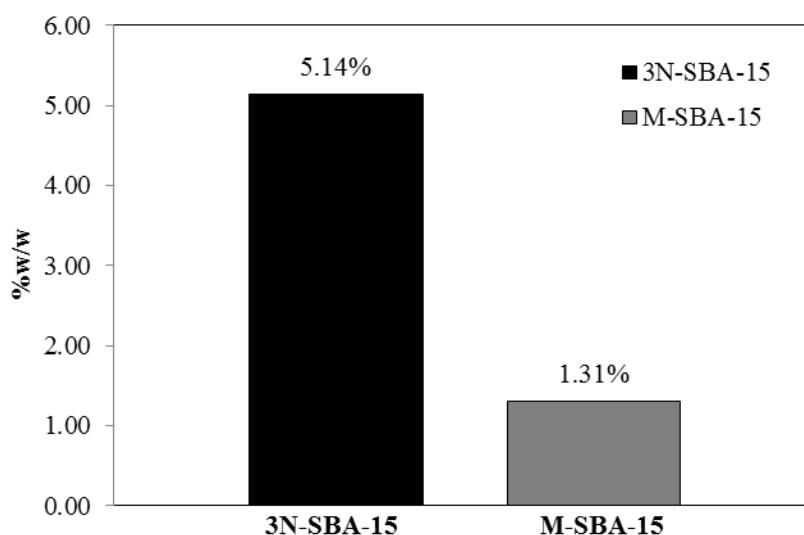


**Figure 4. 6** Nitrogen and sulfur content of 3N-SBA-15 and M-SBA-15

The total nitrogen content on 3N-SBA-15 was 5.14 (%w/w) or 43.87 $\mu mol_N/m^2$ and sulfur content on M-SBA-15 was 1.31 (%w/w) or 0.7476 $\mu mol_S/m^2$. Hence, the presence of amino and mercapto functional groups on 3N-SBA-15 and M-SBA-15, respectively, could be confirmed.

**4.1.5 Point of zero charge and surface charge density**

Acid-base titration method was used to determine the point of zero charge ($pH_{zpc}$). The $pH_{zpc}$ of all synthesized adsorbents are shown in **Table 4. 2**. The $pH_{zpc}$ of each adsorbent were different depended on the surface modification with different functional groups. The $pH_{zpc}$ of SBA-15, 3N-SBA-15 and M-SBA-15 were 5.1, 9.2, and 5.8, respectively.

**Table 4. 2** pH$_{zpc}$ of all synthesized adsorbents

| Adsorbents | Surface functional groups | pH$_{zpc}$ |
|---|---|---|
| SBA-15 | Silanol | 5.1 |
| 3N-SBA-15 | Amino and silanol | 9.2 |
| M-SBA-15 | Mercapto and silanol | 5.8 |

According to **Figure 4. 7** at pH less than pH$_{zpc}$ the surface of adsorbent was positive charge because the surface gained proton (H$^+$), but at pH more than pH$_{zpc}$ the surface of adsorbent was negative charge because the surface lost proton (H$^+$).
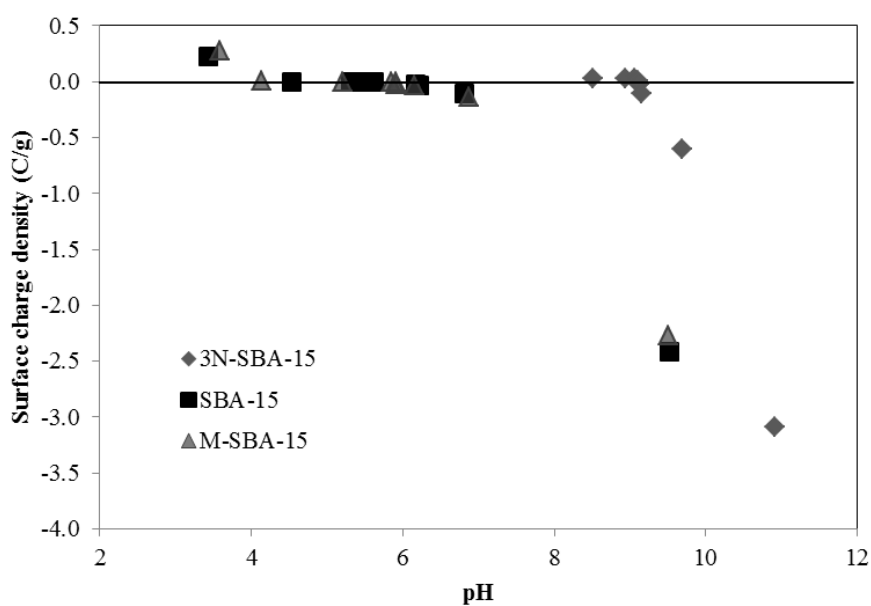


**Figure 4. 7** Surface charge density of synthesized SBA-15,

and functionalized SBA-15 (IS 0.01M)

**4.1.6 Particle size distribution analysis**

The particle size distribution analysis was used to determine diameter of adsorbent by using the average of diameter as shown in **Table 4. 3**.

**Table 4. 3** Average diameters of SBA-15 and functionalized SBA-15 particles

| Adsorbents | Average diameters (µm) |
|---|---|
| SBA-15 | 12.78* |
| 3N-SBA-15 | 9.58* |
| M-SBA-15 | 10.53* |

*Average diameter at D(v,0.5) by analysis 3 times

**Table 4. 3** showed the average diameter of all adsorbents followed the order: SBA-15 > M-SBA-15 > 3N-SBA-15. The result indicated that particle 3N-SBA-15 might be destroyed during grafting with functional groups.

### 4.1.7 Conclusion of characterization

| Adsorbents | Surface functional groups | Surface characteristic | BET surface area (m$^2$/g) | Pore volume (cc/g) | Pore diameter (Å) | Average diameters (µm) | pH$_{zpc}$ |
|---|---|---|---|---|---|---|---|
| SBA-15 | Silanol | Hydrophilic | 614.89 | 0.83 | 61.24 | 12.78 | 5.1 |
| 3N-SBA-15 | Amino and silanol | Hydrophilic | 83.69 | 0.15 | 46.09 | 9.58 | 9.2 |
| M-SBA-15 | Mercapto and silanol | Hydrophobic | 547.65 | 0.76 | 61.21 | 10.53 | 5.8 |
| PAC[a,b] | Carboxyl, phenyl and etc. | Hydrophobic | 980.00 | 0.83 | 54.16 | - | 9.5 |

[a] (Prarat et al., 2011)

[b] (Suriyanon et al., 2013)

## 4.2 ADSORPTION OF CLOFIBRIC ACID (CFA)

### 4.2.1 Adsorption of clofibric acid (CFA) at high concentration

In this part, the adsorption information were done by investigating the adsorption of CFA at high concentration which consisted of adsorption kinetic,

intraparticle diffusion mechanism, and adsorption isotherm that were important for unit operation process.

### 4.2.1.1 Adsorption kinetic

The adsorption kinetic is applied to investigate the adsorption rate and equilibrium time for unit operation treatment process. The study of adsorption kinetics of CFA onto SBA-15 and functionalized SBA-15s was investigated at initial concentration of CFA 10 mg/L. Phosphate buffer 2 mM was used to control the pH of the solution was controlled using at 7. The ratio of adsorbent to adsorbate was fixed at 1g/L. The samples were agitated in a magnetic stirrer at static condition at 25 ℃. The samples were collected between 0 and 24 hr. Adsorption kinetic of CFA onto all adsorbents is illustrated in **Figure 4. 8** as the amount of adsorbate (CFA) adsorbed at time ($q_t$) over time (hr). The result showed that the concentration of CFA decreased rapidly in the first 1 hr. and reach equilibrium within 6 hrs. for all synthesized adsorbents. Comparing with PAC, CFA concentration rapidly decreased in 1 min and reach equilibrium within 3 hrs.
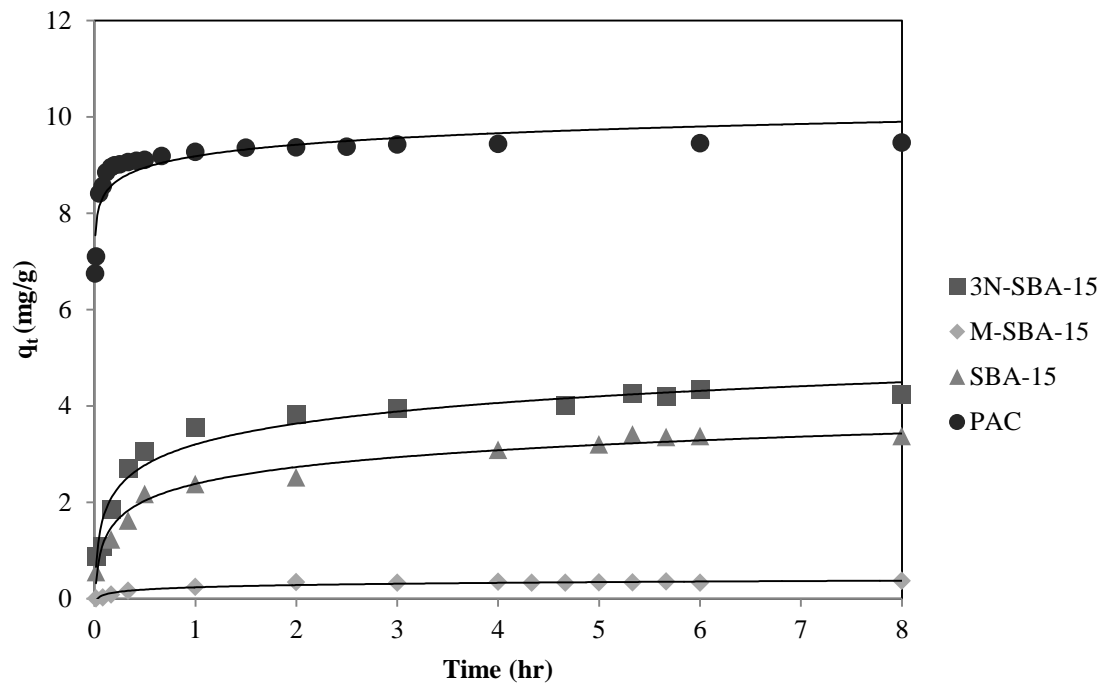
**Figure 4. 8** Adsorption kinetics of CFA by SBA-15, functionalized SBA-15

Adsorption kinetic models were used to evaluate the adsorption efficiency that consists of pseudo-first-order and pseudo-second-order kinetic models. The pseudo-first-order equation can be defined as **Equation 4.4**.

$$\ln\left(q_e - q_t\right) = \ln q_e - k_1 t \qquad (4.4)$$

Where $k_1$ is the pseudo-first-order rate constant (mg/g) and $q_t$ is amounts of adsorbate (mg/g) at time $t$ (min).When plot between 1/q and 1/t, the values of $q_e$ and $k_1$ can be calculated from the slope and intercept, respectively.

The pseudo-second-order model can be presented (Blanchard et al., 1984; Ho and Mackay, 1999) as shown in **Equation 4.5.**

$$\frac{t}{q_t} = \frac{1}{k_2 q_e^{\,2}} + \frac{t}{q_e} \qquad (4.5)$$

Where $k_2$ is pseudo- second-order rate constant (g/mg.hr). Moreover, the initial adsorption rate ($h$) (mg/g.hr) can also be obtained from this model as **Equation 4.6.**

$$h = k_2 q_e^{\ 2} \tag{4.6}$$

**Table 4. 4** showed the calculated parameters for kinetic models of all absorbents. The obtained results were fitted well with the pseudo-second order model with high correlation coefficients ($R^2$) of the linear plots. This result suggests that the rate-limiting step may be chemical adsorption or involving valence forces by exchange or sharing the electron between adsorbent and adsorbate (Hodaifa, Ochando-Pulido, Driss Alami, Rodriguez-Vives, & Martinez-Ferez, 2013). The initial adsorption rates ($h$) of CFA are compared, and the higher initial adsorption rate of 3N-SBA-15 is observed than the others synthesized adsorbents. The initial adsorption rate of all adsorbents followed the order: PAC > 3N-SBA-15 > SBA-15 > M-SBA-15. This result showed that the initial rate adsorption ($h$) of CFA was higher for synthesized hydrophilic adsorbents (3N-SBA-15 and SBA-15) than another hydrophobic adsorbent (M-SBA-15) because of higher adsorption affinity on the hydrophilic surface of CFA. However, they were still lower than PAC's initial adsorption rate because of complexation of organo-functional group on its surface and very board pore size distribution. These results suggest that not only the hydrophilic or hydrophobic interaction involved, but also the other phenomena can occur, such as interparticle diffusion and electrostatic interaction.

**Table 4. 4** Kinetic parameters for CFA adsorption on SBA-15, functionalized SBA-15, and PAC adsorbents at 10 mg/L (pH7 and IS 2mM)

| Adsorbents | $q_{e,exp}$ (mg/g) | $q_{e,cal}$ (mg/g) | Pseudo-second-order | | | | Pseudo-first-order | | |
|---|---|---|---|---|---|---|---|---|---|
| | | | $k_2$ (g/mg.hr) | $h$ (mg/g.hr) | $t_{1/2}$ (hr) | $R^2$ | $q_{e,cal}$ (mg/g) | $k_1$ (g/mg.hr) | $R^2$ |
| SBA-15 | 3.38 | 3.49 | 0.8116 | 9.88 | 0.353 | 0.997 | 1.60 | 0.5539 | 0.724 |
| 3N-SBA-15 | 4.35 | 4.49 | 0.7828 | 15.80 | 0.204 | 0.998 | 2.11 | 0.5247 | 0.791 |
| M-SBA-15 | 0.36 | 0.39 | 4.009 | 0.62 | 0.691 | 0.996 | 0.18 | 0.3881 | 0.789 |
| PAC | 9.44 | 9.46 | 7.97 | 714.71 | 0.013 | 1 | 0.92 | 1.4735 | 0.915 |

## 4.2.1.2 Intraparticle diffusion mechanism

The Weber and Morris intraparticle diffusion model was used to analyze from kinetic data to predict the rate-controlling step in an adsorption process to understand the mechanism of adsorption.The intraparticle diffusion equation can be presented as **Equation 4.7**

$$q_t = k_i t^{1/2} + C \qquad (4.7)$$

Where $q_t$ is the amount of adsorbate adsorbed (mg/g) at time $t$ (min), $k_i$ is the intraparticle diffusion rate constant (mg/g.min$^{1/2}$) and $C$ is the interception, which can be determined from the plot of $q_t$ versus $t^{1/2}$.
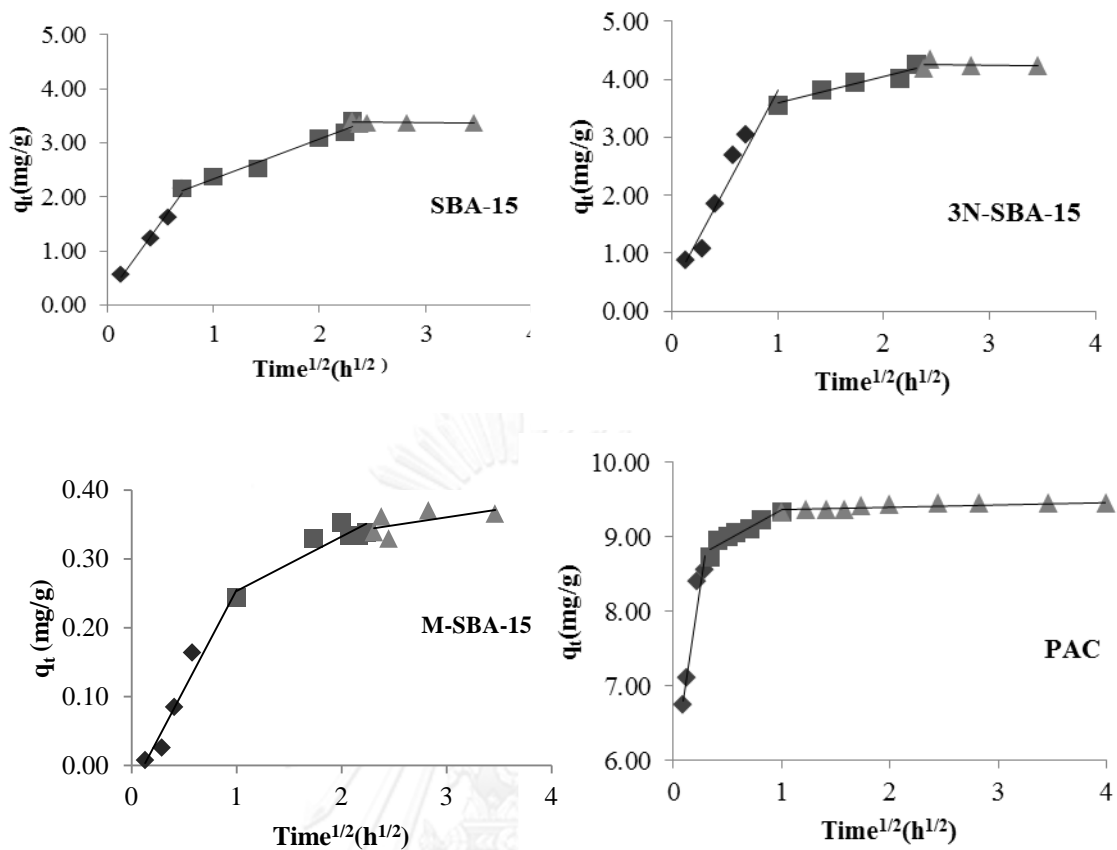
**Figure 4. 9** Intraparticle diffusion plots of CFA adsorbed onto SBA-15, functionalized SBA-15 and PAC (pH 7 and IS 2mM)

Normally, the adsorption mechanism of solid-liquid adsorption has three steps (Albadarin et al., 2012). First of all is the film diffusion process that presents the transport of adsorbate from bulk solution to the external surface of adsorbent. The second step of adsorption mechanism is intraparticle diffusion or pore diffusion process that molecules of adsorbate move into the interior of absorbent. The last step is adsorption process that presents the adsorption of the adsorbate on internal site of the adsorbent or final equilibrium. The last step is very fast when compared with other steps, so it can be considered negligible. Therefore, the rate limiting step can be film diffusion and/or intraparticle diffusion. According to the intraparticle diffusion model, if intraparticle diffusion involves in the adsorption, a plot between $q_t$ and $t^{1/2}$ should be linear and if it passes through the origin, it means that the

intraparticle diffusion is rate-limiting step (Ozcan, Ozcan, & Gok, 2007). As shown in, the intraparticle diffusion plots were multi-linearity of three steps. This suggests that adsorption occurred in three phases of all adsorbents.

The initial stage represents film diffusion that CFA from solution diffuse though the boundary layer to external surface of the adsorbents. The intraparticle or pore diffusion is represented in the second stage that CFA diffuse into pore of adsorbent and the third stage is final equilibrium. As the plot did not pass through the origin, it means that the intraparticle diffusion is not the only rate-limiting step. Therefore, film and intraparticle diffusion mechanism might control the adsorption rate together. However, the adsorption rate of intraparticle diffusion was supposed to be the slowest rate for CFA adsorption on mesoporous silica adsorbents. The intraparticle diffusion rate constant $k_i$, was calculated from the slope of the second stage. The intercept C in the second stage can relate to the thickness of the boundary layer (Kavitha & Namasivayam, 2007); in addition, larger intercepts suggests that intraparticle diffusion has a larger role as the rate-limiting step.

**Table 4. 5** The Weber and Morris intraparticle diffusion parameters for adsorption of CFA (pH 7 and IS 2mM)

| Adsorbents | 1st stage | | | 2nd stage | | |
|---|---|---|---|---|---|---|
| | $k_i$ (mg/g.hr$^{1/2}$) | C | $R^2$ | $k_i$(mg/g.hr$^{1/2}$) | C | $R^2$ |
| SBA-15 | 2.6981 | 0.1643 | 0.9835 | 0.7391 | 1.6023 | 0.9748 |
| 3N-SBA-15 | 3.4011 | 0.4226 | 0.9465 | 0.4621 | 3.1258 | 0.9252 |
| M-SBA-15 | 0.2888 | -0.0336 | 0.9565 | 0.1303 | 0.0994 | 0.9829 |
| PAC | 9.9249 | 5.8857 | 0.9474 | 0.7947 | 8.5669 | 0.9097 |

### 4.2.1.3 Adsorption isotherm

#### 4.2.1.3.1 Adsorption isotherm models

The isotherm models, which are Linear, Langmuir, and Freundlich isotherm were used to analyze the adsorption isotherm data of CFA adsorption onto synthesized adsorbents. The linear form of the Linear isotherm is given by **Equation 4.8**.

$$q_e = K_P C_e \tag{4.8}$$

$q_e$ is the amount of adsorbate adsorbed at equilibrium (mg/L) and $K_P$ is the Linear constant (L/mg). $C_e$ is the concentration of adsorbate at equilibrium (mg/L).

The linear form of the Langmuir isotherm is given by **Equation 4.9**.

$$\frac{1}{q_e} = \frac{1}{K_L q_m C_e} + \frac{1}{q_m} \tag{4.9}$$

Where $q_m$ defines the maximum adsorption capacity (mg/g), $q_e$ is the amount of adsorbate adsorbed at equilibrium (mg/L) and $K_L$ is the Langmuir constant (L/mg).The linear form of the Freundlich isotherm is given by **Equation 4.10**.

$$\log q_e = \log K_{fr} + \frac{1}{n} \log C_e \tag{4.10}$$

Where $K_{fr}$ is the Freundlich constant (mg/g) and $n$ is the adsorption intensity (dimensionless).

The study of adsorption isotherms of CFA onto SBA-15 and functionalized SBA-15 were investigated at an initial CFA concentration range between 6-15 mg/L. Phosphate buffer 2 mM was used to controlled the pH of the solution at 5, 7 and 9. The ratio of adsorbent to adsorbate was fixed at 1g/L. The samples were agitated in a magnetic stirrer at static condition at 25 °C. The samples were collected at 24 hr.

**Table 4. 6** showed the calculated parameters for isotherm models of all absorbents. The obtained results showed the the Freundlich isotherm model gave highest $R^2$ values for all adsorbents. The Freundlich isotherm model is used to explain the adsorption characteristics for the heterogeneous surface. If *n* lies between one and ten, this indicates a favorable sorption process (Goldberg, 2005). From the **Table 4. 6,** the *n* values were more than 1 that indicates the adsorption of CFA onto all adsorbents was favorable. The $K_{fr}$ value is an approximate indicator of adsorption capacity, as the $K_{fr}$ value increases; the adsorption capacity of the adsorbent increases, it mean that the affinity of adsorbate toward the adsorbent (Bui & Choi, 2009). The results showed the affinity of CFA with synthetic adsorbents followed the order: 3N-SBA-15> SBA-15> M-SBA-15. 3N-SBA-15 had highest $K_{fr}$ value of all synthetic adsorbent which might cause by hydrophilic interaction between CFA and adsorbent, however, it was still lower than PAC. The percentage of CFA removal at high concentration of PAC, 3N-SBA-15, SBA-15 and M-SBA-15 were 95.47%, 44.60%, 31.67%, and 3.00%, respectively.

**Table 4. 6** Isotherm parameters for adsorption of CFA (pH7 and 2mM)

| Adsorbents | Freundlich | | | | Langmuir | | | Linear | |
|---|---|---|---|---|---|---|---|---|---|
| | $1/n$ | $n$ | $K_{fr}$ | $R^2$ | $K_L$ (L/mg) | $q_m$ (mg/g) | $R^2$ | $K_p$ (L/mg) | $R^2$ |
| SBA-15 | 0.761 | 1.314 | 0.728 | 0.978 | 0.060 | 10.905 | 0.967 | 0.4433 | 0.920 |
| 3N-SBA-15 | 0.827 | 1.209 | 1.076 | 0.947 | 0.047 | 21.552 | 0.933 | 0.787 | 0.916 |
| M-SBA-15 | 0.966 | 1.035 | 0.033 | 0.992 | 0.005 | 6.431 | 0.988 | 0.0306 | 0.986 |
| PAC | 0.876 | 1.142 | 19.058 | 0.970 | 0.199 | 116.28 | 0.968 | 20.467 | 0.948 |

*4.2.1.3.2 Effect of surface functional groups*

The study of effect of surface functional groups to CFA adsorption was evaluated by comparing adsorption isotherms of CFA onto all adsorbents.

**Figure 4. 10** showed the amount of adsorbate adsorbed at equilibrium ($q_e$) over concentration at equilibrium ($C_e$). The different surface functional groups, which are hydroxyl (silanol), animo, and mercapto affected to adsorption capacities of adsorbents. The obtained results showed that the adsorption capacities of all adsorbents for CFA followed the order: 3N-SBA-15> SBA-15> M-SBA-15 as shown in **Figure 4. 10**.
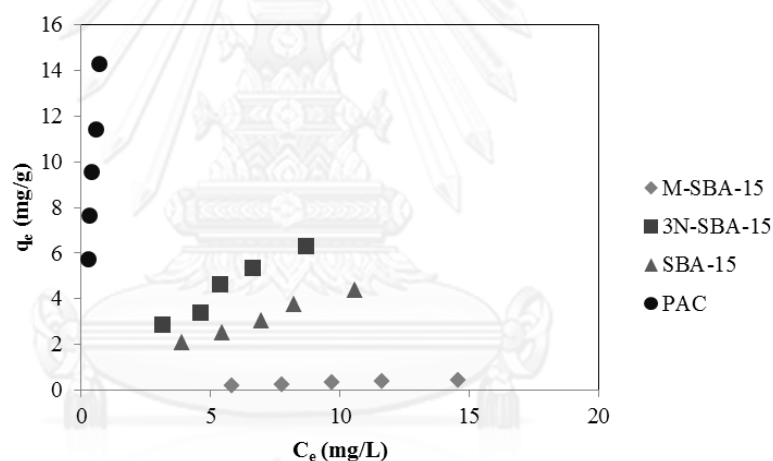


**Figure 4. 10** Effect of surface functional groups of adsorbents onto adsorption capacities of CFA (pH 7 and IS 2mM)

The pK$_a$ of CFA (pK$_a$ =3.18) shows that CFA is negatively charged at pH7. The mechanisms that can occur for their adsorption onto SBA-15 and functionalized SBA-15 are electrostatic interaction between negative charge and positive charge and hydrophilic interaction through hydrogen bonding. At pH 7, SBA-15 and M-SBA-15 have a negative charge, while 3N-SBA-15 has a positive charge. According to the results, 3N-SBA-15 had the highest adsorption capacity for CFA which might be

caused by the combination of hydrogen bond and electrostatic interactions between positive charge on its surface and negative charge of CFA molecule. In contrast, SBA-15 and M-SBA-15 are negatively charged, so the electrostatic repulsion might interfere the adsorption capacities of those two adsorbents. Furthermore, SBA-15 and 3N-SBA-15 had higher adsorption capacities than M-SBA-15 because they are hydrophilic adsorbents, so the hydrophilic interaction also plays an important role at this pH, but M-SBA-15, which is hydrophobic adsorbent, might interact with CFA though Van der Waals interaction more than electrostatic interaction. Therefore, the surface modification with amino functional group can increase the CFA adsorption capacity of adsorbent. However, the adsorption capacities of all adsorbents were still lower than PAC.

Moreover, the specific adsorption capacities per square meter of all synthesized absorbents was plotted to study the effect of the surface area of adsorbents (as shown in **Figure 4. 11**). The results showed that the adsorption capacity per square meter of 3N-SBA-15 might be compared with PAC. The results indicated that surface area were also the important factor in adsorption of CFA. Moreover, the functional groups that were grafted on adsorbents were also another reason in CFA adsorption. As shown in **Figure 4. 11**, the hydrophilic adsorbents (3N-SBA-15 and SBA-15) had higher adsorption capacities per square meter than the hydrophobic ones (M-SBA-15) on the adsorption isotherm of CFA at pH 7.0. From the obtained results, the development of higher surface area of amino functionalized porous silica with high stability should be considered, in order to increase the overall adsorption capacity of CFA comparing with PAC. Furthermore, the adsorption

capacity of CFA per mole of nitrogen in 1 g. of 3N-SBA-15 was plotted as shown in
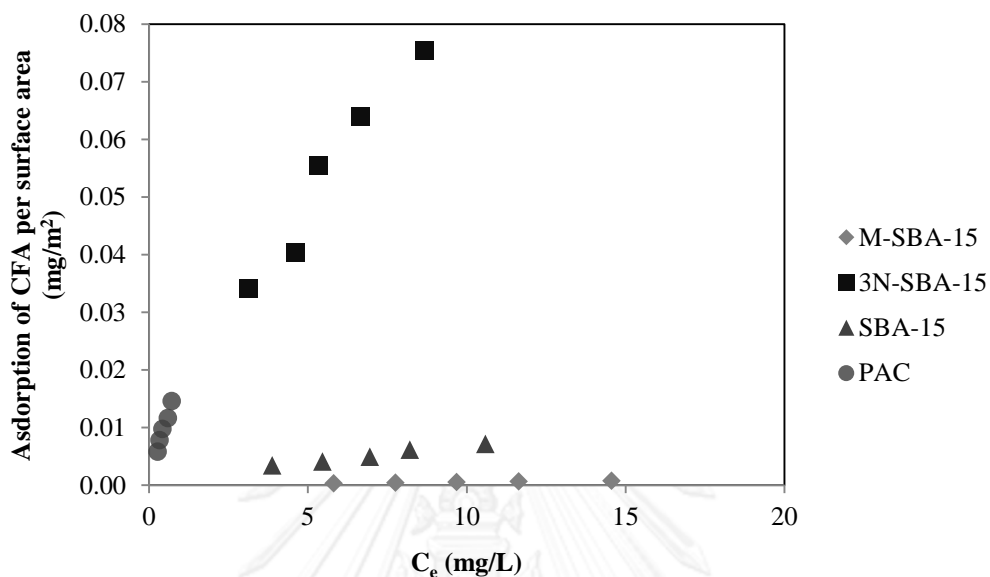
**Figure 4. 12**.



**Figure 4. 11** Effect of surface area of adsorbents onto adsorption of CFA per specific
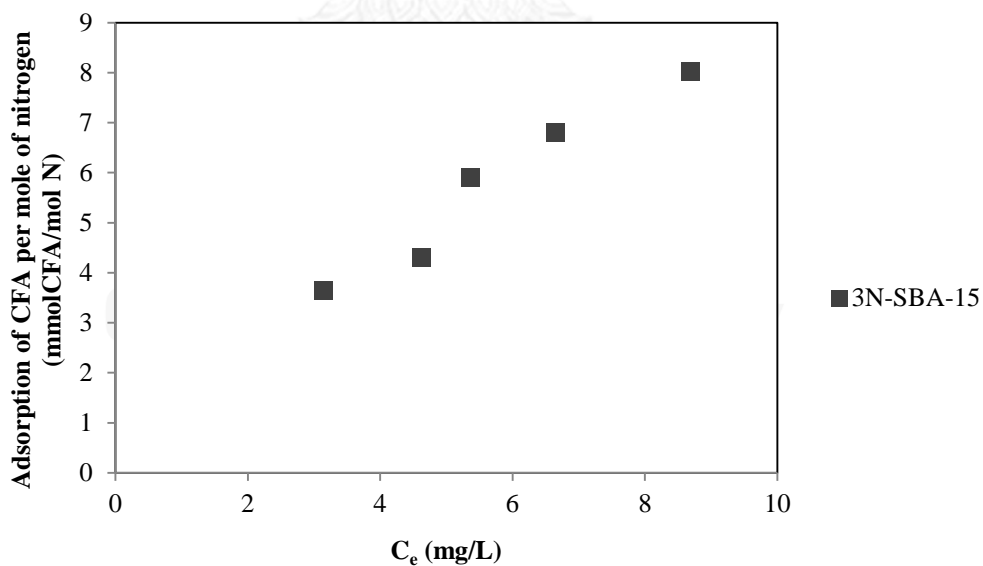
surface area (pH 7 and IS 2mM)



**Figure 4. 12** Effect of the amount of nitrogen of 3N-SBA-15 onto

adsorption of CFA per mole of nitrogen (pH 7 and IS 2mM)

*4.2.1.3.3 Effect of pH*

Effects of pH on adsorption capacities of CFA onto SBA-15 and the functionalized SBA-15 were investigated at pH 5, 7, and 9. The $pH_{zpc}$ of adsorbents were used to determine the surface charge properties of adsorbents. When pH of solution is higher than $pH_{zpc}$, the surface of the adsorbents is negatively charged. The obtained results showed that the adsorption capacities were depended on pH as shown in **Figure 4. 13**. The results showed that the adsorption capacity followed the order: pH5>pH7>pH9. The highest adsorption capacity was pH 5 which strongly related to the attractive electrostatic interaction. At pH 5, all synthesized adsorbents has positive charge, while CFA has negative charge, hence at this pH the adsorption capacities were increased because of attractive electrostatic interactions. At pH 7 and 9, SBA-15 and M-SBA-15 are negatively charged, so the adsorption capacities were decreased because of the electrostatic repulsive interaction.

For 3N-SBA-15 which has positive charge for all study pH (5 to 9) performed the highest adsorption capacities comparing with others (except PAC) for all pH; however, when the pH was increased, positive charge density on its surface will be decreased that lead to the decrease of CFA adsorption capacity of 3N-SBA-15. In case of PAC, it had the similar trend of pH as all synthesized adsorbents and it had the highest adsorption capacity due to the different types of surface functional groups on PAC surface that there have other forces related to the adsorption process.
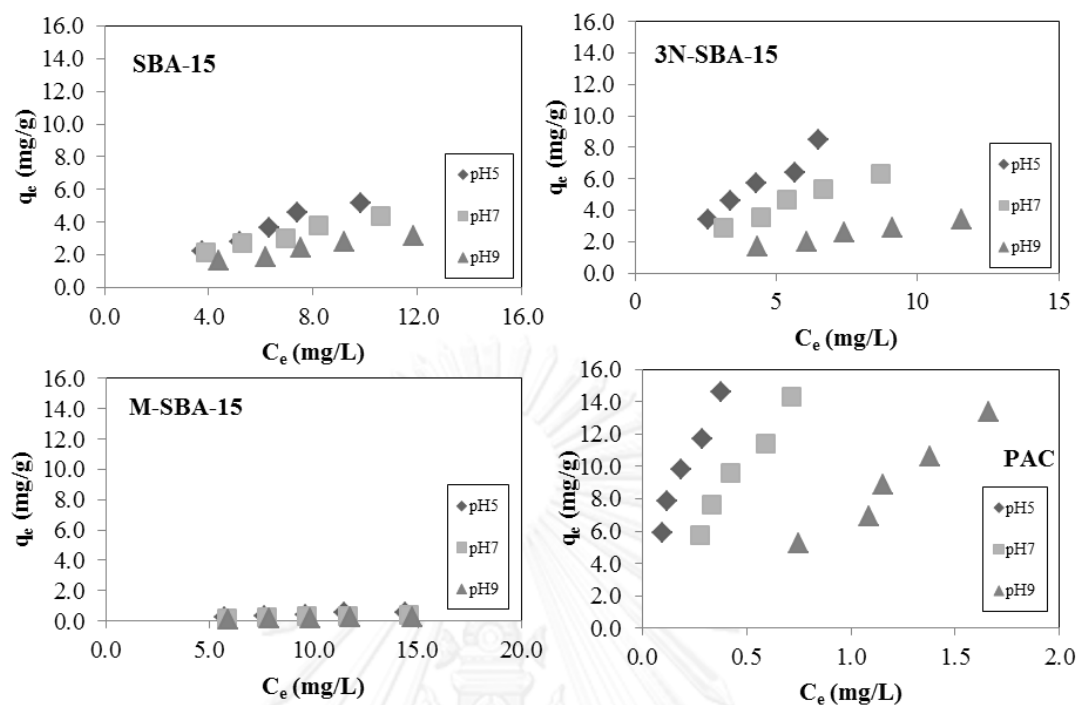
**Figure 4. 13** Effect of pH on CFA adsorption capacities of SBA-15, functionalized SBA-

15

## 4.2.2 Adsorption of clofibric acid (CFA) at low concentration

### 4.2.2.1 Adsorption of clofibric acid (CFA) at low concentration onto 3N-SBA-15

In order to apply for unit operation process at real situation, the adsorption

isotherm of CFA at low concentration (ppb) was investigated. Since 3N-SBA-15 is the

highest adsorption capacity when comparing with other synthesized adsorbents.

Therefore, 3N-SBA-15 was chosen to investigate of adsorption isotherm of CFA onto

3N-SBA-15 at low concentration. Phosphate buffer 2 mM was used to control the pH

of the solution at 7. The ratio of adsorbent to adsorbate was fixed at 1g/L. The

samples were agitated in a magnetic stirrer at static condition at 25 °C. The samples

were collected at 24 hr. The obtained results showed that the Linear isotherm

model gave the highest $R^2$ values. **Table 4. 7** showed the calculated parameters for

isotherm models of absorbent. According to the literature, they found that low concentration of solute is obtained by the Linear isotherm that the amount of solute was adsorbed on a fraction of monolayer capacity (Faust & Aly, 1987). The percentage of CFA removal at low concentration was 56.50%.

**Table 4. 7** Isotherm parameters for adsorption of CFA at low concentration at pH7

| Adsorbents | Linear | | Langmuir | | | Freundlich | | | |
|---|---|---|---|---|---|---|---|---|---|
| | $K_p$ (L/µg) | $R^2$ | $K_L$ (L/µg) | $q_m$ (µg/g) | $R^2$ | $1/n$ | $n$ | $K_{fr}$ | $R^2$ |
| 3N-SBA-15 | 1.252 | 0.992 | 0.0044 | 370.37 | 0.983 | 0.886 | 1.128 | 2.057 | 0.988 |
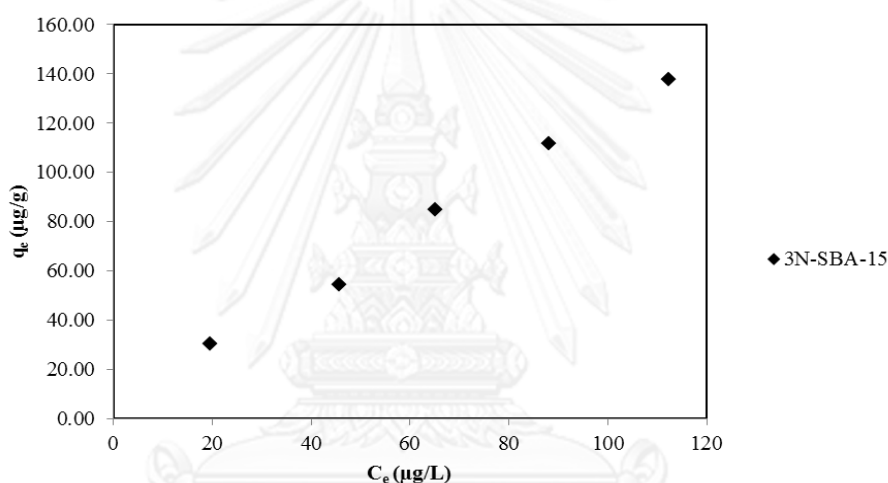


**Figure 4. 14** Adsorption capacities of CFA onto 3N-SBA-15 at low concentration

(pH 7 and IS 2mM)

In addition, the adsorption of CFA per surface area of 3N-SBA-15 was plotted with equilibrium concentration of CFA to demonstrate the effect of surface area to adsorption capacity as shown in **Figure 4. 15** and the adsorption of CFA per mole of nitrogen in 1 g. of 3N-SBA-15 was also plotted to demonstrate the effect of amount of nitrogen in 3N-SBA-15 as shown in **Figure 4. 16**.
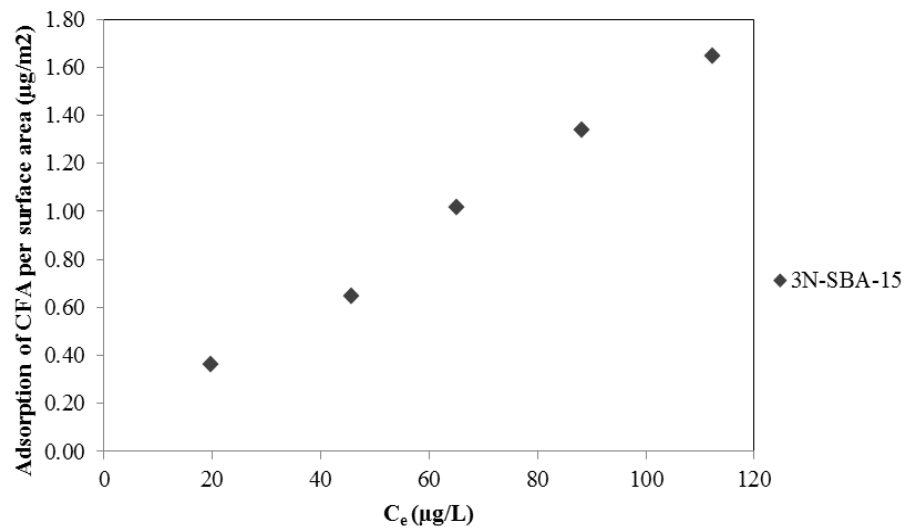
**Figure 4. 15** Adsorption of CFA per surface area at low concentration (pH 7 and IS 2mM)
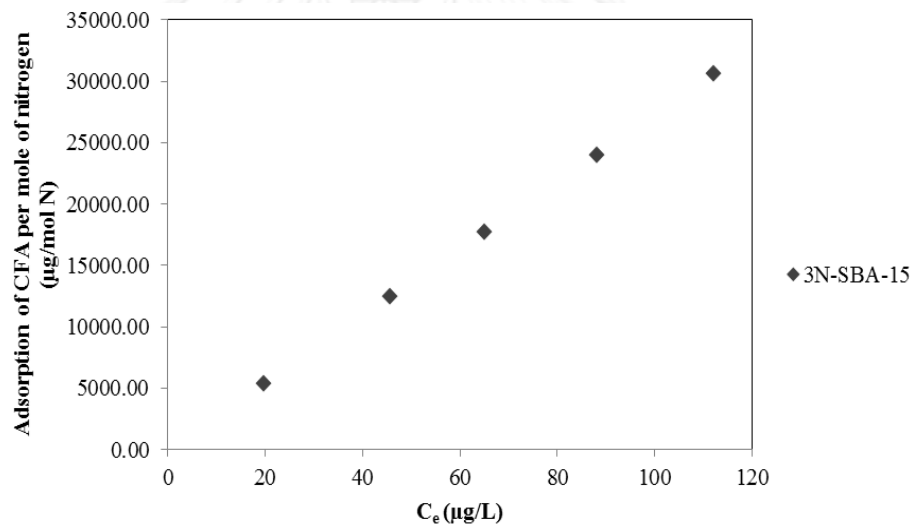


**Figure 4. 16** Adsorption of CFA per mole of nitrogen at low concentration

(pH 7 and IS 2mM)

*4.2.2.2 Comparison between adsorption of clofibric acid (CFA) at low concentration onto 3N-SBA-15 and A-HMS*
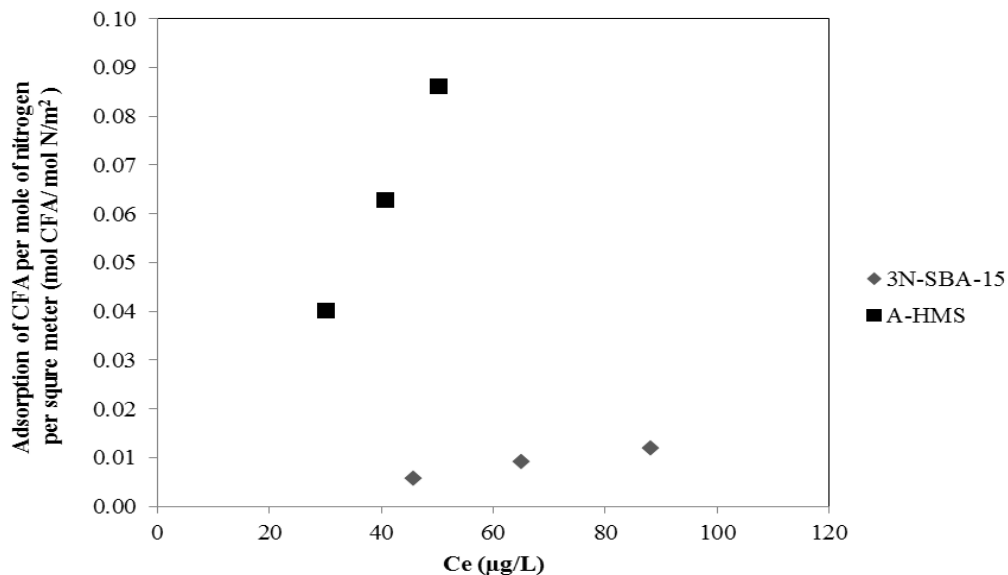


**Figure 4. 17** Adsorption of CFA per mole of nitrogen per squre meter
(mol CFA/mol N/m$^2$)

**Table 4. 8** Calculated mole of CFA per mole of nitrogen on 3N-SBA-15 and A-HMS

| Adsorbents | Initial concentration of CFA (μg/L) | Mole of CFA ($10^{-7}$) | Mole of nitrogen ($10^{-3}$) | Mole of CFA/Mole of nitrogen ($10^{-5}$) |
|---|---|---|---|---|
| 3N-SBA-15 | 100 | 2.53 | 3.67 | 6.89 |
| | 150 | 3.96 | 3.67 | 10.78 |
| | 200 | 5.21 | 3.67 | 14.20 |
| A-HMS | 100 | 1.63 | 1.06 | 15.36 |
| | 150 | 2.54 | 1.06 | 24.00 |
| | 200 | 3.49 | 1.06 | 32.91 |

Furthermore, the study of effect of the amount of amine functional group on adsorbent surface was investigated. The adsorption capacity at low concentration was plotted between mole of CFA per mole of nitrogen in 1 g. of adsorbent and concentration at equilibrium (*Ce*) as shown in **Figure 4. 17**. The data of 3N-SBA-15 used in this study were compared with the data of A-HMS which synthesized by co-

condensation method with mono-amino functional group of the literature from (Suriyanon et al., 2013) as shown in **Table 4. 8** Calculated mole of CFA per mole of nitrogen on 3N-SBA-15 and A-HMS **Table 4. 8**. **Table 4. 8** showed that the adsorption capacities (mg/g) of both two adsorbents were quite similar, but A-HMS had higher amount of CFA adsorption per mol of nitrogen than 3N-SBA-15 as shown in **Figure 4. 17**. It indicated that at low concentration of CFA is not necessary to increase the amount of amino functional group on adsorbent to be higher than obtained from 3N-SBA-15.

### 4.2.3 Adsorption of clofibric acid (CFA) in treated wastewater from swine farm

To study the effect of NOM on CFA adsorption, the discharged wastewater from wastewater treatment plant (WWTP) of swine farm in Chiang Mai province of Thailand was used as background water sample of this study. Before using, water sample was separated natural organic matters (NOM) to be hydrophilic NOM (HPI) and hydrophobic NOM (HPO) by fractionation of ion exchange resin. The result of TOC showed that the concentration of dissolve organic carbon of HPO and HPI were 0.7179 mg/L and 0.7826 mg/L, respectively. The study of effect of NOM on CFA adsorption onto 3N-SBA-15 at high concentration was conducted at an initial CFA concentration range between 6-15 mg/L with pH at treated wastewater. The ratio of adsorbent to adsorbate was fixed at 1g/L. The samples were agitated in a magnetic stirrer at static condition at 25 °C. The samples were collected at 24 hr.

7
6
5
4
$q_e$ (mg/g)
3
2
1
0

0　　　　5　　　　10　　　　15

$C_e$ (mg/L)

◆ CFA with HPO NOM
▲ CFA with HPI NOM
■ CFA without NOM
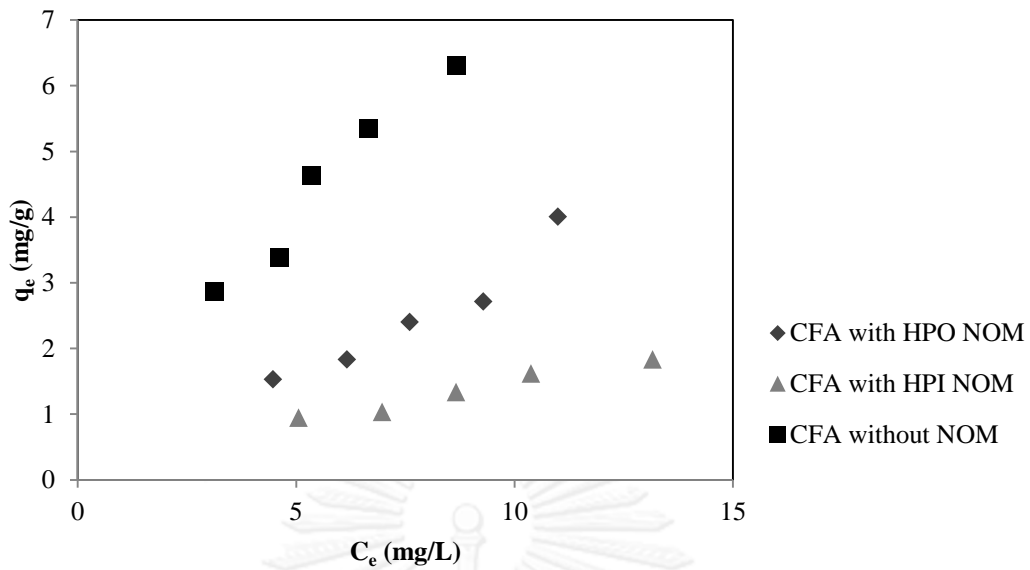
**Figure 4. 18** Effect of NOM on CFA adsorption capacities of 3N-SBA-15

From

**Figure 4. 18** showed the adsorption of CFA with HPO NOM and HPI NOM comparing with the adsorption of CFA at high concentration with pH 7 which is nearly pH of treated wastewater. The obtained results indicated that the presence of both of HPO and HPI NOM can decrease CFA adsorption capacity. It might be caused by two mechanisms that were direct adsorption competition and pore blocking onto 3N-SBA-15 (Ridder et al., 2011).
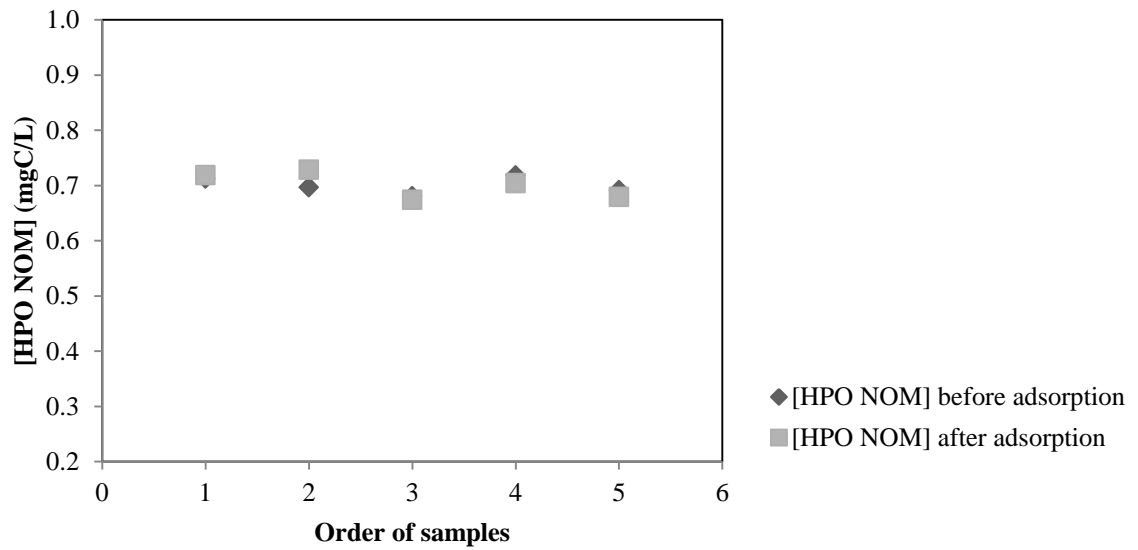
Figure 4. 19 The concentration of hydrophobic NOM before and after CFA adsorption onto 3N-SBA-15
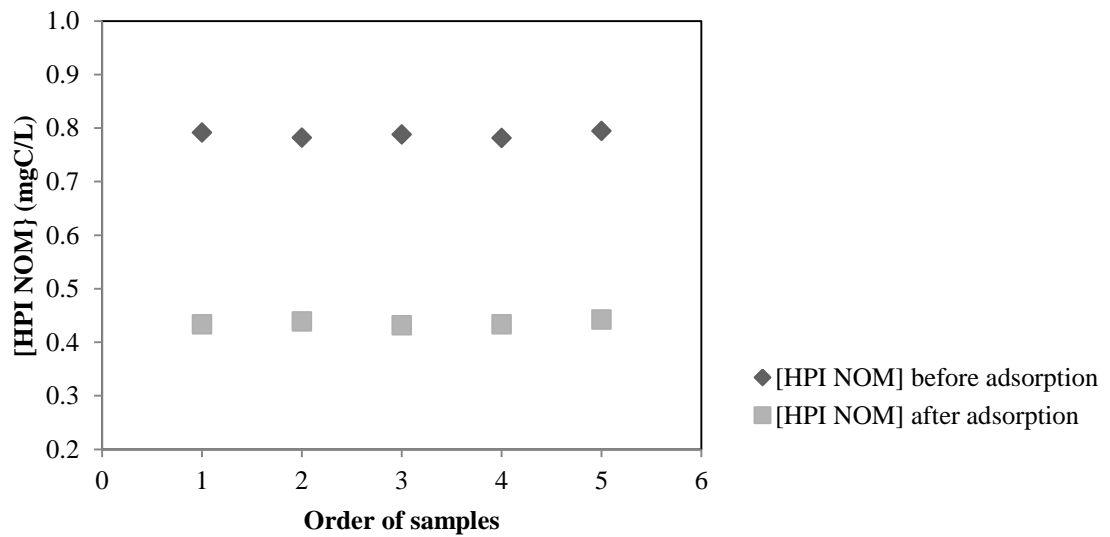


Figure 4. 20 The concentration of hydrophillic NOM before and after CFA adsorption onto 3N-SBA-15

From

Figure 4. 18, it can be indicated that the adsorption capacity of CFA with HPI NOM was lower than the adsorption capacity of HPO NOM. It may be because of

adsorption competition between CFA and HPI NOM that 3N-SBA-15 is hydrophilic adsorbent, so it had the interaction between adsorbent and HPI NOM by hydrophilic interaction through hydrogen bonding.

The adsorption competition can confirm by **Figure 4. 20** that showed the concentration of HPI NOM was decreased from the initial concentration after adsorption. Moreover, HPI NOM can block pore of adsorbent that might decrease the active adsorption sites on surface of adsorbent that could lead to lower adsorption capacity of CFA. Furthermore, HPI NOM can interact with CFA via the hydrophilic interaction (Navon et al., 2011). On the other hand, HPO NOM did not prefer to interact with 3N-SBA-15 that adsorption competition between CFA and HPO NOM did not occur that can confirm by **Figure 4. 19.** Therefore, the higher adsorption capacity of CFA than HPI NOM might have only pore blocking of HPO NOM onto adsorbent that decreased the active adsorption sites on surface of adsorbent (Ridder et al., 2011).

### 4.2.4 Calculation of the mass transfer parameters

*4.2.4.1 Calculation of the mass transfer parameters of all adsorbents*

The mass transfer parameters that consist of liquid film mass transfer coefficient ($k_f$), solid film mass transfer coefficient ($k_s$), overall solid-phase mass transfer coefficient ($K_s$), overall liquid-phase mass transfer coefficient ($K_f$), and constant diffusivity ($D_s$), were calculated from the results of adsorption kinetic by using **Equation 4.11-4. 14**. The calculated mass transfer parameters are shown in **Table 4. 9.**

Mass transfer through liquid film can be described by rate law that calls "Linear driving force" (LDF) as shown **Equation 4. 11**.

$$\frac{\partial \overline{q}}{\partial t} = k_f S_0 (C - C_i)$$ (4.11)

$\overline{q}$ is the average solute concentration in solid (M/V). $C$ is the concentration of the solute in bulk solution (M/V). $C_i$ isthe concentration of solute in liquid interface (M/V). $S_0$ is the surface area of particle per unit volume of adsorbent (M/V) and $k_f$ is the liquid film mass transfer coefficient (L/T).

Mass transfer through particle pore can describe by "Homogeneous solid diffusion model" (HSDM) that has Diffusivity ($D_s$) as shown in **Equation 4.12**.

$$\frac{\partial q}{\partial t} = \frac{D_s}{r^2} \frac{\partial}{\partial r} (r^2 - \frac{\partial q}{\partial r})$$ (4.12)

$r$ is the radial position (L) and $D_s$ is constant diffusivity (L$^2$/T). Crank presents the solution to solve **Equation 4.12** that can be rewritten in **Equation 4.13** (Crank, 1956)

$$\frac{\overline{q}}{q_\infty} = 6 \left( \frac{D_s t}{R^2} \right)^{1/2} \left[ \pi^{1/2} + L \right]$$

**(4.13)**

The slope of a plot between $\dfrac{\overline{q}}{q_\infty}$ and $t^{1/2}$ is $6 \left( \dfrac{D_s}{\pi R^2} \right)^{1/2}$ that can calculate $D_s$ from the slope value and $q_\infty$ is average solute concentration in solid at infinite time.

Mass transfer through solid film can be express in rate law that calls "Linear driving force" (LDF) as shown in **Equation 4.14**.

$$\frac{\partial \overline{q}}{\partial t} = k_s S_0 (q_i - \overline{q})$$ (4.14)

$q_i$ is the solid concentration at interface (M/V) and $k_s$ is the solid film mass transfer coefficient (L/T).

The presence of Overall solid-phase mass transfer coefficient ($K_s$) can be rewritten as **Equation 4.15.**

$$\frac{\partial \bar{q}}{\partial t} = K_s S_0 (q_e - \bar{q}) \tag{4.15}$$

$K_s$ is Overall solid-phase mass transfer coefficient and $q_e$ is value of $q$ at equilibrium (M/V).

$$\frac{1}{K_s} = \frac{m}{k_f} + \frac{1}{k_s} \tag{4.16}$$

$m$ is slope of a plot between $q$ and $C$. In case of the presence of Overall liquid-phase mass transfer coefficient ($K_f$) can be rewritten as **Equation 4.17**.

$$\frac{\partial \bar{q}}{\partial t} = K_f S_0 (C - C_e) \tag{4.17}$$

$C_e$ is value of $C$ at equilibrium (M/V).

$$\frac{1}{K_f} = \frac{1}{k_f} + \frac{1}{mk_s} \tag{4.18}$$

According to **Equation 4.16** and **4.18**, it has relationship between $K_s$ and $K_f$ as **Equation 4.19**.

$$K_f = mK_s \tag{4.19}$$

Furthermore, It has relationship between $k_s$ and $D_s$ as **Equation 4.20** (Glueckauf, 1955)

$$k_s = \frac{5D_s}{R} \tag{4.20}$$

By $S_o = 3/R$ for spherical particle

**Table 4. 9** Calculated mass transfer parameters of SBA-15, functionalized SBA-15, and PAC (pH 7 and IS 2mM)

| Adsorbents | $k_f (10^{-3})^1$ (cm/hr) | $k_s (10^{-5})^1$ (cm/hr) | $K_f (10^{-6})^1$ (cm/hr) | $K_s (10^{-5})^1$ (cm/hr) | $D_s (10^{-9})^1$ (cm$^2$/hr) |
|---|---|---|---|---|---|
| SBA-15 | 2.34 | 5.50 | 24.15 | 5.45 | 7.03 |
| 3N-SBA-15 | 2.41 | 18.92 | 138.81 | 17.82 | 18.12 |
| M-SBA-15 | 0.1525 | 5.70 | 1.73 | 5.63 | 6.00 |
| PAC | 851.78 | 124.34 | 550.84 | 124.26 | 908.67 |

*1 = Calculation of mass transfer parameters are shown in APPENDIX D CALCULATION OF MASS TRANSFER PARAMETERS

### 4.2.4.2 Comparison of the mass transfer parameters of SBA-15

The application of the mass transfer parameters at high concentration were compared with the mass transfer parameters at low concentration which were calculated from the result of adsorption kinetic data of previous literature (Suriyanon et al., 2013) that the adsorption of CFA was studied at low concentration onto SBA-15 as shown in **Table 4. 10.** The obtain result indicated that the mass transfer parameters at low concentration were slightly higher than the mass transfer parameters at high concentration. It might be caused by different of fixed ionic strength of both low and high concentration experiments. At low concentration experiment (from previous literature) the effect of ionic strength (IS=0.01M) should be higher than at high concentration experiment (IS=2 mM) (in this study).

**Table 4. 10** Calculated mass transfer parameters of SBA-15 at high concentration and SBA-15 at low concentration of CFA (pH 7 and IS 2mM)

| Adsorbents | $k_f$ ($10^{-3}$) (cm/hr) | $k_s$ ($10^{-5}$) (cm/hr) | $K_f$ ($10^{-6}$) (cm/hr) | $K_s$ ($10^{-5}$) (cm/hr) | $D_s$ ($10^{-9}$) (cm$^2$/hr) |
|---|---|---|---|---|---|
| SBA-15 (at high concentration of CFA) | 2.34 | 5.50 | 24.15 | 5.45 | 7.03 |
| SBA-15 (at low concentration of CFA)[a] | 2.80* | 6.70* | 21.81* | 6.66* | 8.57* |

* The adsorption kinetic parameters of low concentration were calculated from (Suriyanon et al., 2013)

CHAPTER V

CONCLUSION AND RECOMMENDATIONS

5.1 CONCLUSION

According to the adsorption kinetic study at high concentration, the concentration of CFA decreased rapidly in the first 1 hr. and reach equilibrium within 6 hrs. for all synthesized adsorbents. The results were fitted well with the pseudo-second order for all adsorbents. The initial adsorption rates ($h$) of CFA of 3N-SBA-15 was higher than the others synthesized adsorbents. Intraparticle diffusion is not the only rate-limiting step. Therefore, film and intraparticle diffusion mechanism might control the adsorption rate together.

The Freundlich isotherm model gave highest $R^2$ values for all adsorbents. At pH 7 the adsorption capacities of all adsorbents for CFA followed the order: 3N-SBA-15> SBA-15> M-SBA-15. The mechanisms that can occur for their adsorption onto SBA-15 and functionalized SBA-15 are attractive electrostatic interaction combining with hydrogen bonding. Hydrophilic interaction also plays an important role comparing with hydrophobic interaction. Moreover, the result showed that surface area might not the main reason in adsorption of CFA, but it might be the functional groups that were grafted on adsorbents.

Effects of pH on adsorption capacities of CFA were investigated at pH 5, 7, and 9. The results showed that the adsorption capacity followed the order: pH5>pH7>pH9. The highest adsorption capacity was pH 5 which strongly related to the attractive electrostatic interaction.

The studies of adsorption isotherm of CFA onto 3N-SBA-15 at low concentration were investigated and the Linear isotherm model can fit well to the

isotherm .The presence of NOM can decrease CFA adsorption capacity both of hydrophobic and hydrophilic NOM by direct adsorption competition and pore blocking onto 3N-SBA-15.

The calculation of the mass transfer parameters were reported and were compared with the mass transfer parameters at low concentration which were calculated from the result of adsorption kinetic data of Suriyanon, 2013. The obtain result indicated that the mass transfer parameters at low concentration were slightly higher than the mass transfer parameters at high concentration. It might be because of at low concentration the ionic strength was higher than at high concentration.

## 5.2 RECOMMENDATIONS

1. The study of adsorption mechanism should be done at low concentration for application of unit operation process.

2. Improvement of the adsorption mechanism should use high efficiency equipment that has high performance to identify.

3. The study of the effect of NOM in wastewater should use various sources of wastewater.

4. Mesoporous materials should be developed by using different functional groups to improve adsorption capacity of adsorbent.

5. The regeneration after use of all adsorbents should be studied.

6. The study of the effect of combination of pharmaceuticals should be studied to understand adsorption selectivity of adsorbents.

7. Development of high stability and high surface area of amino functionalized porous silica should be investigated, in order to enhance the adsorption capacity to be comparable level with PAC.

# REFERENCES

Abechi, E. S., Gimba, C. E., Uzairu, A., & Kagbu, J. A. (2011). Kinetics of adsorption of methylene blue onto activated carbon prepared from palm kernel shell. *Archives of Applied Science Research, 3*, 154-164.

Ahmad, A., Rafatullah, M., Sulaiman, O., Ibrahim, M. H., Chii, Y. Y., & Siddique, B. M. (2009). Removal of Cu(II) and Pb(II) ions from aqueous solutions by adsorption on sawdust of Meranti wood. *Desalination, 247*(1-3), 636-646. doi: 10.1016/j.desal.2009.01.007

Albadarin, A. B., Mangwandi, C., Muhtaseb, A. A. H., Walker, G. M., Allen, S. J., & Ahmad, M. N. M. (2012). Kinetics and thermodynamics of chromium ions adsorption onto low-cost dolomite adsorbent. *Chem. Eng. J., 179*, 193-202.

Bai, Y., Wu, F., Liu, C., Guo, J., Fu, P., Li, W., & Xing, B. (2008). Interaction between carbamazepine and humic substances: a fluorescence spectroscopy study. *Environ. Toxicol. Chem., 27*(1), 95-102.

Barnes, K. K., Kolpin, D. W., Furlong, E. T., Zaugg, S. D., Meyer, M. T., & Barber, L. B. (2008). A national reconnaissance of pharmaceuticals and other organic wastewater contaminants in the United States--I) groundwater. *Sci Total Environ, 402*(2-3), 192-200. doi: 10.1016/j.scitotenv.2008.04.028

Boyd, G. R., Reemtsma, H., Grimm, D. A., & Mitra, S. (2003). Pharmaceuticals and personal care products (PPCPs) in surface and treated waters of Louisiana, USA and Ontario, Canada.. *Science of the Total Environment, 311*(1-3), 135-149.

Bui, T. X., & Choi, H. (2009). Adsorptive removal of selected pharmaceuticals by mesoporous silica SBA-15. *J Hazard Mater, 168*(2-3), 602-608. doi: 10.1016/j.jhazmat.2009.02.072

Bui, T. X., & Choi, H. (2010). Influence of ionic strength, anions, cations, and natural organic matter on the adsorption of pharmaceuticals to silica. *Chemosphere, 80*(7), 681-686. doi: 10.1016/j.chemosphere.2010.05.046

Bui, T. X., Kang, S. Y., Lee, S. H., & Choi, H. (2011). Organically functionalized mesoporous SBA-15 as sorbents for removal of selected pharmaceuticals from water. *J Hazard Mater, 193*, 156-163. doi: 10.1016/j.jhazmat.2011.07.043

Bui, T. X., Pham, V. H., Le, S. T., & Choi, H. (2013). Adsorption of pharmaceuticals onto trimethylsilylated mesoporous SBA-15. *J Hazard Mater, 254-255*, 345-353. doi: 10.1016/j.jhazmat.2013.04.003

Buser, H. R., Müller, M. D., & Theobald, N. (1998). Occurrence of the pharmaceutical drug clofibric acid and the herbicide mecoprop in various Swiss Lakes and in the North Sea *Environmental Science and Technology, 32*, 188-192.

Carabineiro, S. A., Thavorn-Amornsri, T., Pereira, M. F., & Figueiredo, J. L. (2011). Adsorption of ciprofloxacin on surface-modified carbon materials. *Water Res, 45*(15), 4583-4591. doi: 10.1016/j.watres.2011.06.008

Castiglioni, S., Bagnati, R., Fanelli, R., Pomati, F., Calamari, D., & Zuccato, E. (2006). Removal of pharmaceuticals in sewage treatment plants in Italy. *Environmental Science and Technology, 40*, 357-363.

Cooney, D. O. (1998). Adsorption Design for Wastewater Treatment.

Crank, J. (1956). Mathematic of Diffusion. *Oxford at the Clarendon Press*.

Cunningham, V. L., Binks, S. P., & Olson, M. J. (2009). Human health risk assessment from the presence of human pharmaceuticals in the aquatic environment. *Regulatory Toxicology and Pharmacology, 53*, 39-45.

Dabrowski, A. (2001). Adsorption- from theory to practice. *Advance in Colloid and Interface Science, 93*, 135-224.

Diaz-Cruz, M. S., & Barcelo, D. (2006). Determination of antimicrobialresidues and metabolites in the aquatic environment by liquid chromatography tandem mass spectrometry. . *Anal. Bioanal. Chem, 386*, 973-985.

Dickey, F. H. (1949). *Preparation of specific adsorbents.* Paper presented at the Proceedings of the national academy of sciences

Domínguez, J. R., González, T., Palo, P., & Cuerda-Correa, E. M. (2011). Removal of common pharmaceuticals present in surface waters by Amberlite XAD-7 acrylic-ester-resin: Influence of pH and presence of other drugs. *Desalination, 269*(1-3), 231-238. doi: 10.1016/j.desal.2010.10.065

Fabrega, A., Sanchez-Cespedes, J., Soto, S., & Vila, J. (2008). Quinolone resistance in the food chain. *Int J Antimicrob Agents, 31*(4), 307-315. doi: 10.1016/j.ijantimicag.2007.12.010

Faust, S. D., & Aly, O. M. (1987). *Adsorption processes for water treatment*: Butterworth.

Fent, K., Weston, A. A., & Caminada, D. (2006). Ecotoxicology of human pharmaceuticals. *Aquat Toxicol, 76*(2), 122-159. doi: 10.1016/j.aquatox.2005.09.009

Ferrari, B. t., Paxéus, N., Giudice, R. L., Pollio, A., & Garric, J. (2003). Ecotoxicological impact of pharmaceuticals found in treated wastewaters: study of

carbamazepine, clofibric acid, and diclofenac. *Ecotoxicology and Environmental Safety, 55*(3), 359-370. doi: 10.1016/s0147-6513(02)00082-9

Fick, J., Soderdtrom, H., Lindberg, R. H., Phan, C., Tysklind, M., & J., L. D. G. (2009). Contamination of surface, ground, and drinking water from pharmaceutical production. *Environmental Toxicology and Chemistry, 28*, 2522-2527.

Figueroa, R. A., Leonard, A., & MacKay, A. A. (2004). Modeling tetracycline antibiotic sorption to clays. *Environmental Science Technology, 38*, 2522-2527.

Glueckauf, E. (1955). Theory of chromatography. *Trans Faraday Soc., 51*, 1540.

Gogate, P. R., & Pandit, A. B. (2004). A review of imperative technologies for wastewater treatment I: oxidation technologies at ambient conditions. *Advances in Environmental Research, 8*(3-4), 501-551. doi: 10.1016/s1093-0191(03)00032-7

Goldberg, S. (2005). Equations and Models Describing Adsorption Processes in Soils. . *Soil Science Society of America, 677*.

Goodman, L. S., Gilman, A. G., Rall, T. W., Nies, A. s., & Taylor, P. (1990). Goodman and Gilman's the pharmaceutical basis of therapeutics. *Pergamon, 8*.

Gros, M., Petrovic, M., Ginebreda, A., & Barcelo, D. (2010). Removal of pharmaceuticals during wastewater treatment and environmental risk assessment using hazard indexes. *Environ Int, 36*(1), 15-26. doi: 10.1016/j.envint.2009.09.002

Haller, M. Y., Muller, S. R., McArdell, C. S., Alder, A. C., & Suter, M. J. F. (2002). Quantification of veterinary antibiotics (sulfonamides and trimethoprim) in animal manure by liquid chromatography–mass spectrometry. *Journal of Chromatography A, 952*, 111-120.

Halling-Sorensen, B., Holten Lützhøft, H.-C., Andersen, H. R., & Ingerslev, F. (2000). Environmental risk assessment of antibiotics: comparison of mecillinam, trimethoprim and ciprofloxacin. *Journal of Antimicrobial Chemotherapy, 46*, 53-58.

Hamoudi, S., El-Nemr, A., & Belkacemi, K. (2010). Adsorptive removal of dihydrogenphosphate ion from aqueous solutions using mono, di- and tri-ammonium-functionalized SBA-15. . *J Colloid Interface Sci, 343*(2).

Heberer, T. (2002). Occurrence, fate, and removal of pharmaceutical residues in the aquatic environment: a review of recent research data. *Toxicology Letter, 131*, 5-17.

Heberer, T., Butz, S., & Stan, H. J. (1995). Analysis of phenoxycarboxylic acids and other acidic compounds in tap, ground, surface, and sewage water at the low ppt-level. *Int. J. Environ. Anal. Chem., 58*, 43-54.

Hepplewhite, C., Newcombe, G., & Knappe, D. R. U. (2004). NOM and MIB, Who Wins in the Competition for Activated Carbon Adsorption Sites? . *Water Science and Technology, 49*(9), 257-265.

Hernandez-Ruiz, S., Abrell, L., Wickramasekara, S., Chefetz, B., & Chorover, J. (2012). Quantifying PPCP interaction with dissolved organic matter in aqueous solution: combined use of fluorescence quenching and tandem mass spectrometry. *Water Res, 46*(4), 943-954. doi: 10.1016/j.watres.2011.11.061

Ho, Y. S., & Mckay, G. (1999). Pseudo-second order model for sorption processes *Process Biochemistry, 34*, 451-465.

Hodaifa, G., Ochando-Pulido, J. M., Driss Alami, S. B., Rodriguez-Vives, S., & Martinez-Ferez, A. (2013). Kinetic and thermodynamic parameters of iron adsorption onto olive stones. *Industrial Crops and Products, 49*, 526-534. doi: 10.1016/j.indcrop.2013.05.039

Hoffmann, F., Cornelius, M., Morell, J., & Froba, M. (2006). Silica-based mesoporous organic-inorganic hybrid materials. *Angew Chem Int Ed Engl, 45*(20), 3216-3251. doi: 10.1002/anie.200503075

Hongsawat, P., Prarat, P., Ngamcharussrivichai, C., & Punyapalakul, P. (2013). Adsorption of ciprofloxacin on surface functionalized superparamagnetic porous silicas. . *Desalination and Water Treatment*, 1-14.

Kar, S., & Roy, K. (2010). First report on interspecies quantitative correlation of ecotoxicity of pharmaceuticals. *Chemosphere, 81*, 738-747.

Kavitha, D., & Namasivayam, C. (2007). Experimental and kinetic studies on methylene blue adsorption by coir pith carbon. *Bioresour. Technol., 98*, 14-21.

Kolpin, D. W., Furlong, E. T., Meyer, M. T., Thurman, E. M., Zaugg, S. D., Barber, L. B., & Buxton, H. T. (2002). Pharmaceuticals, hormones, and other organic wastewater contaminants in US streams, 1999–2000: a national reconnaissance. *Environmental Science Technology, 36*, 1202-1211.

Lagergren, S. (1898). Zurtheorie der sogenannten adsorption gelosterstoffe. *K. Vet. Akad. Hand, 24*(1-39).

Lajeunesse, A., & Gagnon, C. (2007). Determination of acidic pharmaceutical products and carbamazepine in roughly primary-treated wastewater by solid-phase extraction and gaschromatography-tandem mass spectrometry. *Int. J. Environ. Anal. Chem., 87*(8), 565-578.

Langmuir, I. (1916). The constitution and fundamental properties of solids and liquids. part i. solids. *J. Am. Chem. Soc., 38*(11), 2221-2295.

Li, Y., Zhang, F., Liang, X., & Yediler, A. (2013). Chemical and toxicological evaluation of an emerging pollutant (enrofloxacin) by catalytic wet air oxidation and ozonation in aqueous solution. *Chemosphere, 90*(2), 284-291. doi: 10.1016/j.chemosphere.2012.06.068

Lindsey, M. E., Meyer, M. Y., & Thurman, E. M. (2001). Analysis of trace levels of sulfonamide and tetracycline antimicrobials in groundwater and surface water using solid-phase extraction and liquid-chromatography/mass spectrometry. *Analytical of Chemistry, 73*, 4640-4646.

Liu, M., Hou, L.-a., Yu, S., Xi, B., Zhao, Y., & Xia, X. (2013). MCM-41 impregnated with A zeolite precursor: Synthesis, characterization and tetracycline antibiotics removal from aqueous solution. *Chemical Engineering Journal, 223*, 678-687. doi: 10.1016/j.cej.2013.02.088

Loffler, D., Rombke, J., Meller, M., & Ternes, T. A. (2005). Environmental fate of pharmaceuticals in water/sediment systems. *Environmental Science Technology, 39*, 5209-5218.

Matilainen, A., Gjessing, E. T., Lahtinen, T., Hed, L., Bhatnagarf, A., & Sillanpää, M. (2011). An overview of the methods used in the characterisation of natural organic matter (NOM) in relation to drinking water treatment. *Chemosphere, 83*, 1431-1442.

Molu, Z. B., & Yurdakoç, K. (2010). Preparation and characterization of aluminum pillared K10 and KSF for adsorption of trimethoprim. *Microporous and Mesoporous Materials, 127*(1-2), 50-60. doi: 10.1016/j.micromeso.2009.06.027

Navon, R., Hernandez-Ruiz, S., Chorover, J., & Chefetz, B. (2011). Interactions of carbamazepine in soil: effects of dissolved organic matter. . *J. Environ. Qual., 40*(3), 942-948.

Newcombe, G., & Cook, D. (2002). Influences on the Removal of Tastes and Odours by PAC. *Aqua, 51*(8), 463-474.

Nie, Y., Deng, S., Wang, B., Huang, J., & Yu, G. (2013). Removal of clofibric acid from aqueous solution by polyethylenimine-modified chitosan beads   *Frontiers of Environmental Science & Engineering*.

Ozcan, A., Ozcan, A. S., & Gok, O. (2007). Adsorption kinetics and isotherms of anionic dye of reactive blue 19 from aqueous solutions onto DTMA-sepiolite. *Hazardous Materials and Wastewater*.

Pan, B., Ning, P., & Xing, B. (2009). Part V-sorption of pharmaceuticals and personal care products. *Sci. Pollut. Res., 16*(1), 106-116.

Pocostales, P., Álvarez, P., & Beltrán, F. J. (2011). Catalytic ozonation promoted by alumina-based catalysts for the removal of some pharmaceutical compounds from water. *Chemical Engineering Journal, 168*(3), 1289-1295. doi: 10.1016/j.cej.2011.02.042

Prarat, P., Ngamcharussrivichai, C., Khaodhiar, S., & Punyapalakul, P. (2011). Adsorption characteristics of haloacetonitriles on functionalized silica-based porous materials in aqueous solution. *J Hazard Mater, 192*, 1210-1218.

Punyapalakul, P., & Sitthisorn, T. (2010). Removal of ciprofloxazin and carbamazepine by adsorption on functionalized mesoporous silicates. *World Academy of Science, Engineering and Technology, 69*, 546-550.

Radjenovic, J., Petrovic, M., & Barcelo, D. (2007). Analysis of pharmaceuticals in wastewater and removal using a membrane bioreactor. *Anal Bioanal Chem, 387*(4), 1365-1377. doi: 10.1007/s00216-006-0883-6

Rafatullah, M., Sulaiman, O., Hashim, R., & Ahmad, A. (2009). Adsorption of copper (II), chromium (III), nickel (II) and lead (II) ions from aqueous solutions by meranti sawdust. *J Hazard Mater, 170*(2-3), 969-977. doi: 10.1016/j.jhazmat.2009.05.066

Ray, C., Melin, G., & B, L. R. (2008). The recalcitrance of clofibric acid to microbial degradation. *Water Pollution, 111*, 186.

Ridder, D. J., Verliefde, A. R., Heijman, S. G., Verberk, J. Q., Rietveld, L. C., van der Aa, L. T., . . . van Dijk, J. C. (2011). Influence of natural organic matter on equilibrium adsorption of neutral and charged pharmaceuticals onto activated carbon. . *Water Science and Technology, 63*, 973-985.

Rosal, R., Rodríguez, A., & Gaecia-Calvo, E. (2009). Ozonation of clofibric acid catalyzed by titanium dioxide. *J Hazard Mater, 169*, 411-418.

Rosal, R., Rodríguez, A., Perdigón-Melón, J. A., Mezcua, M., Agüera, A., Hernando, M. D., . . . Fernánández-Alba, A. R. (2008). Removal of pharmaceuticals and kinetics of mineralization by $O_3/H_2O_2$ in a biotreated municipal wastewater. *Water Res, 42*, 3719-3728.

Rossner, A., Snyder, S. A., & Knappe, D. R. (2009). Removal of emerging contaminants of concern by alternative adsorbents. *Water Res, 43*(15), 3787-3796. doi: 10.1016/j.watres.2009.06.009

Sanderson, H., Johnson, D. J., Reitsma, T., Brain, R. A., Wilson, C. J., & Solomon, K. R. (2004). Ranking and prioritization of environmental risks of pharmaceuticals in surface waters. *Regulatory Toxicology and Pharmacology, 39*, 158-183.

Saravanan, M., Karthika, S., Malarvizhi, A., & Ramesh, M. (2011). Ecotoxicological impacts of clofibric acid and diclofenac in common carp (Cyprinus carpio) fingerlings: hematological, biochemical, ionoregulatory and enzymological responses. *Journal of Hazardorus Material, 195*, 188-194.

Saravanan, M., & Ramesh, M. (2013). Short and long-term effects of clofibric acid and diclofenac on certain biochemical and ionoregulatory responses in an Indian major carp, *Cirrhinus mrigala Chemosphere, 93*, 388-396.

Schlusener, M. P., Bester, K., & Spiteller, M. (2003). Determination of antibiotics such as macrolides, ionophores and tiamulin in liquid manure by HPLC-MS/MS. *Anal Bioanal Chem, 375*(7), 942-947. doi: 10.1007/s00216-003-1838-9

Sing, K. S. W. (1982). Reporting physisorption data for gas/solid systems with special reference to determination of surface area and porosity. *Pure & Appl. Chem, 54*, 2201-2218.

Stein, A., Melde, B. J., & Schroden, R. C. (2000). Hybrid inorganic-organic mesoporous silicates-nanoscopic reactors coming of age. *Advanced Materials, 12*, 1403-1419.

Stumpf, M., Ternes, T. A., Wilken, R.-D., Rodrigues, S. V., & Bauman, W. (1999). Polar drug residues in sewage and neutral waters in the state of Rio de Janeiro, Brazil. *Science of the Total Environment, 225*, 135-141.

Suriyanon, N., Punyapalakul, P., & Ngamcharussrivichai, C. (2013). Mechanistic study of diclofenac and carbamazepine adsorption on functionalized silica-based porous materials. *Chemical Engineering Journal, 214*, 208-218. doi: 10.1016/j.cej.2012.10.052

Tanev, P. T., & Chibwe, M. (1994). Titanium-containing mesoporous molecular sieves for catalytic oxidation of aromatic compounds *Nature, 368*, 321-323.

Ternes, T. A., Meisenheimer, M., McDowell, D., Sacher, F., Brauch, H. J., Haist-Gulde, B., . . . Zulei-Seibert, N. (2002). Removal of pharmaceuticals during drinking water treatment. *Environmental Science and Technology, 36*, 3855-3863.

Thomas, A., & Adriano, J. (2006). Human Pharmaceutical, Hormones and Fragrances: The Challenge of Micropollutants in Urban Water Management. *IWA Publishing London*, 293-322.

Tixier, C., Singer, H. P., & Oellers, S. (2003). Occurrence and Fate of carbamazepine, clofibric acid, diclofenac, ibuprofen, ketoprofen, and naproxen in surface waters. *Environmental Science and Technology, 37*, 61-68.

Vazquez-Roig, P., Segarra, R., Blasco, C., Andreu, V., & Picó, Y. (2009). Determination of pharmaceuticals in soils and sediments by pressurized liquid extraction and

liquid chromatography tandem mass spectrometry. *Journal of Chromatography A, 1217*, 2471–2483.

Weber, W. J., & Morris, J. C. (1962). *Advances in water pollution research: removal of biologically resistant pollutants from waste waters by adsorption.* Paper presented at the international Conference on Water Pollution Symposium.

Westerhoff, P., Yoon, Y., Snyder, S. A., & Wert, E. (2005). Fate of endocrine-disruptor, pharmaceutical, and personal care product chemicals during simulated drinking water treatment processes. *Environmental Science and Technology, 39*, 6649-6663.

Yang, W., Zheng, F., Xue, X., & Lu, Y. (2001). Investigation into adsorption mechanisms of sulfonamides onto porous adsorbents. *J Colloid Interface Sci, 362*(2), 503-509. doi: 10.1016/j.jcis.2011.06.071

Ye, Z. Q., Weinberg, H. S., & Meyer, M. T. (2007). Trace analysis of trimethoprim and sulfonamide, macrolide, quinolone, and tetracycline antibiotics in chlorinated drinking water using liquid chromatography electrospray tandem mass spectrometry. *Anal. Chem., 79*, 1135-1144.

Yu, Z., Peldszus, S., & Huck, P. M. (2008). Adsorption characteristics of selected pharmaceuticals and an endocrine disrupting compound-Naproxen, carbamazepine and nonylphenol-on activated carbon. *Water Res, 42*(12), 2873-2882. doi: 10.1016/j.watres.2008.02.020

Zhao, D., Feng, J., Huo, Q., Melosh, N., Fredrickson, G. H., Chmelka, B. F., & Stucky, G. D. (1998). Triblock copolymer syntheses of mesoporous silica with periodic 50 to 300 angstrom. *Pores. Science, 279*, 548-552.

Zwiener, C., & Frimmel, F. H. (2000). Oxidative treatment of pharmaceuticals in water. *Water Res, 34*, 1881-1885.

APPENDIX A

CALIBRATION CURVE

**Analysis concentration of CFA by High Performance Liquid Chromatography (HPLC) with UV detector at high concentration**

<u>**Laboratory Equipment and chemical reagent**</u>

1. High Performance Liquid Chromatography (HPLC) (Prostar, Varian, Germany)

2. Stock solution 0f CFA concentration 100 mg/L

3. Phosphate buffer

4. Volumetric flask

5. Micropipette

6. Deionized water

<u>**Preparation of stock solution of CFA**</u>

CFA 100 mg. was dissolved in deionized water by volumetric flask 1000 mL and was stored in the dark at 4 °C.

Preparation of standard solution of CFA

Pipetted stock solution of CFA followed Table A.1 into volumetric flask 100 mL by calculation from **Equation 1**

$$C_1V_1 = C_2V_2 \qquad\qquad (1)$$

<u>Example</u> Preparation of standard solution of CFA at 10 mg/L from stock solution 100 mg/L in 100 mL of volumetric flask

$$C_1V_1 = C_2V_2$$
$$100 \text{ mg/L} \times V_1 = 10 \text{ mg/L} \times 100 \text{ mL}$$
$$V_1 = 10 \text{ mL}$$

∴ Pipetted stock solution of CFA 10 mL into 100 mL of volumetric flask and adjusted volume of solution by phosphate buffer 2mM until final volume was 100 mL

**Table A. 1** Volume of stock solution

| Concentrations of CFA (mg/L) | Volume of stock solution (mL) |
|:---:|:---:|
| 6 | 6.00 |
| 8 | 8.00 |
| 10 | 10.00 |
| 12 | 12.00 |
| 15 | 15.00 |

## Standard curve

The concentrations of standard solution of CFA were analyzed by HPLC with UV detector at 230 nm. Standard curve was plotted between area of chromatogram and concentration of standard solution of CFA



**Figure A. 1** Standard curve of CFA analysing by HPLC

After we had standard curve, the concentration of CFA was calculated by using equation from standard curve that replaced by area of chromatogram from HPLC.

Analysis concentration of CFA by High Performance Liquid Chromatography (HPLC) with UV detector at low concentration

Laboratory Equipment and chemical reagent

1. High Performance Liquid Chromatography (HPLC) (Prostar, Varian, Germany)

2. Stock solution 0f CFA concentration 10 mg/L

3. Phosphate buffer

4. Volumetric flask

5. Micropipette

6. Deionized water

Preparation of stock solution of CFA

CFA 100 mg. was dissolved in deionized water by volumetric flask 1000 mL and was stored in the dark at 4 ℃.

Preparation of standard solution of CFA

Pipetted stock solution of CFA followed **Table A.1** into volumetric flask 100 mL by calculation from **Equation 1**

$$C_1V_1 = C_2V_2 \tag{1}$$

Example Preparation of standard solution of CFA at 10 mg/L from stock solution 100 mg/L in 100 mL of volumetric flask

$$C_1V_1 = C_2V_2$$
$$10 \text{ mg/L} \times V_1 = 50 \text{ µg/L} \times 100 \text{ mL}$$
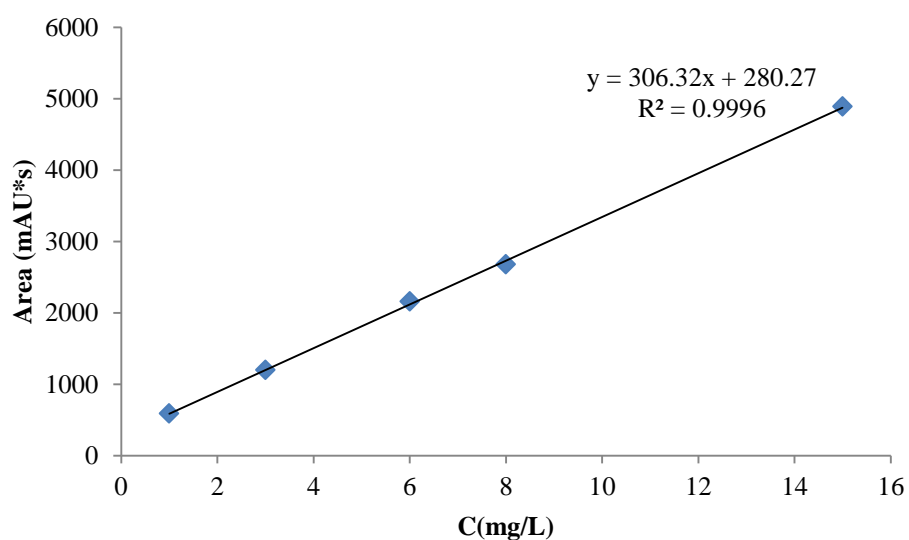$$V_1 = 0.5 \text{ mL}$$

∴ Pipetted stock solution of CFA 0.5 mL into 100 mL of volumetric flask and adjusted volume of solution by phosphate buffer 2mM until final volume was 100 mL

Table A. 2 Volume of stock solution

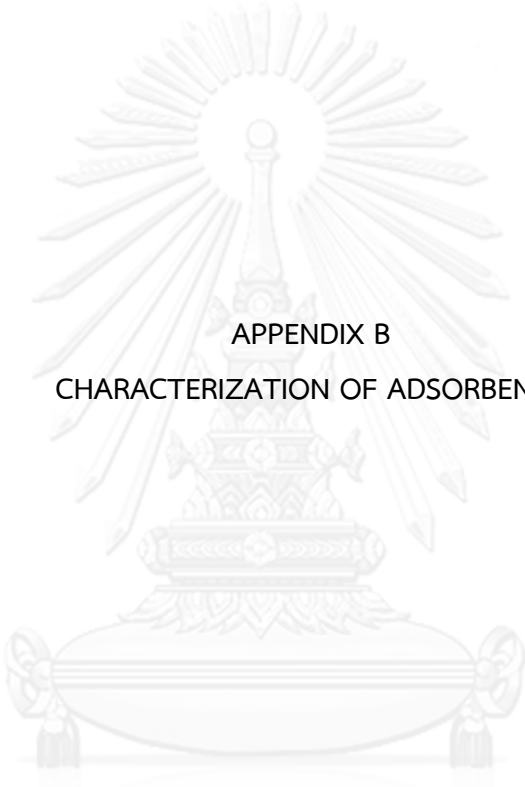| Concentrations of CFA (mg/L) | Volume of stock solution (mL) |
|---|---|
| 50 | 0.50 |
| 100 | 1.00 |
| 150 | 1.50 |
| 200 | 2.00 |
| 250 | 2.50 |

## Standard curve

The concentrations of standard solution of CFA were analyzed by HPLC with UV detector at 230 nm. Standard curve was plotted between area of chromatogram and concentration of standard solution of CFA.
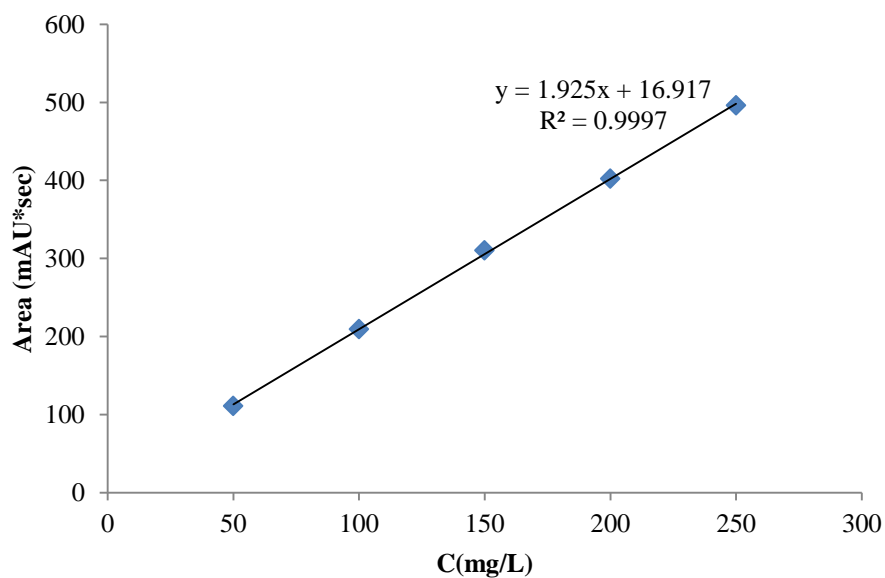


Figure A. 2 Standard curve of CFA analysing by HPLC at low concentration

After we had standard curve, the concentration of CFA was calculated by using equation from standard curve that replaced by area of chromatogram from HPLC.
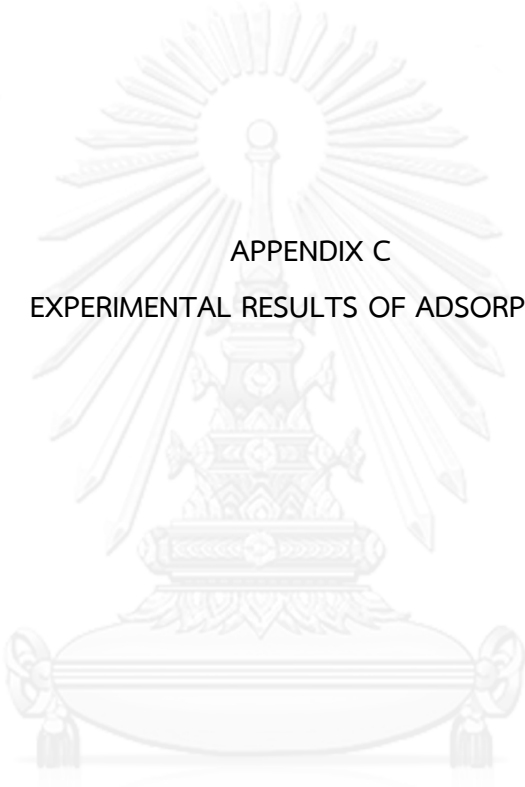
**Analysis concentration of CFA by High Performance Liquid Chromatography (HPLC) with UV detector in treated wastewater from swine farm**

**Laboratory Equipment and chemical reagent**

1. High Performance Liquid Chromatography (HPLC) (Prostar, Varian, Germany)

2. Stock solution 0f CFA concentration 100 mg/L

3. Volumetric flask

4. Micropipette

5. Hydrophilic NOM

6. Hydrophobic NOM

**Preparation of stock solution of CFA**

CFA 100 mg. was dissolved in hydrophilic NOM or hydrophobic NOM by volumetric flask 1000 mL and was stored in the dark at 4 °C.

Preparation of standard solution of CFA

Pipetted stock solution of CFA followed **Table A.1** into volumetric flask 100 mL by calculation from **Equation 1**

$$C_1V_1 = C_2V_2 \tag{1}$$

<u>Example</u> Preparation of standard solution of CFA at 10 mg/L from stock solution 100 mg/L in 100 mL of volumetric flask

$$C_1V_1 = C_2V_2$$
$$100 \text{ mg/L} \times V_1 = 10 \text{ mg/L} \times 100 \text{ mL}$$
$$V_1 = 10 \text{ mL}$$

∴ Pipetted stock solution of CFA 10 mL into 100 mL of volumetric flask and adjusted volume of solution by hydrophilic NOM or hydrophobic NOM until final volume was 100 mL

**Table A. 3** Volume of stock solution

| Concentrations of CFA (mg/L) | Volume of stock solution (mL) |
| --- | --- |
| 6 | 6.00 |
| 8 | 8.00 |
| 10 | 10.00 |
| 12 | 12.00 |
| 15 | 15.00 |

**Standard curve**

The concentrations of standard solution of CFA were analyzed by HPLC with UV detector at 230 nm. Standard curve was plotted between area of chromatogram and concentration of standard solution of CFA



**Figure A. 3** Standard curve of CFA in hydrophilic NOM analysing by HPLC at low concentration
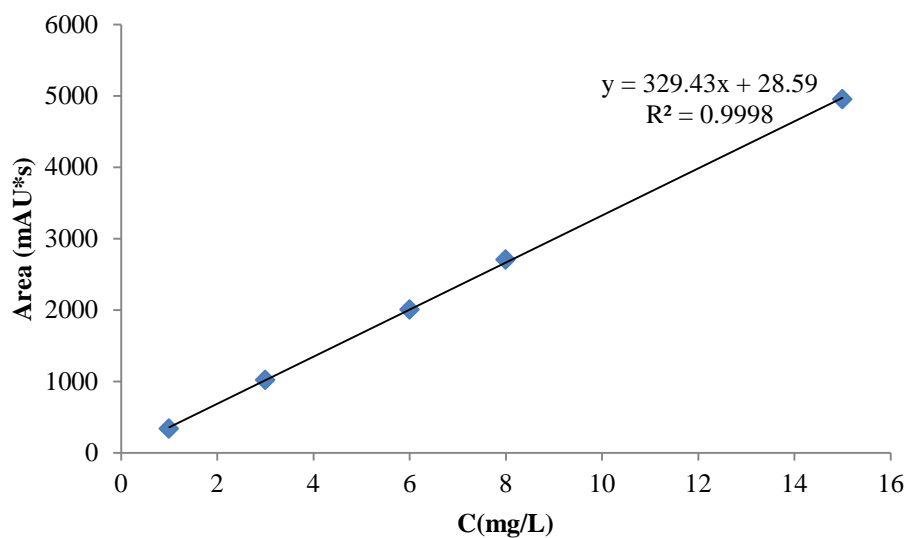
**Figure A. 4** Standard curve of CFA in hydrophobic NOM analysing by HPLC at low concentration

After we had standard curve, the concentration of CFA was calculated by using equation from standard curve that replaced by area of chromatogram from HPLC.

APPENDIX B

CHARACTERIZATION OF ADSORBENTS

**Table B. 1** Surface charge density of SBA-15 and functionalized SBA-15 by acid-base titration

| SBA-15 | | 3N-SBA-15 | | M-SBA-15 | |
|---|---|---|---|---|---|
| pH | Surface charge (C/g) | pH | Surface charge (C/g) | pH | Surface charge (C/g) |
| 3.43 | 0.2243 | 8.51 | 0.0306 | 3.59 | 0.2788 |
| 4.34 | -0.0182 | 8.94 | 0.0273 | 4.14 | 0.0079 |
| 4.95 | -0.0118 | 9.06 | 0.0286 | 5.2 | 0.0008 |
| 5.54 | -0.0031 | 9.1 | 0.0087 | 5.85 | -0.0013 |
| 5.62 | -0.0028 | 9.11 | 0.0033 | 5.91 | -0.0014 |
| 6.17 | -0.0206 | 9.12 | -0.0193 | 5.91 | -0.0186 |
| 6.21 | -0.0294 | 9.13 | -0.0266 | 6.15 | -0.0295 |
| 6.81 | -0.1030 | 9.16 | -0.1088 | 6.87 | -0.1424 |
| 9.52 | -2.4132 | 9.69 | -0.6064 | 9.51 | -2.2688 |
| 10.27 | -7.1978 | 10.92 | -3.0841 | 10.42 | -7.6353 |

APPENDIX C
EXPERIMENTAL RESULTS OF ADSORPTION

**Table C. 1** Adsorption kinetic of CFA onto SBA-15 and functionalized SBA-15

| Time (min) | Equilibrium concentration of CFA (mg/L) | | | |
|---|---|---|---|---|
| | SBA-15 | 3N-SBA-15 | M-SBA-15 | PAC |
| 0 | 10.00 | 10.00 | 10.00 | 10.00 |
| 1 | 9.446 | 9.132 | 9.992 | 2.898 |
| 5 | 8.470 | 8.916 | 9.974 | 1.437 |
| 10 | 8.769 | 8.144 | 9.915 | 1.048 |
| 20 | 8.381 | 7.304 | 9.836 | 0.939 |
| 30 | 7.831 | 6.950 | 9.675 | 0.894 |
| 60 | 7.623 | 6.439 | 9.757 | 0.670 |
| 120 | 7.481 | 6.175 | 9.652 | 0.632 |
| 180 | 7.149 | 6.056 | 9.670 | 0.572 |
| 240 | 6.913 | 6.309 | 9.647 | 0.561 |
| 260 | 7.291 | 6.242 | 9.665 | - |
| 280 | 7.291 | 5.984 | 9.665 | - |
| 300 | 6.799 | 6.190 | 9.661 | - |
| 320 | 6.595 | 5.735 | 9.661 | - |
| 340 | 6.647 | 5.812 | 9.638 | - |
| 360 | 6.624 | 5.664 | 9.670 | 0.550 |
| 480 | 6.624 | 5.759 | 9.629 | 0.538 |
| 720 | 6.643 | 5.759 | 9.634 | 0.538 |

**Table C. 2** Adsorption isotherm of CFA onto SBA-15 at pH5, 7, and 9

| SBA-15 | Initial concentration of CFA (mg/L) | Equilibrium concentration of CFA (mg/L) | Adsorption capacities (mg/g) |
|---|---|---|---|
| pH5 | 6 | 3.747 | 2.253 |
| | 8 | 5.172 | 2.828 |
| | 10 | 6.329 | 3.671 |
| | 12 | 7.389 | 4.611 |
| | 15 | 9.846 | 5.154 |
| pH7 | 6 | 3.882 | 2.118 |
| | 8 | 5.466 | 2.533 |
| | 10 | 6.957 | 3.042 |
| | 12 | 8.214 | 3.786 |
| | 15 | 10.592 | 4.408 |
| pH9 | 6 | 4.379 | 1.620 |
| | 8 | 6.165 | 1.835 |
| | 10 | 7.549 | 2.451 |
| | 12 | 9.192 | 2.808 |
| | 15 | 11.849 | 3.151 |
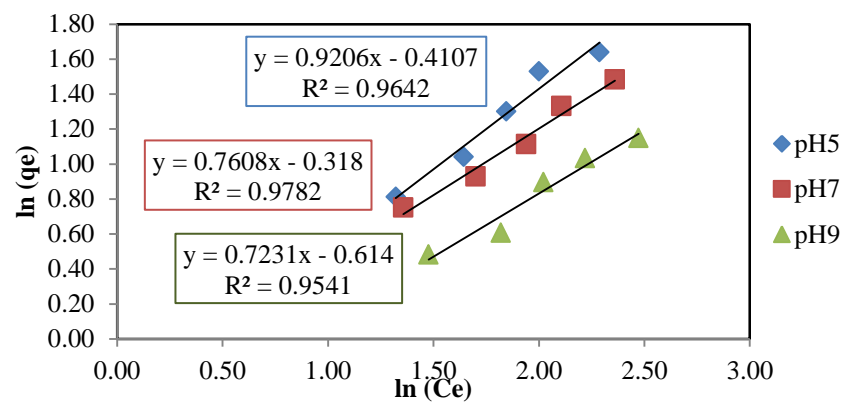


**Figure C. 1** Plotted Freundlich isotherm at high concentration of CFA onto SBA-15 at pH5, 7, and 9
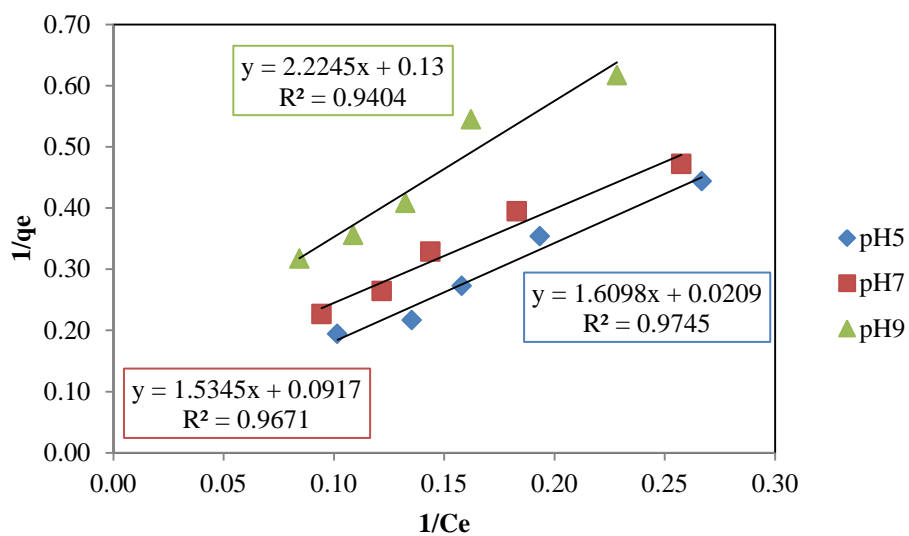
**Figure C. 2** Plotted Langmuir isotherm at high concentration of CFA onto SBA-15 at pH5, 7, and
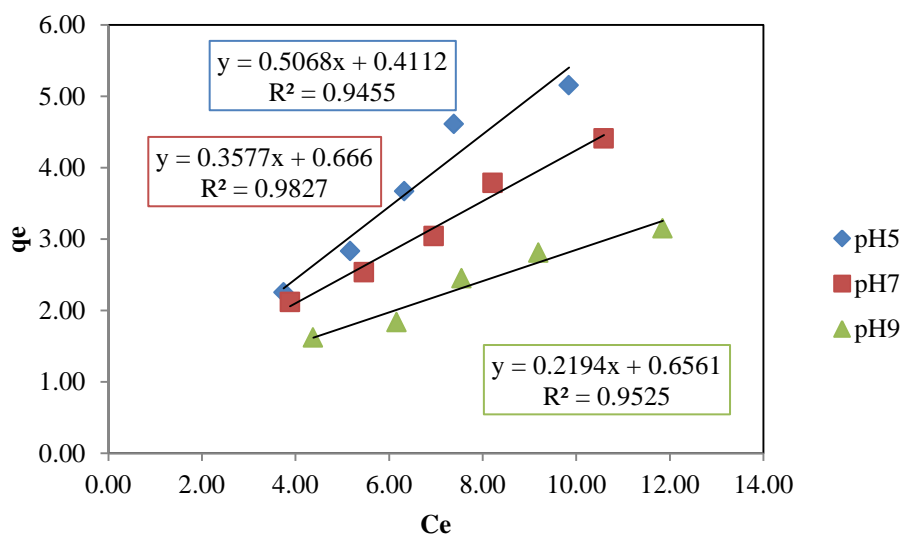


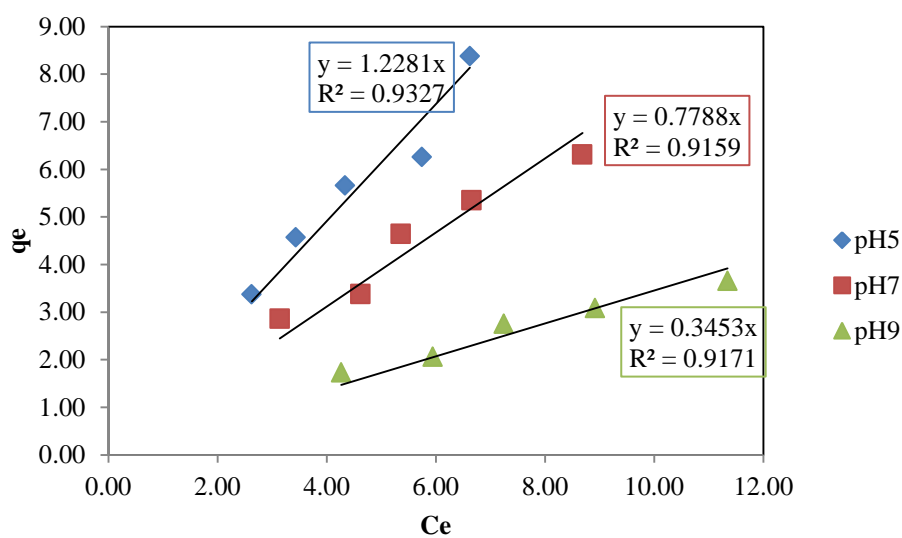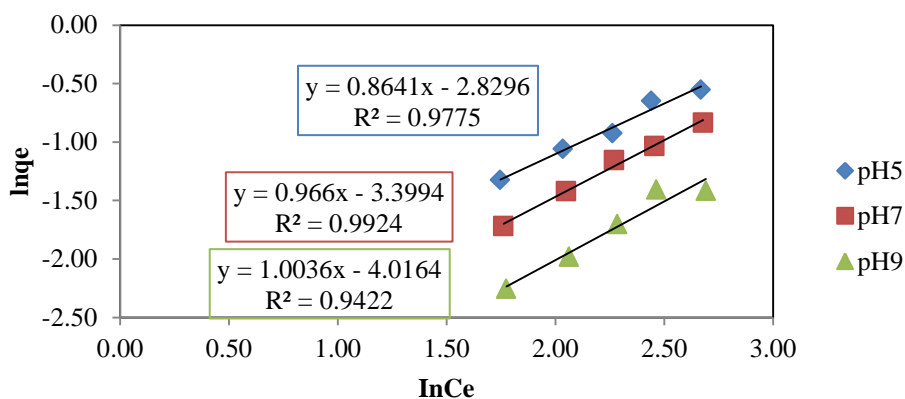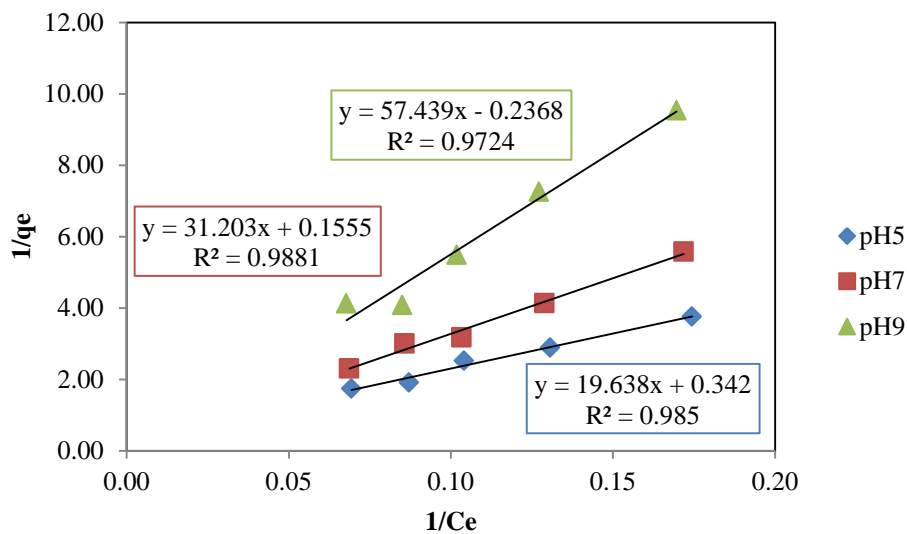**Figure C. 3** Plotted Liner isotherm at high concentration of CFA onto SBA-15 at pH5, 7, and 9

**Table C. 3** Adsorption isotherm of CFA onto 3N-SBA-15 at pH5, 7, and 9

| 3N-SBA-15 | Initial concentration of CFA (mg/L) | Equilibrium concentration of CFA (mg/L) | Adsorption capacities (mg/g) |
|---|---|---|---|
| pH5 | 6 | 2.590 | 3.409 |
| | 8 | 3.380 | 4.619 |
| | 10 | 4.267 | 5.732 |
| | 12 | 5.641 | 6.358 |
| | 15 | 6.502 | 8.497 |
| pH7 | 6 | 3.139 | 2.860 |
| | 8 | 4.618 | 3.381 |
| | 10 | 5.358 | 4.641 |
| | 12 | 6.652 | 5.347 |
| | 15 | 8.686 | 6.313 |
| pH9 | 6 | 4.340 | 1.659 |
| | 8 | 6.053 | 1.946 |
| | 10 | 7.386 | 2.613 |
| | 12 | 9.093 | 2.906 |
| | 15 | 11.57 | 3.423 |
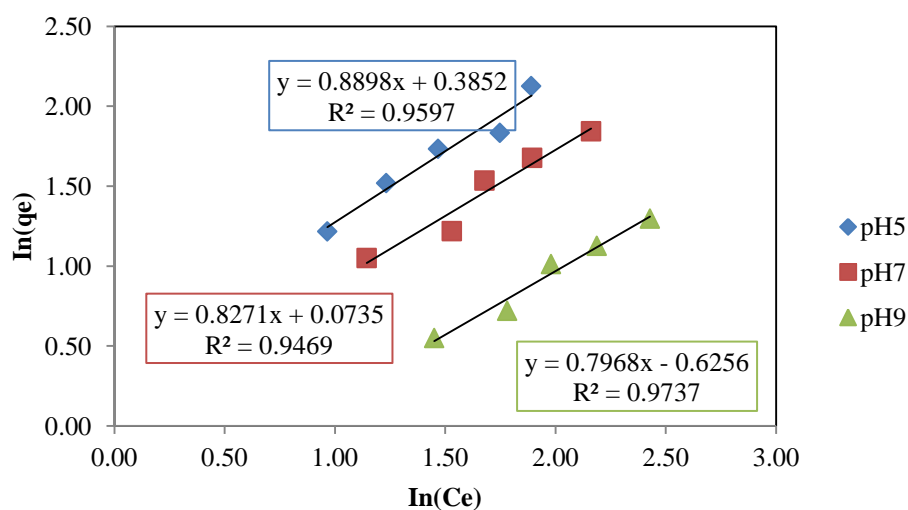


**Figure C. 4** Plotted Freundlich isotherm at high concentration of CFA onto 3N-SBA-15 at pH5, 7, and 9
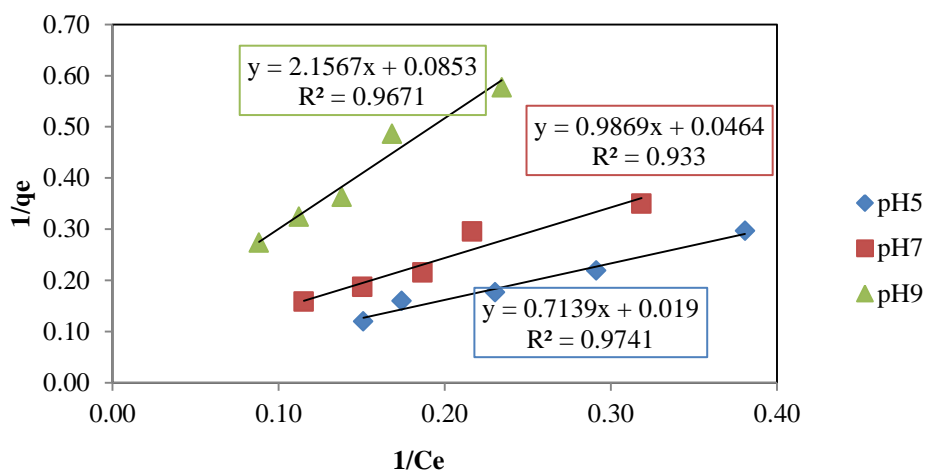
**Figure C. 5** Plotted Langmuir isotherm at high concentration of CFA onto 3N-SBA-15 at pH5, 7, and 9
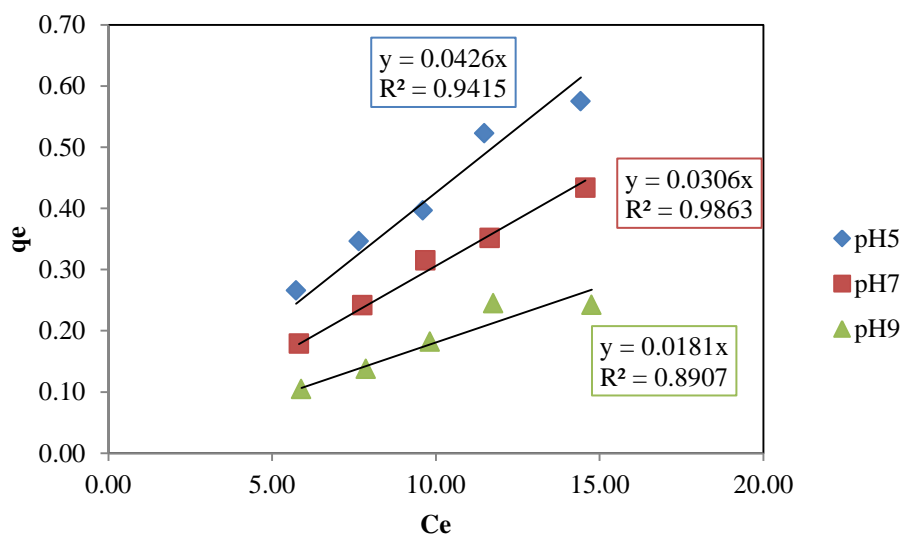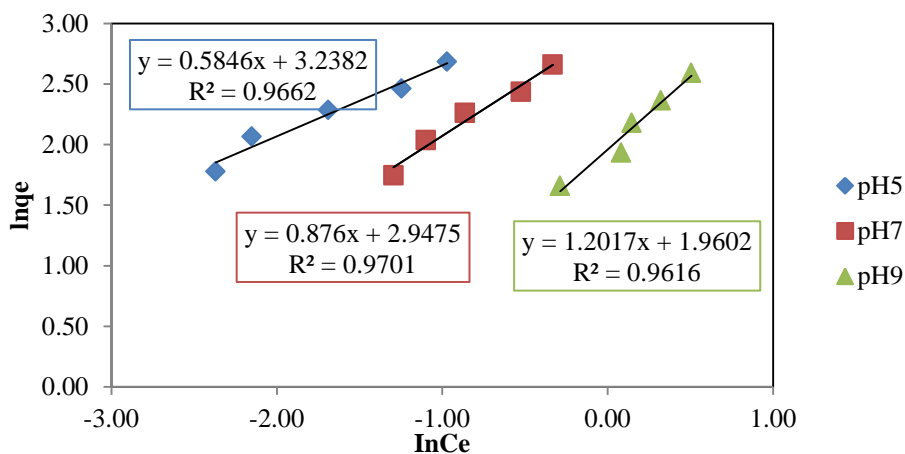


**Figure C. 6** Plotted Linear isotherm at high concentration of CFA onto 3N-SBA-15 at pH5, 7, and 9

**Table C. 4** Adsorption isotherm of CFA onto M-SBA-15 at pH5, 7, and 9

| M-SBA-15 | Initial concentration of CFA (mg/L) | Equilibrium concentration of CFA (mg/L) | Adsorption capacities (mg/g) |
|---|---|---|---|
| pH5 | 6 | 5.733 | 0.266 |
| | 8 | 7.653 | 0.346 |
| | 10 | 9.603 | 0.396 |
| | 12 | 11.477 | 0.522 |
| | 15 | 14.424 | 0.575 |
| pH7 | 6 | 5.820 | 0.179 |
| | 8 | 7.758 | 0.241 |
| | 10 | 9.684 | 0.315 |
| | 12 | 11.644 | 0.355 |
| | 15 | 14.566 | 0.433 |
| pH9 | 6 | 5.895 | 0.104 |
| | 8 | 7.862 | 0.137 |
| | 10 | 9.817 | 0.182 |
| | 12 | 11.755 | 0.244 |
| | 15 | 14.757 | 0.242 |



**Figure C. 7** Plotted Freundlich isotherm at high concentration of CFA onto M-SBA-15 at pH5, 7, and 9
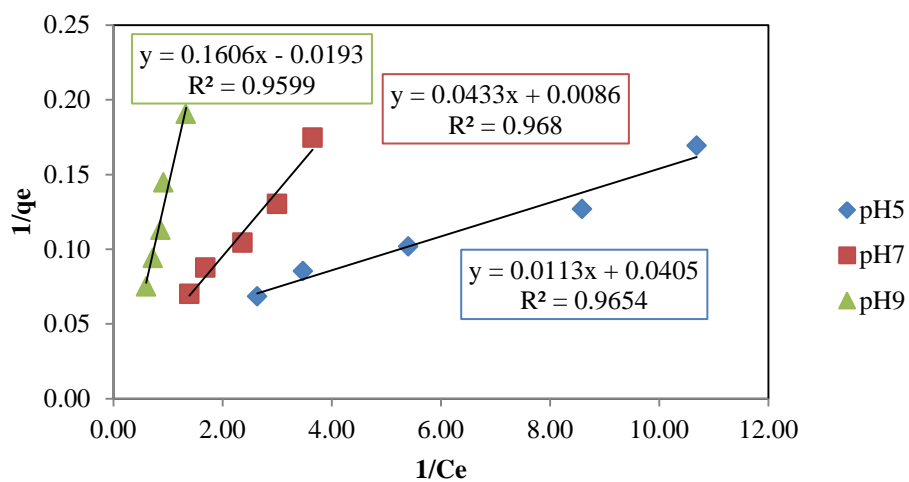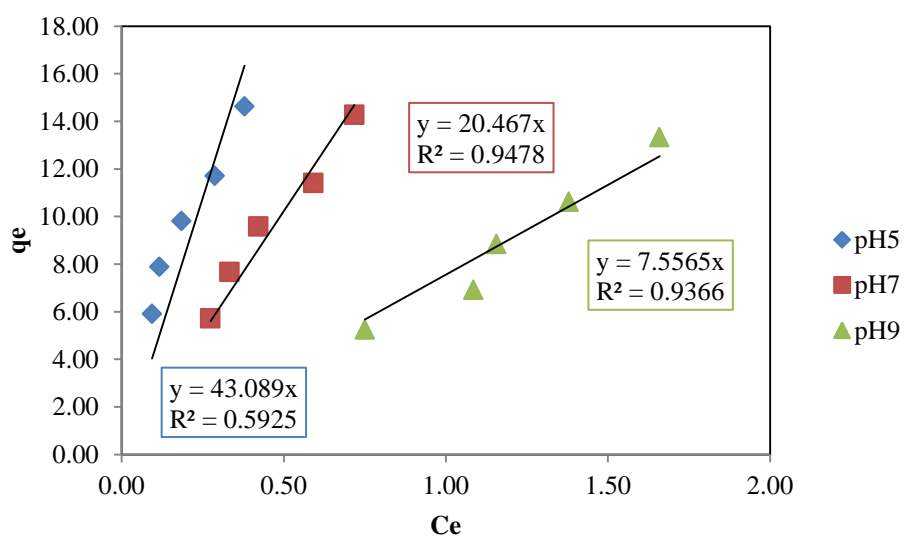
**Figure C. 8** Plotted Langmuir isotherm at high concentration of CFA onto M-SBA-15 at

pH5, 7, and 9



**Figure C. 9** Plotted Freundlich isotherm at high concentration of CFA onto M-SBA-15

at pH5, 7, and 9

**Table C. 5** Adsorption isotherm of CFA onto PAC at pH5, 7, and 9

| PAC | Initial concentration of CFA (mg/L) | Equilibrium concentration of CFA (mg/L) | Adsorption capacities (mg/g) |
|---|---|---|---|
| pH5 | 6 | 0.093 | 5.906 |
| | 8 | 0.116 | 7.883 |
| | 10 | 0.184 | 9.815 |
| | 12 | 0.287 | 11.712 |
| | 15 | 0.379 | 14.620 |
| pH7 | 6 | 0.274 | 5.725 |
| | 8 | 0.333 | 7.666 |
| | 10 | 0.421 | 9.578 |
| | 12 | 0.592 | 11.407 |
| | 15 | 0.718 | 14.282 |
| pH9 | 6 | 0.750 | 5.249 |
| | 8 | 1.085 | 6.914 |
| | 10 | 1.156 | 8.843 |
| | 12 | 1.379 | 10.620 |
| | 15 | 1.659 | 13.340 |



**Figure C. 10** Plotted Freundlich isotherm at high concentration of CFA onto PAC at pH5, 7, and 9

**Figure C. 11** Plotted Langmuir isotherm at high concentration of CFA onto PAC at pH5, 7, and 9



**Figure C. 12** Plotted Linear isotherm at high concentration of CFA onto PAC at pH5, 7, and 9

**Table C. 6** Adsorption isotherm of CFA onto 3N-SBA-15 at low concentration at pH7

| Adsorbent | Intial concentration (μg/L) | Equilibrium concentration (μg/L) | Adsorption capacity (μg/g) | Adsorption capacity (μg/m2) | Adsorption capacity (mol CFA/molN/m$^2$) |
|---|---|---|---|---|---|
| 3N-SBA-15 | 50 | 19.679 | 30.320 | 0.362 | 0.003 |
| | 100 | 45.757 | 54.242 | 0.648 | 0.006 |
| | 150 | 65.082 | 84.917 | 1.014 | 0.009 |
| | 200 | 88.198 | 111.801 | 1.335 | 0.012 |
| | 250 | 112.250 | 137.749 | 1.645 | 0.015 |
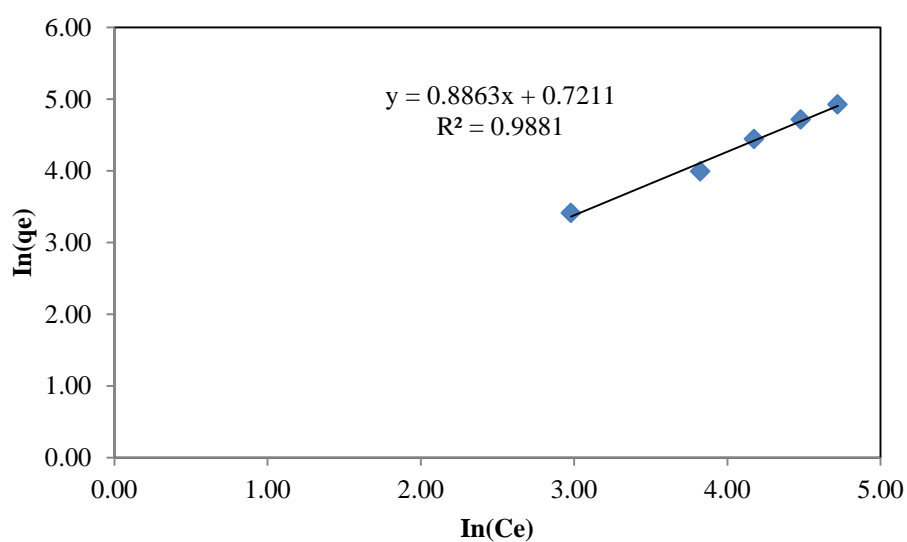


**Figure C. 13** Plotted Freundlich isotherm at low concentration of CFA onto 3N-SBA-15 at pH7
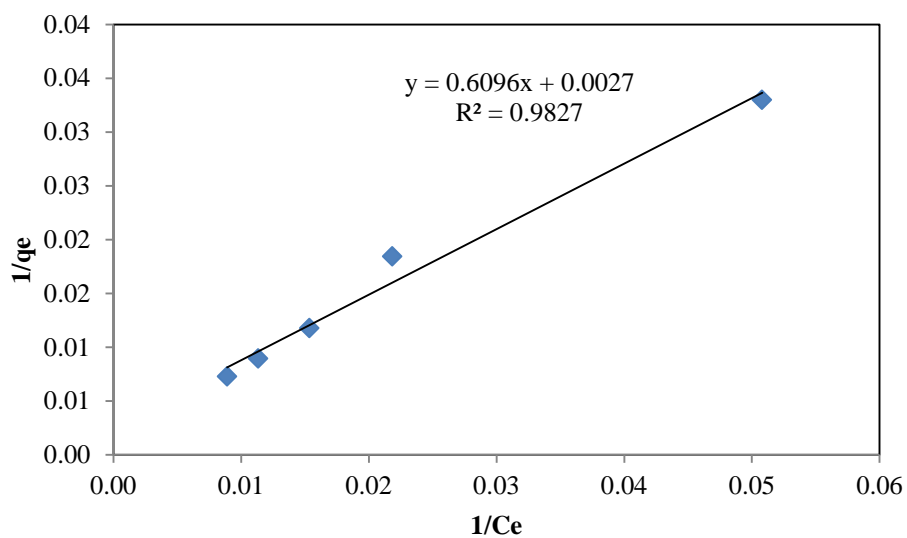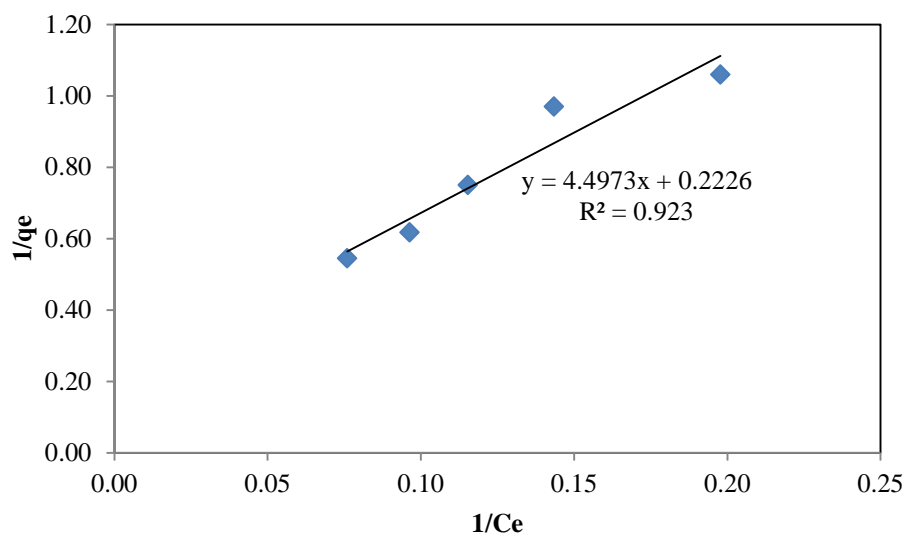
**Figure C. 14** Plotted Langmuir isotherm at low concentration of CFA onto 3N-SBA-15
at pH7
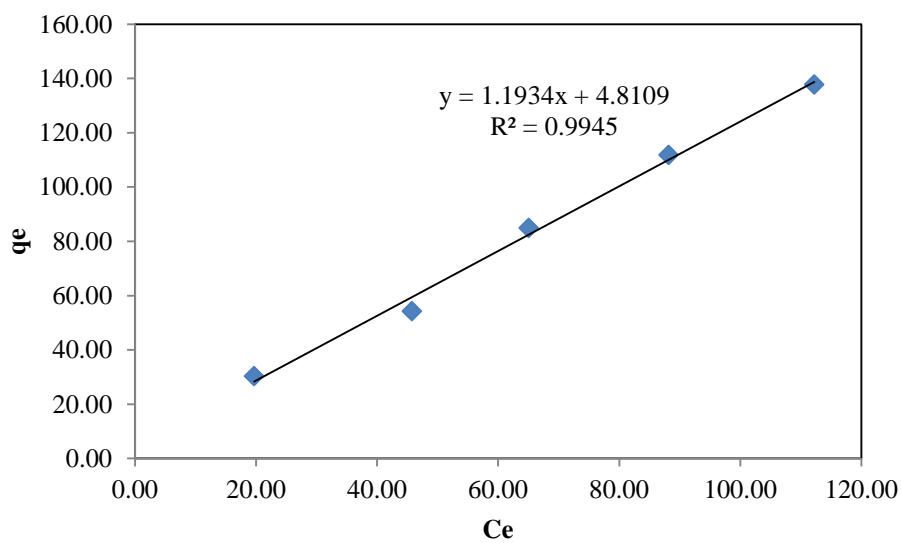


**Figure C. 15** Plotted Linear isotherm at low concentration of CFA onto 3N-SBA-15 at
pH7

**Table C. 7** Adsorption isotherm of CFA in treated wastewater from swine farm

| Natural organic matter (NOM) | Initial concentration (mg/L) | Equilibrium concentration (mg/L) | Adsorption capacity (mg/g) |
|---|---|---|---|
| Hydrophillic NOM | 6 | 5.055 | 0.944 |
| | 8 | 6.968 | 1.031 |
| | 10 | 8.666 | 1.333 |
| | 12 | 10.380 | 1.619 |
| | 15 | 13.165 | 1.835 |
| Hydrophobic NOM | 6 | 4.469 | 1.530 |
| | 8 | 6.166 | 1.833 |
| | 10 | 7.599 | 2.401 |
| | 12 | 9.283 | 2.716 |
| | 15 | 10.993 | 4.007 |
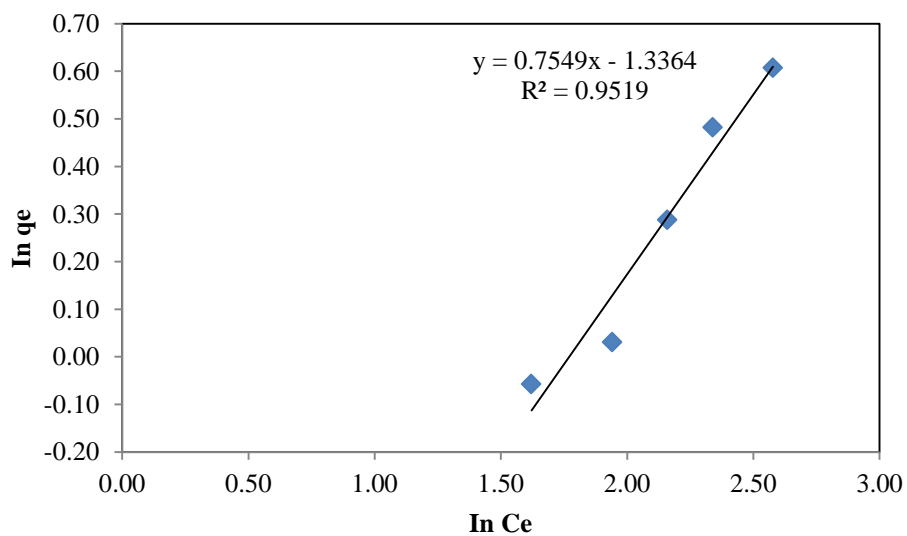


**Figure C. 16** Plotted Feundlich isotherm at high concentration of CFA onto 3N-SBA-15 in HPI NOM

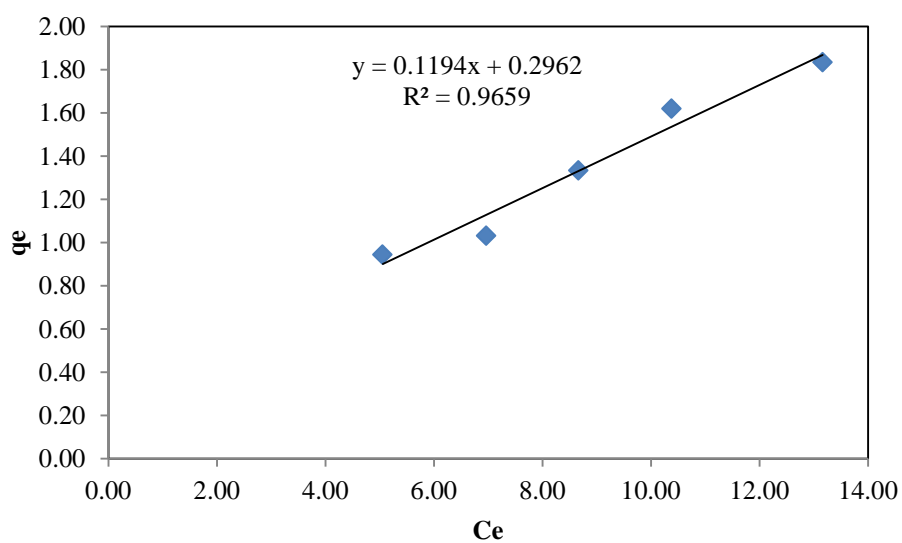**Figure C. 17** Plotted Langmuir isotherm at high concentration of CFA onto 3N-SBA-15 in HPI NOM



**Figure C. 18** Plotted Linear isotherm at high concentration of CFA onto 3N-SBA-15 in HPI NOM
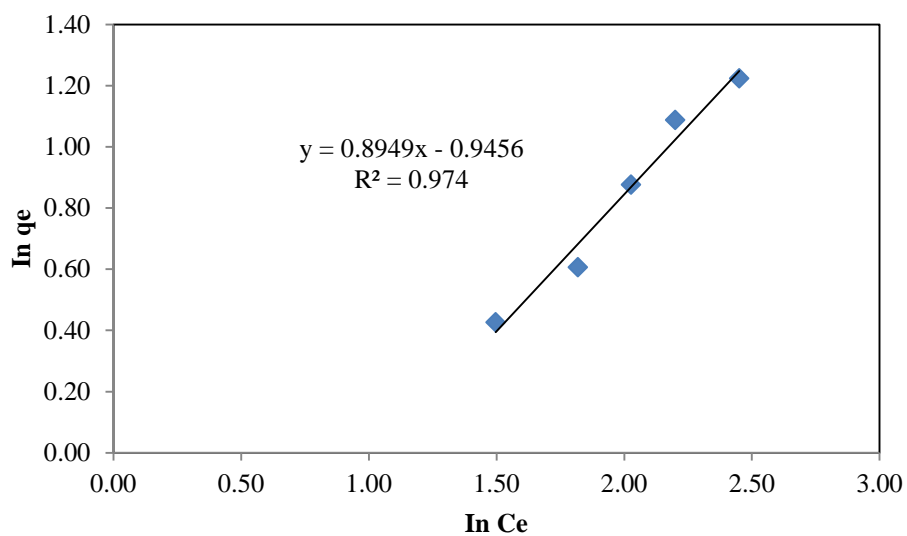
**Figure C. 19** Plotted Feundlich isotherm at high concentration of CFA onto 3N-SBA-15 in HPO NOM
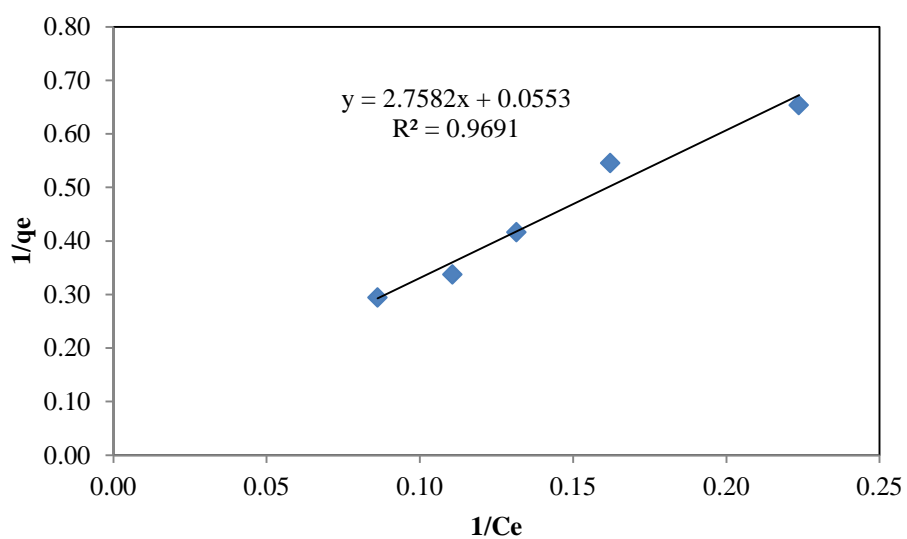


**Figure C. 20** Plotted Langmuir isotherm at high concentration of CFA onto 3N-SBA-15 in HPO NOM
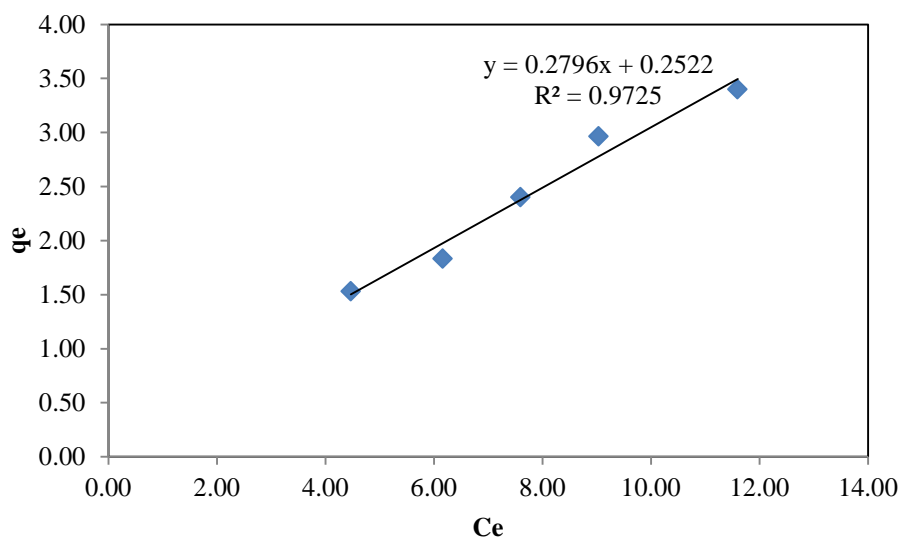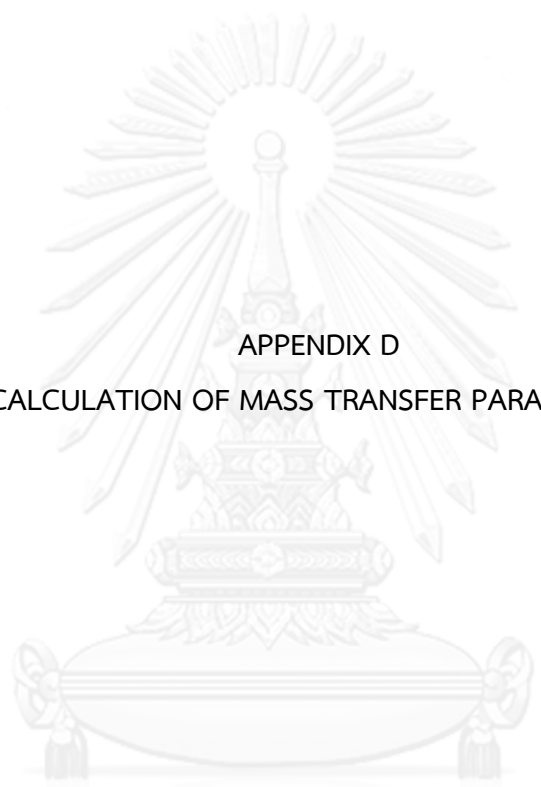
**Figure C. 21** Plotted Linear isotherm at high concentration of CFA onto 3N-SBA-15 in HPO NOM

**Table C. 8** Initial and equilibrium concentration of HPI NOM

| Initial concentration of CFA in HPI NOM (mg/L) | Initial concentration of HPI NOM (mg/L) | Equilibrium concentration of HPI NOM (mg/L) |
|---|---|---|
| 6 | 0.794 | 0.442 |
| 8 | 0.781 | 0.433 |
| 10 | 0.788 | 0.432 |
| 12 | 0.782 | 0.438 |
| 15 | 0.792 | 0.433 |

**Table C. 9** Initial and equilibrium concentration of HPO NOM

| Initial concentration of CFA in HPO NOM (mg/L) | Initial concentration of HPO NOM (mg/L) | Equilibrium concentration of HPO NOM (mg/L) |
|---|---|---|
| 6 | 0.691 | 0.679 |
| 8 | 0.718 | 0.704 |
| 10 | 0.681 | 0.674 |
| 12 | 0.696 | 0.728 |
| 15 | 0.712 | 0.719 |

APPENDIX D

CALCULATION OF MASS TRANSFER PARAMETERS

**Mass transfer parameters**

(2)
$$q_t = \frac{q_e{}^2 k_2 t}{1 + k_2 q_e t}$$

$$\frac{\partial q}{\partial t} = \frac{q_e{}^2 k_2 \left(1 + q_e t - q_e\right)}{\left(1 + q_e k_2 t\right)^2} \qquad (3)$$

## 1. SBA-15

Example of calculation of mass transfer parameters for SBA-15

## 1.1 Liquid film mass transfer coefficient

$$\frac{\partial \overline{q}}{\partial t} = k_f S_0 (C - C_i) \qquad (4)$$
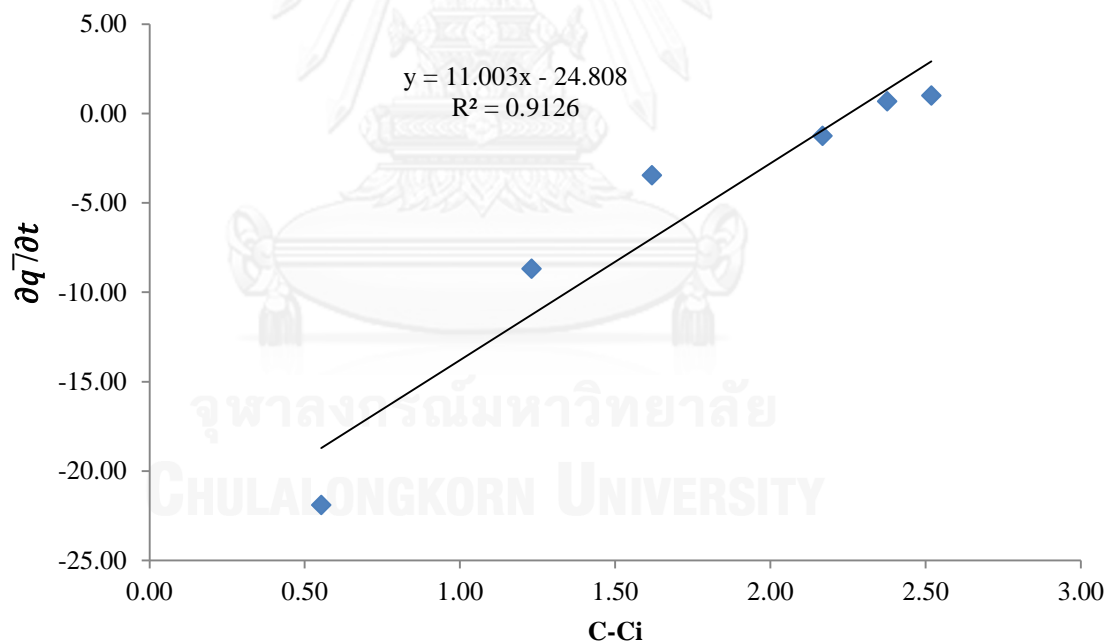


**Figure D. 1** Graph for calculation of liqiud film mass transfer coefficient of SBA-15

**Table D. 1** Calculated parameters for liqiud film mass transfer coefficient of SBA-15

| $\dfrac{\partial \overline{q}}{\partial t}$ | C-C$_i$ (mg/L) |
|:---:|:---:|
| -21.905 | 0.553 |
| -8.699 | 1.230 |
| -3.467 | 1.619 |
| -1.260 | 2.169 |
| 0.673 | 2.377 |
| 0.999 | 2.519 |

$$S_0 = \frac{3}{R} = 4694.836 \text{ cm}^2/\text{cm}^3 \qquad (5)$$

$$Slope = k_f S_0 \qquad (6)$$

$$11.003 = k_f \times 4694.836$$

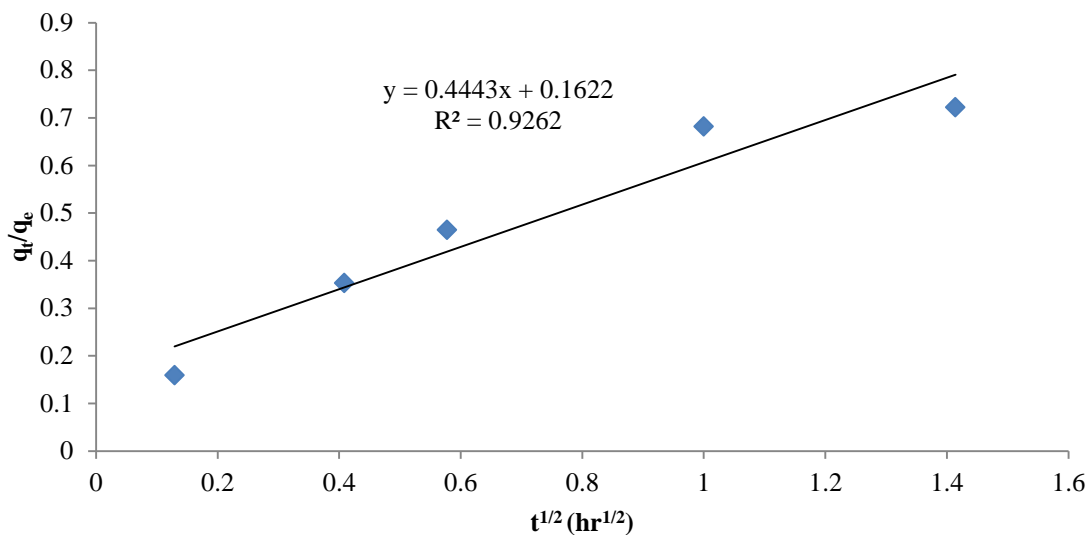$$k_f = 2.344 \times 10^{-3} \text{ cm/hr.}$$

## 1.2 Diffusivity



**Figure D. 2** Graph for calculation of diffusivity **of SBA-15**

**Table D. 2** Calculated parameters for diffusivity of SBA-15

| $q_t/q_e$ | $t^{1/2}(hr^{1/2})$ |
|---|---|
| 0.159 | 0.129 |
| 0.353 | 0.408 |
| 0.464 | 0.577 |
| 0.681 | 1.000 |
| 0.722 | 1.414 |

$$Slope = 6\left(\frac{D_s}{\Pi R^2}\right)^{\frac{1}{2}} \tag{7}$$

$$0.444 = 6\left(\frac{D_s}{\Pi\left(6.39\times10^{-4}\right)^2}\right)^{\frac{1}{2}}$$

$$D_s = 7.034\times10^{-9}\,cm^2/hr.$$

## 1.3 Solid film mass transfer coefficient

$$k_s = \frac{5D_s}{R} \tag{8}$$

$$k_s = \frac{5(7.034\times10^{-9})}{6.39\times10^{-4}}$$

$$k_s = 5.504\times10^{-5}\,\text{cm/hr.}$$

## 1.4. Overall solid-phase mass transfer coefficient

$$\frac{1}{K_s} = \frac{m}{k_f} + \frac{1}{k_s} \tag{9}$$

$$\frac{1}{K_s} = \left(\frac{0.444}{2.344\times10^{-3}}\right) + \frac{1}{5.504\times10^{-5}}$$

$$K_s = 5.447\times10^{-5}\,\text{cm/hr.}$$

## 1.5. Overall liquid-phase mass transfer coefficient

$$\frac{1}{K_f} = \frac{1}{k_f} + \frac{1}{mk_s} \tag{10}$$

$$\frac{1}{K_f} = \left(\frac{1}{2.344\times10^{-3}}\right) + \left(\frac{1}{0.4444\times5.504\times10^{-5}}\right)$$

$$K_f = 2.415\times10^{-5}\,\text{cm/hr.}$$

## 2. 3N-SBA-15

Table D. 3 Calculated parameters for mass transfer parameters of 3N-SBA-15

| Adsorbent | $\frac{\partial\overline{q}}{\partial t}$ | $C-C_i$ (mg/L) | $q_t/q_e$ | $t^{1/2}$ (hr$^{1/2}$) |
|---|---|---|---|---|
| 3N-SBA-15 | -31.891 | 1.0837 | 0.200 | 0.129 |
| | -16.831 | 1.856 | 0.249 | 0.288 |
| | -5.793 | 2.696 | 0.427 | 0.408 |
| | -2.084 | 3.049 | 0.621 | 0.577 |
| | | | 0.703 | 0.707 |
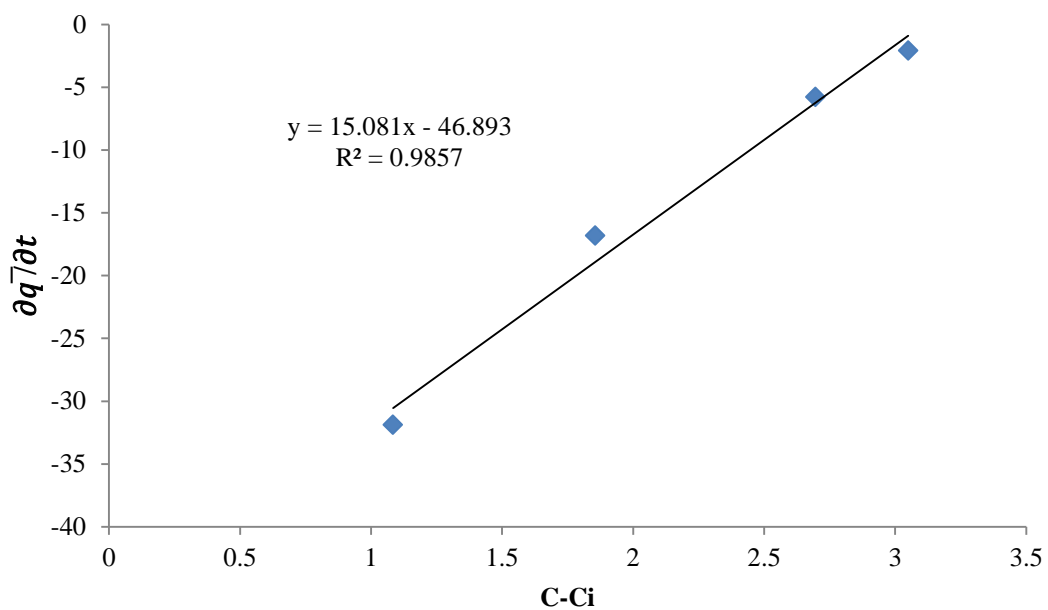
**Figure D. 3** Graph for calculation of liqiud film mass transfer coefficient of 3N-SBA-15

$$y = 15.081x - 46.893$$
$$R^2 = 0.9857$$
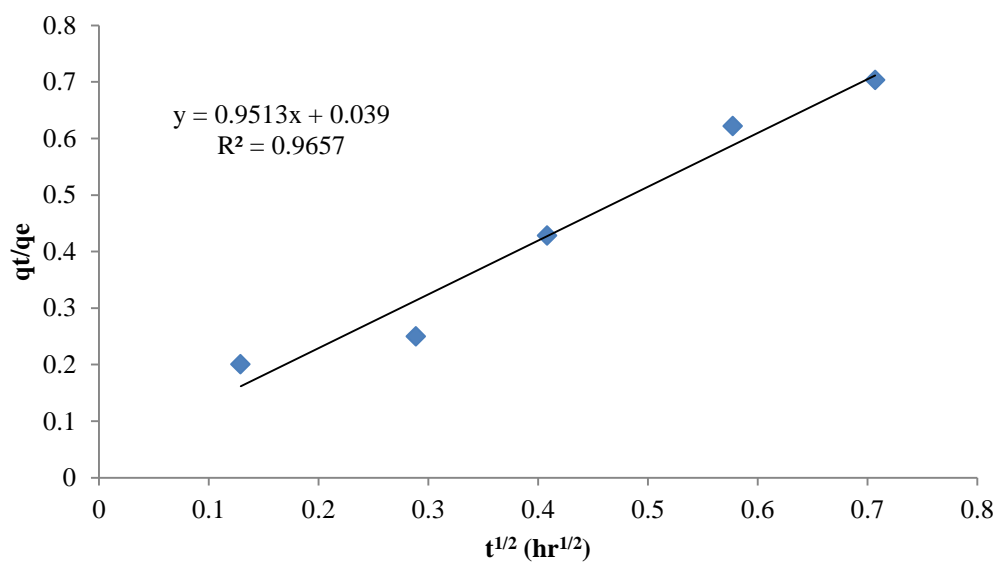


**Figure D. 4** Graph for calculation of diffusivity of 3N-SBA-15

$$y = 0.9513x + 0.039$$
$$R^2 = 0.9657$$

### 3. M-SBA-15

**Table D. 4** Calculated parameters for mass transfer parameters of M-SBA-15

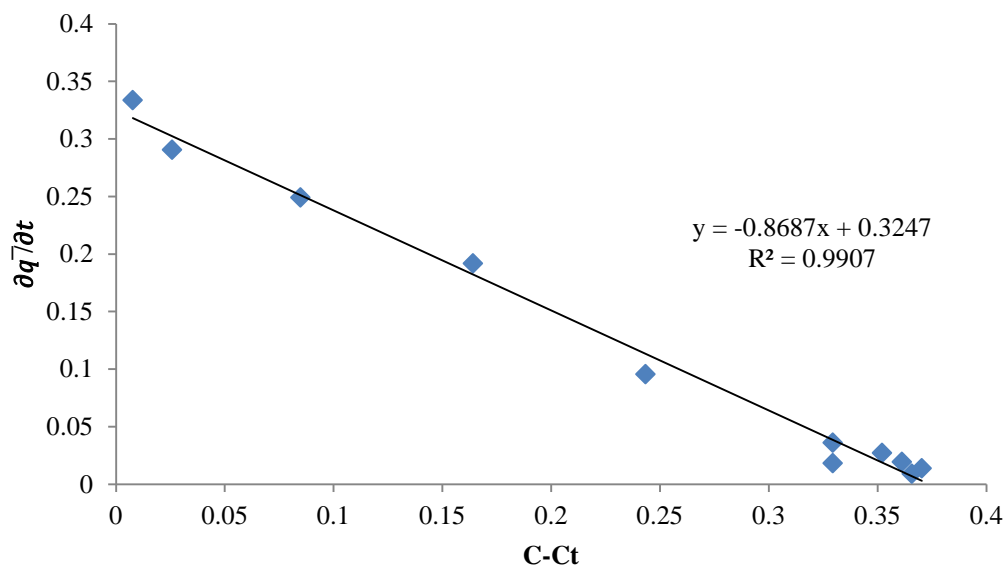| Adsorbent | $\dfrac{\partial \overline{q}}{\partial t}$ | C-C$_i$ (mg/L) | q$_t$/q$_e$ | t$^{1/2}$(hr$^{1/2}$) |
|---|---|---|---|---|
| M-SBA-15 | 0.334 | 0.008 | 0.0196 | 0.129 |
| | 0.291 | 0.026 | 0.214 | 0.408 |
| | 0.249 | 0.085 | 0.415 | 0.577 |
| | 0.192 | 0.164 | 0.616 | 1.000 |
| | 0.095 | 0.243 | 0.834 | 1.732 |
| | 0.036 | 0.329 | | |
| | 0.027 | 0.352 | | |
| | 0.0192 | 0.361 | | |
| | 0.0181 | 0.329 | | |
| | 0.014 | 0.370 | | |
| | 0.009 | 0.366 | | |



$$y = -0.8687x + 0.3247$$
$$R^2 = 0.9907$$

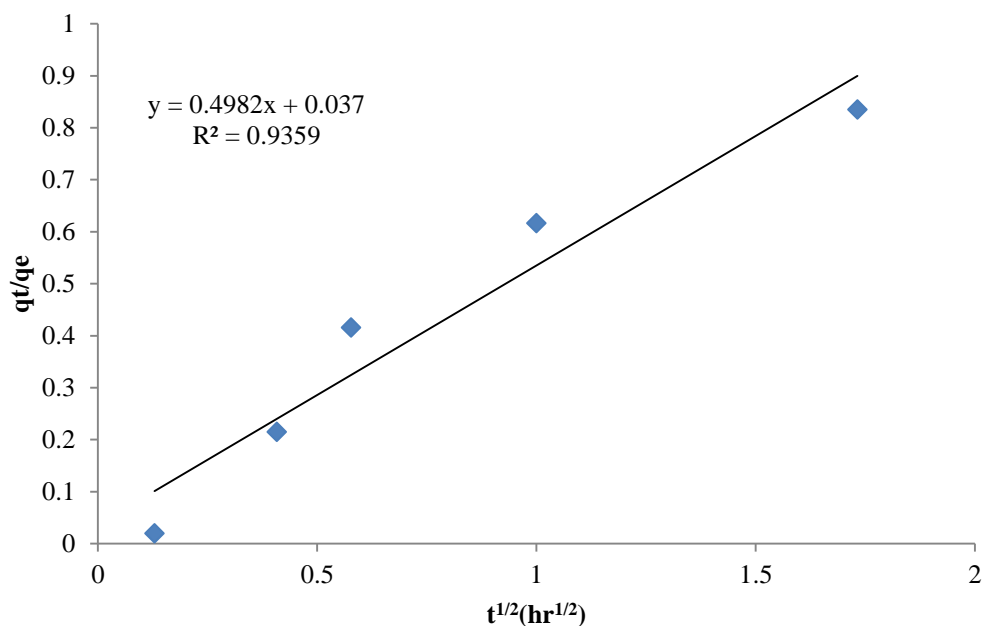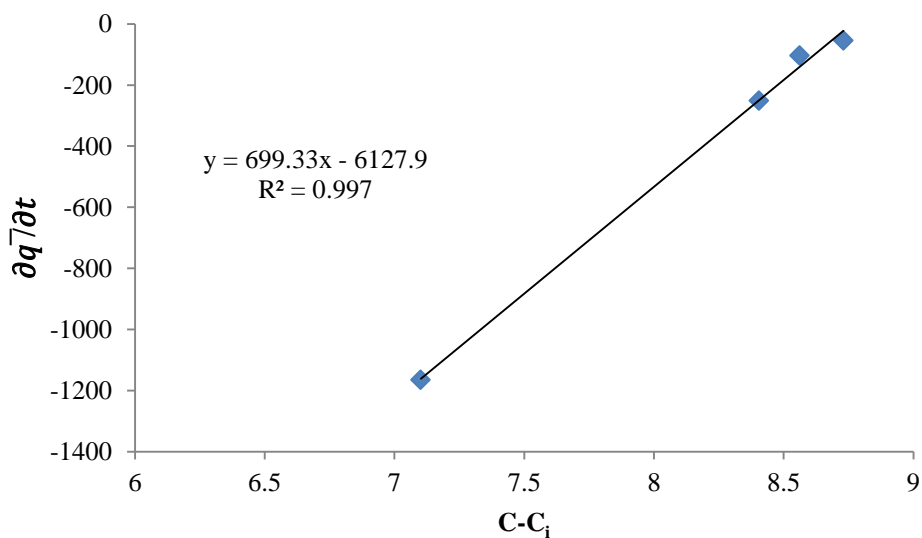Figure D. 5 Graph for calculation of liqiud film mass transfer coefficient of M-SBA-15

**Figure D. 7** Graph for calculation of diffusivity of M-SBA-15

## 4. PAC

**Table D. 5** Calculated parameters for mass transfer parameters of PAC

| Adsorbent | $\dfrac{\partial \overline{q}}{\partial t}$ | C-C$_i$ (mg/L) | $q_t/q_e$ | t$^{1/2}$(hr$^{1/2}$) |
|-----------|------------|--------------|-----------|--------------|
| PAC | -1165.339 | 7.101 | 0.712 | 0.0913 |
| | -250.876 | 8.405 | 0.749 | 0.129 |
| | -103.352 | 8.562 | 0.887 | 0.224 |
| | -54.775 | 8.731 | 0.904 | 0.289 |
| | | | 0.922 | 0.342 |



**Figure D. 8** Graph for calculation of liqiud film mass transfer coefficient of PAC
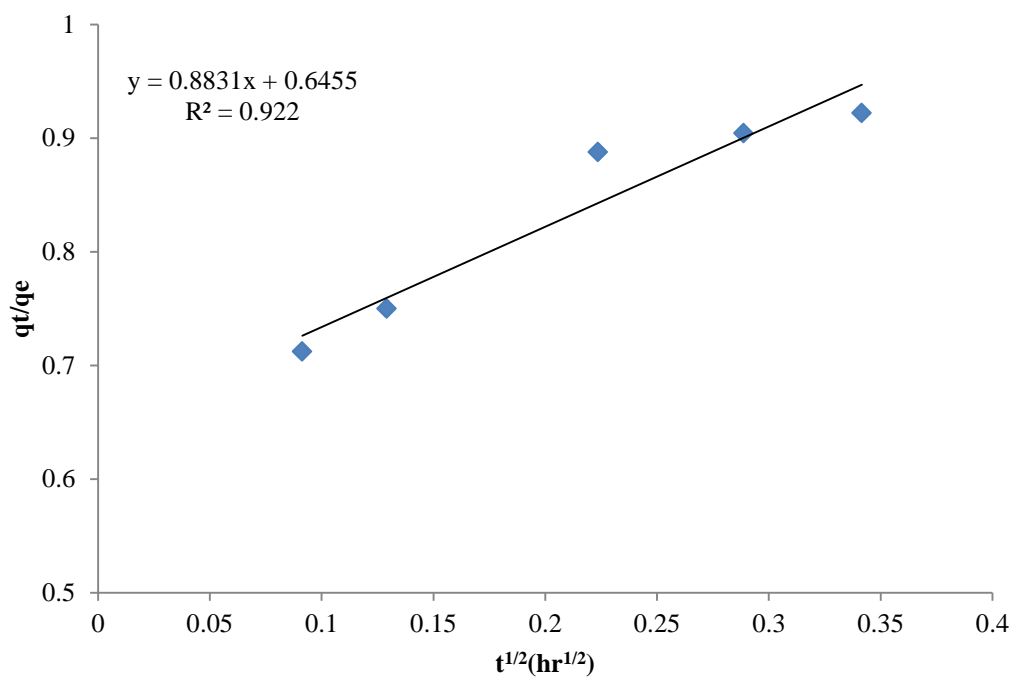
y = 0.8831x + 0.6455
R² = 0.922

**Figure D. 9** Graph for calculation of diffusivity of PAC

## 5. SBA-15 at low concentration

**Table D. 6** Calculated parameters for mass transfer parameters of SBA-15 at low concentration

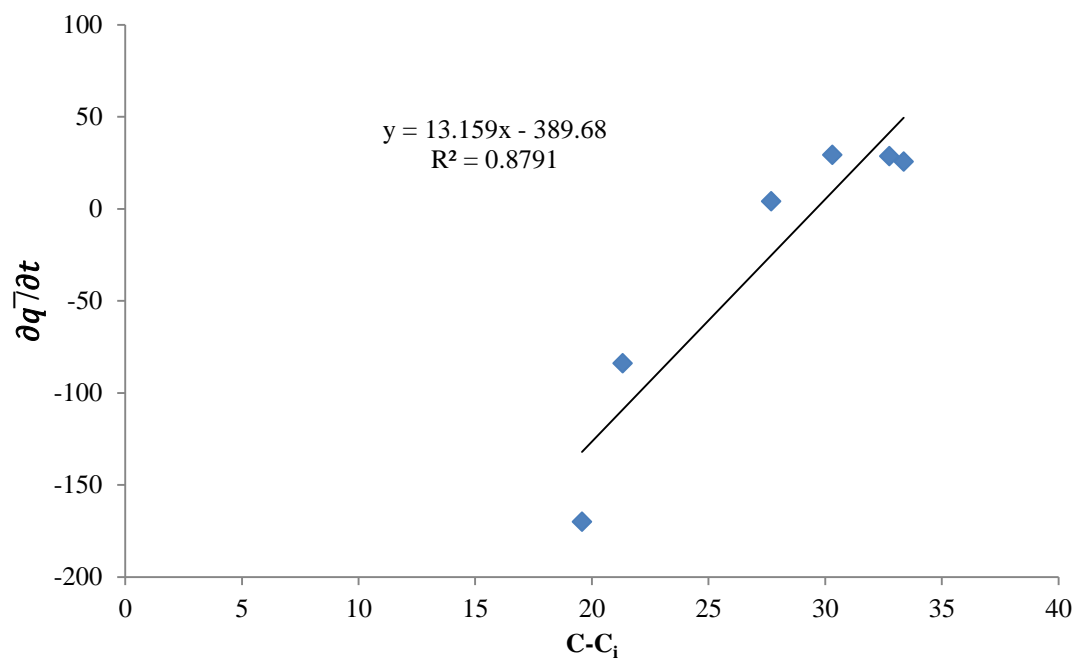| Adsorbent | $\dfrac{\partial \bar{q}}{\partial t}$ | $C-C_i$ (mg/L) | $q_t/q_e$ | $t^{1/2}$(hr$^{1/2}$) |
|---|---|---|---|---|
| SBA-15 | -169.962 | 19.58 | 0.422 | 0.408 |
| | -83.861 | 21.33 | 0.505 | 0.577 |
| | 4.112 | 27.69 | 0.550 | 0.707 |
| | 29.186 | 30.31 | 0.714 | 1.000 |
| | 28.646 | 32.76 | | |
| | 25.577 | 33.37 | | |

**Figure D. 10** Graph for calculation of liqiud film mass transfer coefficient of SBA-15 at low concentration
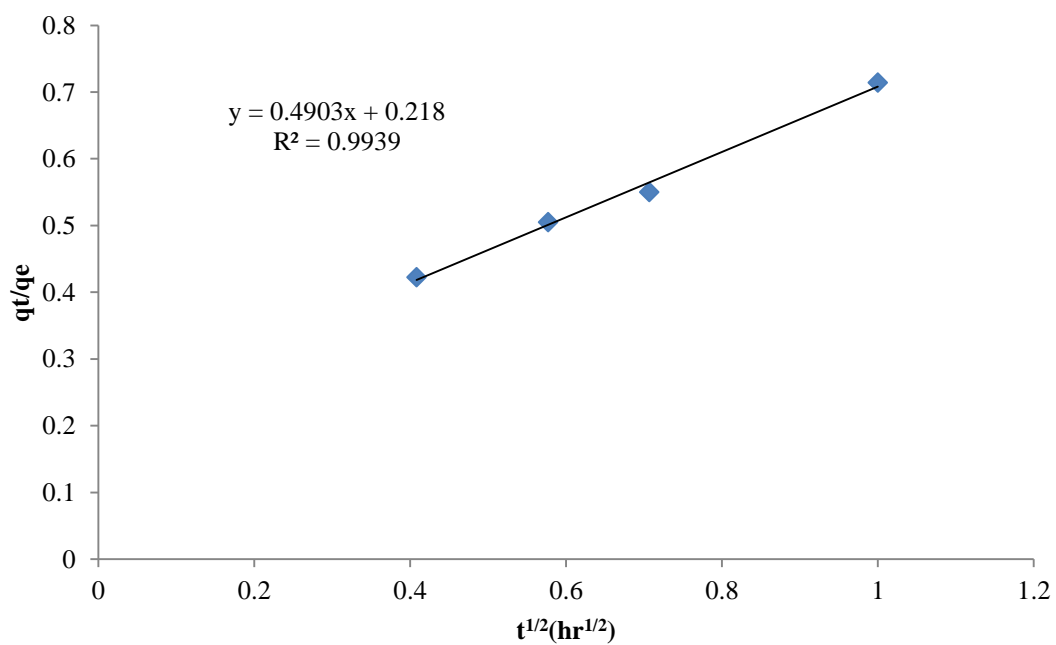


**Figure D. 11** Graph for calculation of diffusivity of SBA-15 at low concentration

**Table D. 7** Calculated mass transfer parameters and radius of SBA-15, functionalized SBA-15, and PAC

| Adsorbents | $k_f$ ($10^{-3}$) (cm/hr) | $k_s$ ($10^{-5}$) (cm/hr) | $K_f$ ($10^{-6}$) (cm/hr) | $K_s$ ($10^{-5}$) (cm/hr) | $D_s$ ($10^{-9}$) (cm$^2$/hr) | Radius (µm) |
|---|---|---|---|---|---|---|
| SBA-15 | 2.34 | 5.50 | 24.15 | 5.45 | 7.03 | 6.39 |
| 3N-SBA-15 | 2.41 | 18.92 | 138.81 | 17.82 | 18.12 | 4.79 |
| M-SBA-15 | 0.15 | 5.70 | 1.73 | 5.63 | 6.00 | 5.27 |
| PAC | 851.78 | 124.34 | 550.84 | 124.26 | 908.67 | 6.39 |
| SBA-15 (at low concentration of CFA) | 2.80 | 6.70 | 21.81 | 6.66 | 8.57 | 36.54 |

## VITA

Miss Jutima Permrungruang was born on December 23, 1989 in Bangkok province. She graduated Bachelor's degree of Science of chemistry from Chulalongkorn University. After that she continued study in Master's degree of science in Environmental management, Chulalongkorn University

Some part of this thesis has been published in the Annual Conference on Engineering and Information Technology held at The Toshi Center Hotel, Tokyo, Japan between 28 to 30 March 2014